Polar Auxin Transport And Auxin Induced Development:

Root System And Signaling Molecules Give The Clue

Dissertation

zur

Erlangung des Doktorgrades (Dr. rer. nat.)

der

Mathematisch-Naturwissenschaftlichen Fakultät

der

Rheinischen Friedrich-Wilhelms-Universität Bonn

vorgelegt von

Markus Schlicht

aus

Bonn

Bonn 2008

Angefertigt mit Genehmigung der Mathematisch-Naturwissenschaftlichen Fakultät der Rheinischen Friedrich-Wilhelms-Universität Bonn

1. Referent: Prof. Dr. František Baluška
2. Referent: Prof. Dr. Diedrik Menzel

Tag der Promotion: 12.12.2008

Diese Dissertation ist auf dem Hochschulschriftenserver der ULB Bonn http://hss.ulb.uni-bonn.de/diss_online elektronisch publiziert.

Erscheinungsjahr: 2008

1. Introduction:

Signaling molecules, including steroids, peptids, radicals of oxygen and nitrogen as well as the six classical phytohormone groups (auxins, abscisic acid, cytokinines, ethylene, jasmonates and gibberellines) are extremely important in plants. Controlled plant growth would not be possible without these regulators. Phytohormones are generally small molecules. Their distribution throughout the plant body occurs in many different ways, i.e., from cell to cell (e.g. auxin), across vascular bundles (e.g. cytokinines) or via the intercellular space (e.g. ethylene). As a general rule all known phytohormones have a broad and complex spectrum of activity. Some phytohormone effects appear immediately and some reactions are revealed only several hours after hormone application. Instantaneous reactions are supposed to be channeled by membrane associated enzymes (Schopfer and Liszkay 2006). Delayed effects are often caused, when an alteration of transcriptional activity is involved (e.g. Theologis et *al.* 1985). Differentiation processes are rather controlled by a complex balanced equilibrium of regulator molecules than by a single class of molecule (Aloni et *al.* 2006a) and often external factors, such as light (Cheng et *al.* 2007) or nutrients (Jain et *al.* 2007; Shishova et *al.* 2007) are of importance. Some combinations of phytohormones act synergistically, like auxin and ethylene (Eklöf et *al.* 2000; Ruzicka et *al.* 2007), while others work antagonistically like auxin and cytokinines (Nordström et *al.* 2004; Aloni et *al*. 2006b). Moreover, hormones can mediate external signals to be transformed into physiological activity (e.g. auxin function for gravitropism).

Historically, auxin is the earliest phytohormone studied. Charles Darwin postulated in his book „The Power of Movement in Plants" a hypothetical substance, which enables phototropism in etiolated coleoptiles, that phototropic reactions are characteristic for growing tissues and are less easily detected in fully differentiated ones.

In his studies he showed that the tip of the coleoptile plays a decisive role in the detection of the light stimulus, but the bending reaction, through cellular elongation growth on the shaded side, occurs some distance beneath the tip. Accordingly, Darwin implied a mechanism for signal transmission downwards through the tissue.

Removing of the tip prevents a phototropic reaction. A re-attachment of the cut-off part of the tip rescues the bending reaction. All this pointed to the existence of a substance, which originates at the tip to the organ, is basipetal transported and promotes cellular elongation in the target area.

In 1926, substantial evidence for the existence of this hypothetical substance was provided by Frits Warmolt Went, who gave it the name auxin. The name is deduced from the greek word „auxein", „to grow". Chemically, auxin is indolyl-3-acetic acid (IAA) and it is derived from the amino acid tryptophan. Besides IAA, several molecules with a comparable spectrum of growth promoting activity are known. They are originating from plants (Woodward et *al.* 2005a), microorganisms (Spaepen et *al.* 2007) or are even synthetically produced (Fig. 1.3). The term auxin may refer collectively to molecules, which are capable of promoting growth by cell elongation of the gramineous coleoptile used as a bioassay. Nevertheless, in the narrow sense the term auxin is used for the most potent native auxin, namely IAA.

Nearly every developmental stage (embryonal and postembryonal) and every growth process of a plant (formation of lateral organs, growth of leafs) is affected directly (Teale et *al.* 2005, 2006; Heisler et *al.* 2005) or indirectly (Pagnussant et *al.* 2004) by IAA. Furthermore, phototropism and gravitropism (Went et *al.*1937; Friml et *al.* 2002a; Li et *al*. 2005) are closely connected to auxin action.

The polar transport of auxin (PAT) is a unique feature, which separates the effect of auxin from that of all other signaling molecules in plants. While almost all tissues of the plant body could produce auxin, the bulk of it originates in primordia and young leaves near the stem apical meristem (Ljung et *al.* 2001; Aloni et *al*. 2003). It is transported along the complete plant body from cell to cell to the root tip. This transport is always directional, ATP-dependent and substrate specific. The transport velocity is beyond diffusion and can run opposite to a concentration gradient.

The cellular auxin propagation is dependent of transport proteins located at the plasma membrane (Muday and DeLong 2001). One class of these comprises specialized influx - efflux carriers another one the ABC transporters (Petrasek et *al.*2006; Bandyopadhyay et *al.* 2007; Zazimalova et *al*. 2007). Following the classical chemiosmotic model of auxin transport, the central role in the cell to cell transport of auxin is played by efflux carriers (facilitators), which provide a checkpoint of the transport mechanism (Zazimalova et *al.* 2007). The pH value of the apoplastic cell wall is maintained at approximately pH 5 resulting in an uncharged form of extracellular IAA, which can diffuse through the plasma membrane easily (Gutknecht and Walter 1980). The pH of the cellular lumen is maintained at pH about 7 by proton pumps continuously pumping hydrogen ions (H^+) from the cytoplasm to the extracellular space. In the cytoplasm, IAA is ionized at this pH condition and is not permeable anymore to the cell membrane, requiring efflux carrier proteins. Such an efflux is limited to specialized cell surface areas at the polar cell poles, thus providing a base of a directional transport.

Several proteins, which have been classified as members of the PIN-family are known to export auxin. The polar localization of these at distinct subcellular domains corresponding to the direction of PAT makes them ideal tools to study the setup and maintance of the cellular IAA export mechanism (Gälweiler et *al.* 1998; Terasaka et *al.* 2005). However, some MDR/PGP-transporters (Multidrug Resistance/P-Glycoprotein transporter) apparently can also export auxin (Petrasek et *al.* 2006; Geisler et *al.* 2005) and might be accountable for some auxin effects, though they are much less well studied.

Evidence is emerging that the domain-specific asymmetric localization of efflux and influx carriers require localized targeting of vesicles and interactions with the actin cytoskeleton (Rahman et *al.* 2007).

A perfect model system in plants to analyze PAT is the root apex, which is defined here as the apical part of the root up to the beginning of the elongation zone encompassing a stretch of several hundred micrometers in Arabidopsis or even several millimeters as in maize. Root apices have a simple anatomy and morphology (Fig. 1.1), which makes them a suitable system to understand the complex interactions between the environment and endogenous plant polarity cues. They are composed of two major parts. Central vascular cylinder (stele) enclosed by the endodermis and by the cortex, which is further enclosed by the epidermis. In comparison shoot apices have a more complex geometry (Baluska et *al.* 1990, 1994, 2001, 2003 2006; Verbelen et *al.* 2006). Interestingly, despite the simple structure the root apex shows the rather complex phenomenon of the polar auxin transport (Bilou et *al.* 2005). Out of eight PIN proteins in *Arabidopsis thaliana*, five members are expressed in the root apex. They are part of an intricate system, which operates the auxin flow loop in the root apex (Bandyopadhyay et *al.* 2007). Shoot derived auxin transported down the stele by PIN1, arrives at the central part of the root cap, and is then channeled to the lateral root cap via activities of PIN3, 4 and 7. After that it is transported through the cortex upwards to the transition zone by PIN2, where again PIN3 and 7 direct the auxin flow inwards to the stele and back again to the apical root tip (Blilou et *al.*

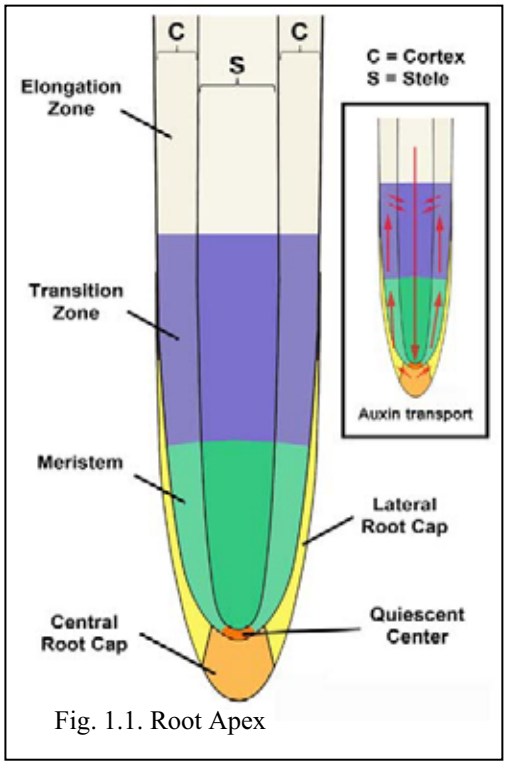

Fig. 1.1. Root Apex

2005). In contrast, despite its higher anatomical complexity shoot apices express only PIN1 for polar transport of auxin.

This network of auxin transporters at the root apex controls a dynamic feedback loop (see Fig 1.1) of auxin flow, which allows rapid reactions to environmental signals like gravitropism or light.

A central point to understand all the facets of auxin activities is the identification of possible interaction partners on the cellular level. Around 20 years ago the first auxin binding protein (ABP1) was found (Hesse et *al.* 1989). Located at the cellular periphery ABP1 participates in the extracellular aspects of auxin induced cell elongation, by activating H^+-ATPases in the plasma membrane. The proton efflux acidifies and loosens the cell walls thus enabling turgor-driven cell expansion (e.g. Christian et *al.* 2006).

Three years ago, two research groups found independent of each other an intracellular auxin receptor. This receptor controls the degradation of a subset of transcription factors (Dharmasiri et *al.* 2005; Kepinski and Leyser 2005).

However, many aspects of auxin action are still not understood. The apparent competence of auxin to alter root architecture may involve other components and interactions such as Reactive Oxygen Species (ROS) and Nitric Oxide (NO). These known stress molecules in plants play crucial parts during cell apoptosis (e.g. Torres et *al.* 1998) and defense against pathogens (Bolwell et *al.* 1999). And recently a more fundamental role in basic growth processes has been discussed. For example, ROS assist in cell elongation by inducing acidification of cell walls (Schopfer and Liszkay 2006) and serve additionally as landmark signal for tip orientated growth in root hairs (e.g. Foreman et *al.* 2003). NO has a marked function in the formation of lateral and adventivous roots (Pagnussant et *al.* 2003, 2004). All these examples are processes, which are induced by auxin, but are depending on ROS and NO, respectively, as down-stream signals.

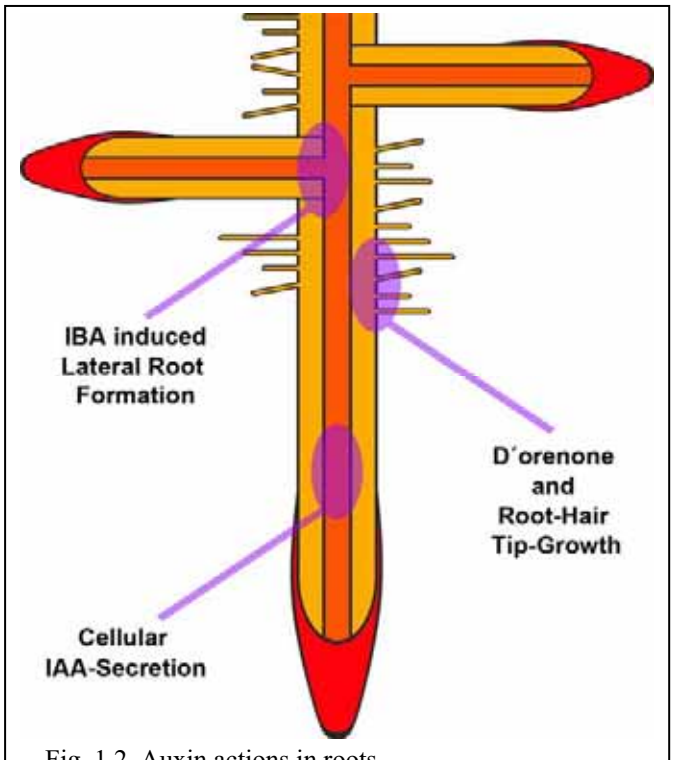

Fig. 1.2. Auxin actions in roots

In the present work several aspects of auxin actions in roots are studied (Fig. 1.2). First, the cellular basis of IAA efflux from cells and polar auxin transport in root apices is analyzed. A second aim is to scrutinize the role of classical stress signaling molecules for root-architecture-modifying effects of auxin. Furthermore, a third facet of this study will be the impact of the novel signaling molecule, D´orenone, on auxin signaling in root apices.

1.1. The cellular basis of the auxin efflux

PAT is important for growth regulation and control of polarity and pattern formation in plants (Swarup and Bennett 2003; Bhalero and Bennett 2003, Friml et *al.* 2003; Friml and Wisniewska 2005; Leyser 2005). In the last few years our knowledge on several proteins, known to be involved in auxin transport has dramatically increased (Gälweiler et *al.* 1998; Bhalero and Bennett 2003; Petrasek et *al.* 2006; Geisler et *al.* 2005), but we are still in need of more detailed information as to how exactly auxin moves across cellular boundaries.

According to the chemiosmotic theory, efflux of auxin is mediated by polarly localized putative auxin efflux carriers within the plasma membrane. Auxin transporters like PIN proteins are pumping IAA across the cell border into the apoplast. This theory predicts that the localization of PINs at the plasma membrane is tightly linked with the activity of polar auxin transport.

Surprisingly, PIN proteins show a fast recycling between plasma membrane and endosomal compartments (Geldner et *al.* 2001, 2003), and recycling is indispensable for PAT (Petrasek et *al.* 2005). Known auxin transport inhibitors, like 2,3,5-Triiodobenzoic acid (TIBA), 1-Naphthylphthalamic acid (NPA) or actomorphine are potent endocytosis blocker, that prevent the internalization of PINs (Geldner et *al.* 2001; Paciorek et *al.* 2005; Schlicht et *al.* 2006). Vice versa, secretion inhibitors such as Brefeldin A (BFA) and Monensin block rapidly the polar auxin transport (Paciorek et *al.* 2005). Delbarre et *al.* (1996) have shown that a drastic drop of PAT occurs within 15 minutes of BFA-treatment.

Brefeldin A eliminates exocytosis and causes the formation of subcellular structures in the cells of root tips, which are called BFA-induced compartments (e.g. Baluska et *al.* 2002). These compartments are locally defined accumulations of endocytic vesicles, endosomes and trans-golgi network elements (Samaj et *al.* 2004). Components of the IAA transport machinery, like PIN1, recycle between the plasma membrane and endosomes and are enriched consequently within BFA-compartments. It is significant that BFA rapidly inhibits PAT, while more than two hours are needed to internalize a better part of auxin exporters (Geldner et *al.* 2001).

PAT depends on the actin cytoskeleton, and this dependency is not consistent with the passive chemiosmotic theory. According to Baluska et *al.* (2001) the formation and maintenance of cellular polarity is enabled by actin. This connection is observable particularly clearly in cells of the transition zone. Root cells are polarized in the longitudinal direction and the cross walls between them separate apical and basal pole of neighboring cells in a cell file. These cell poles are enriched with filamentous actin and are connected by actin bundles. These bundles run along the sides of the nucleus, almost forming a spindle-like structure around the nucleus and hold it tight in the cell center. This actin cytoskeleton provides a transport system for endocytic and secretory vesicles through the cell. Depolymerisation of actin filaments by toxins, like Latrunculin B or Cytochalasin D, stops vesicular trafficking and inhibits polar auxin transport.

Only recently, the contribution of phospholipids and phospholipid-converting enzymes in the regulation of endocytosis and exocytosis has been realized. For instance, phospholipase Dζ2 regulates vesicle trafficking at the plasma membrane (endo- and exocytosis). A substantial portion of the polar transport of auxin in root apices is driven by vesicle-mediated secretion regulated by the PLDζ2 activity and its product phosphatidic acid (PA). The genetic ”Knock-Out“ mutant of PLDζ2 has a strongly reduced endocytosis and flawed auxin reactions (Li et *al.* 2007). In the *pldζ2* mutant and also after 1-butanol treatment, auxin fluxes measured by the IAA-sensitive microelectrode are strongly suppressed despite undisturbed localization of PINs (Li et *al.* 2007; Mancuso et *al.* 2007). Interestingly, mutants over expressing PLDζ2 show a reversed behavior, i.e., amplified endocytosis and increased auxin transport (Li et *al.* 2007; Mancuso et *al.* 2007).

After the phototropism of coleoptiles (see above), gravitropism of the root is the longest known auxin-controlled process in plants (Ciesielski, 1872). For gravitropism PAT is even more important than transcriptional auxin signaling. Several mutants with defects in root auxin transport, like *Aux1* or *PIN2,* are agravitropic, but mutants of transcriptional auxin signaling, for example *TIR1*, can still sense and grow along the gravity vector. Interestingly, gravitropic bending of root apices is also strongly reduced or completely prevented, if ROS (reactive oxygen species) formation is blocked (Joo et *al.* 2001, 2005). Noteworthy, the most common and for this feature used ROS-formation inhibitors (Wortmannin und LY294005) are potent endocytosis reducing chemicals (Lam et *al*. 2007).

Moreover, changing the endogenous ROS-level, either reducing or increasing by chemical treatment, disturbs endocytosis (see diploma thesis by G. Njio). Together with the knowledge that

IAA itself can affect endocytosis (Paciorek et *al.*2005) a strong link between PLDζ2 maintained endocytosis, endogenous ROS-level and auxin transport is becoming evident.

One aim of this thesis is a better understanding of how vesicle trafficking and the cytoskeleton provide a basis for cellular auxin transfer. For this antibody labelings of root sections with a new high-class IAA-specific antibody were done, giving an until now unmatched resolution of subcellular located free IAA (see also Schlicht et *al*. 2006). Beside the snapshots of „in-situ" labelings, several „in-vivo" observations with GFP-fusion proteins and auxin flux measurements were done.

1.2. Auxin modifies root architecture by affecting the status of ROS (*reactive oxygen species*)

ROS are radical forms of oxygen produced photochemically or enzymatically. Besides unstable radicals like superoxide anion ($O2^{\cdot -}$) or the highly reactive hydroxyl radical ($OH^{\cdot}$) stable molecular oxidants such as hydrogen peroxide (H_2O_2) and ozone (O_3) are also considered as ROS. Because of their highly reactive and oxidizing properties these molecules cause a wide range of damage to cellular structures and macromolecular components, including DNA and proteins (Taylor and Millar 2007).

In addition to the damaging effects within plant cells, some forms of ROS mainly H_2O_2 and nitric oxide (NO) play also a crucial role as defense agents against pathogens (Delledonne et *al.* 1998; Durner et *al.* 1998). This includes reactive nitrogen species (RNS), for instance $NO^{\cdot}$ and peroxynitrite ($ONOO^{-}$), which is formed *in vivo* by the reaction of the free radical superoxide with the free radical nitric oxide. Recent studies have shown that ROS/ RNS not only play a role in stress reactions and defense (Mala and Lamattina 2001), but also in signaling and cell-cell communication (Zelko et *al.* 2002; Appel and Hirt et *al.* 2004) and this involves a crosstalk with auxin signaling.

Auxin may act by two different mechanisms. The first is a direct effect on the transcriptional level (Abel 2007), involving an auxin receptor (Dharmasiri et *al.* 2005; Kepinski and Leyser 2005). The second is acting much faster and therefore cannot primarily depend on transcriptional regulation (Schopfer and Liszkay 2006). Schopfer and coworkers have shown that auxin triggers ROS/RNS molecules, which in turn promote cell expansion by loosening the cell walls (Schopfer and Liszkay 2006) and it has further been demonstrated that auxin triggered ROS signals fed into cGMP and MAP-kinase pathways (Pagnussant et *al.* 2003, 2004). Eventually these pathways have their own modulatory effect on gene transcription, revealing surprisingly strong similarities between stress adaptation and auxin

answers. This indicates a possible shared origin of stress adaptation and auxin response.

A new interesting avenue that may help to understand ROS/RNS-based auxin signaling is to take a closer look at the effects of indole butyric acid (IBA), which is a naturally occurring IAA analogue (Fig.1.3.) known from several plant species (Epstein and Ludwig-Müller 1993).

Unlike auxin, it is generally believed that IBA has nearly no transcriptional induction capacity on its own (e.g. Oono et *al.* 1998), it rather serves mainly as a transport and storage form of IAA (Bartel et *al.* 1997; Zolman et *al.* 2001). IAA can be converted to IBA (Ludwig-Müller and Epstein 1994) and it is thought that IBA is turned back to IAA in a ß-oxidation like process (Poupart and Waddell 2000). In plants ß-oxidation is localized in the peroxisomes (Gerhardt 1992; Kindl 1993). Mutants with defects of peroxisomal biosynthesis or β-oxidation are "blind" to externally applied IBA (Zolman et *al.* 2000, 2001a, b; Zolman and Bartel 2004; Woodward and Bartel 2005b) indicating that ß-oxidation-like conversion of IBA to IAA is the explanation for IBA to be effective. However, independent experimental proof for this hypothesis is still missing.

In auxin bioassays IBA shows only weak growth promoting activity (Woodward et *al.* 2005a) with the exception of adventivous and lateral root induction. At this, IBA has a stronger effect than IAA (Zolman et *al.* 2000).

Parallel to the present work, a recent publication is showing that IBA, much like IAA, uses nitric oxide as downstream signal to induce adventivous and lateral roots (Kolbert et *al.* 2007). This suggests a strong link between auxin-induced root formation and RNS-mediated signaling and it argues against a mechanism that requires a change of transcriptional activity.

Fig. 1.3. Indole acetic acid (IAA) and Indole butyric acid

Another experimental tool to divide transcriptional and redox-based activities of auxin is the protein-degradation inhibitor Terfestatin A. Transcriptional auxin signaling pathways depend on TIR^{scf} complex-mediated degradation of transcriptional repressor proteins. Auxin-triggered degradation of the Aux/IAAs leads to the derepression of auxin response factors-mediated transcription. The F-box protein TIR1, which is part of the TIR^{scf} ubiquitin ligase complex, is an auxin receptor. Upon auxin binding TIR1 recruits specific transcriptional repressors (the Aux/IAA repressors) for ubiquitination by the proteasome complex. This marking process leads to specific gene expression in response to auxins.

Terfestatin A binds specifically the TIR^{scf} proteasome complex and deactivates this ubiquitination machinery and such preventing auxin specific changes of the gene repression (Yamazoe et *al.* 2005).

In this thesis work, the effects of IAA and IBA are compared in different plant model systems (*Zea mays* and *Arabidopsis thaliana*) using wild types and mutant plant lines. Particular emphasis is laid on the involvement of ROS/RNS in root growth and development, transcriptional activity and localization and transport of auxin.

1.3. Auxin influences the polarized tip-growth of root hairs

Root hairs are tip-growing tubular outgrowths emerging from specialized root epidermis cells known as trichoblasts (Dolan *et al.* 1993) and expanding locally at their apical dome (Schiefelbein, 2000). The development of the root hair cell can be divided into three stages: determination of hair and non-hair cellular identity in the rhizodermis (Schiefelbein 2000), initiation of hair outgrowth, and apical growth at the tip (Baluska *et al.* 2000).

Once initiated, the rapid tip-focused growth is maintained by a polarized cytoarchitecture and supported by cytoplasmic streaming directing secretory vesicles to the tip. The presence of internal gradients, the trans-membrane flux of ions, especially Ca^{2+}, and the tip-focused formation of ROS are all integral elements of tip growth. To facilitate these dynamic processes, the cytoskeleton of root hairs turns over rapidly, supporting a high rate of vesicle trafficking and polarized cytoarchitecture (Šamaj et *al*. 2004; Campagnoni and Blatt, 2007).

Root hair formation is regulated by phytohormone-based signaling pathways, especially those triggered by ethylene and auxin (Pitts et *al.* 1998; Rahman et *al.* 2002). Auxin transport provides vectorial information for the planar localization of hair outgrowth at the apical end of the trichoblasts, which are the ends facing the root tip. (Grebe 2004, Fischer et *al.* 2006) Once initiated, tip-focused growth of the hair bulge is based on a critical level of auxin in the trichoblast (Lee and Cho, 2006; Cho *et al.* 2008). Auxin export out of trichoblasts is driven by the PIN2 auxin efflux carrier (Blilou *et al.* 2005).

The conclusion that auxin levels in trichoblasts strongly influence root hair growth comes from the observation that trichoblast-specific over-expression of the serine/threonine kinase, PINOID, and the PIN3 efflux carrier resulted in increased auxin efflux from these cells, and root hair growth was inhibited due to a decrease of cellular auxin levels below the required threshold value (Lee and Cho, 2006). More recently, trichoblast-specific overexpression of three other efflux transporter (PIN2, PIN4, PGP4) was reported to block

root hair tip growth, but root hair tip-growth is restored by exogenously applied auxin (Lee and Cho, 2006; Cho *et al.* 2008). Altogether these observations implicate the existence of an auxin monitoring system in trichoblasts, which stops tip-growth, when the endogenous level of auxin drops below a critical level.

Several inhibitors are also able to stop tip growth of root hairs,. for example, Latrunculin B and Cytochalasin D, which disrupt filamentous actin (Baluška *et al.* 2001), or Wortmannin, which blocks the phosphoinositide signal pathways and interrupts endocytosis (Lam *et al.* 2007). Moreover the fungal metabolite, Hypaphorine inhibits root hair growth. This substance is made by the ectomycorrhiza fungus, *Pisolithus tinctorius* (Reboutier et *al.* 2002), to suppress root hair formation in its eucalyptus tree host.

Hypaphorine is an indolic compound, and as such a natural antagonist of IAA. It competes with auxin for auxin-binding proteins (Kawano et *al.* 2001) and prevents transcription of IAA-inducible genes (Reboutier et *al.* 2002). The stop of root hair growth is accompanied by a collapse of the tip-focused calcium gradient (Dauphin et *al.* 2007) and disturbances of the cytoskeleton of the root hair. External auxin rescues tip growth in these Hypaphorine-treated root hairs (Ditengou *et al.* 2003). It might be noted, that the Hypaphorine effect is host specific. Non host plants are only affected at concentrations of more than 100μM.

1.4. D'orenone as possible interactor of auxin actions.

The C_{18}-ketone D'orenone (Fig.1.4) has been postulated to be an early cleavage product of ß-carotene *en route* to trisporic acids; these act as morphogenetic factors during the sexual reproduction of zygomycetes (Gooday 1978, 1983; Gessler et *al.* 2002; Schachtschabel et *al.* 2005; Schachtschabel and Boland 2007).

An early report connecting the action of fungal apocarotenoids to that of auxin *in planta* described the inhibitory effect of trisporic acids on the auxin-induced elongation of coleoptiles of *Avena sativa* (Blaydes and Saus, 1978). This observation gave the inspiration to study the effect of trisporoids on root growth, focusing on early and late intermediates of the biosynthetic pathway to trisporic acids (Sutter *et al.,* 1996). The C_{18}-ketone (5*E*,7*E*)-6-methyl-8-(2,6,6–trimethylcyclohex-1-enyl) octa-5,7-die-2-one (D'orenone) significantly inhibits the

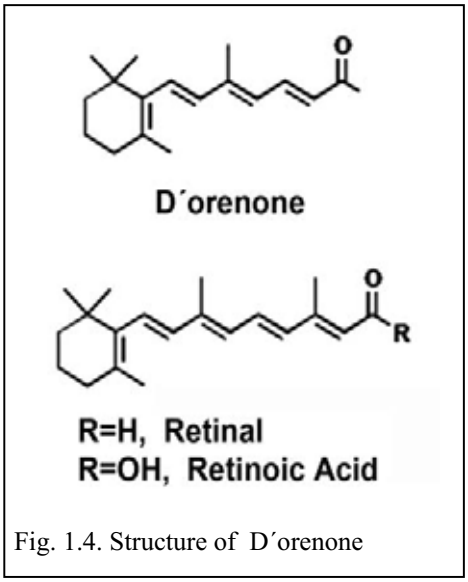

Fig. 1.4. Structure of D´orenone

polarized growth of root hairs at nanomolar concentrations (Schlicht et *al.* 2008). This effect could be monitored in different plant species. Significant parts of this study are based on the current thesis work and will be presented and discussed here in detail.

The third part of this work uses the D´orenone features described above to explore the role of auxin actions that underlie the sensory-driven root growth responses in general, and these will be compared with the processes controlling polarized tip-growth of root hairs.

2. Material and Methods

2.1. Plant material and inhibitor treatments

Maize grains (*Zea mays* L.) of wild type and *Semaphore1, lrt1, rum1* and *lrt1-rum1* mutants were soaked for 6 h and germinated in well moistened rolls of filter paper for 4 d in darkness at 20^{o}C. Young seedlings with straight primary roots, either 50-70 mm long (wildtype, *lrt1* and *rum1*), or 25-60 mm (of the slower growing *Semaphore1* and *lrt1-rum1*) were selected for inhibitor treatments and subsequent immunolabeling studies. For pharmacological experiments, root apices were submerged into appropriate solutions at room temperature. For Brefeldin A treatment, a 10^{-2} M stock solution (made in DMSO) was used and further diluted in distilled water to achieve effective working concentration of 10^{-4} M immediately before submerging root apices for 10min or 2h. Latrunculin B, NPA, TIBA, Flurenol, Chlorflurenol, Chlorflurenolmethyl and IAA were used at 10^{-5} M for 2h.

Seeds of wild type *Arabidopsis thaliana (ecotype Columbia), GFP lines* or mutants (see table 3.1.), were surface-sterilized and placed on the ½ strength MS culture medium (Murashige and Skoog, 1962) without vitamins and containing 1% sucrose (1.5% for ß-oxidation mutants and wild type controls) that was solidified by 0.8 % phytagel. Plates with seeds were stored at 4°C for 48 hours to break dormancy and then vertically mounted under continuous light for 3-4 days or in darkness for one week in the case of D´orenone treatments, because this inhibitor is sensitive to light.

For microscopy 3-4 day-old seedlings were transferred to microscopic slides that were modified into thin chambers made of cover-slips. Chambers were filled with the same liquid medium but without phytagel and placed in sterile glass cuvettes containing the medium at a level that reached the open lower end of the chambers. This allowed free exchange of medium to take place between chambers and the cuvette. Seedlings were grown in a vertical position under continuous light for up to 24 hours. During this period, the seedlings stabilized their root growth and generated new root hairs. Inhibitors and chemicals for treatments (retinal, retinol, retinoic acid, Wortmannin, Terfestatin A, IAA, IBA, Latrunculin B, NPA, TIBA, cPTIO, SNAP, D'orenone and analogues) were added to the ½ strength MS culture medium (Murashige and Skoog, 1962). D'orenone, D´orenol and 3,4-dihydro-D'orenone were synthesized as described previously (Schachtschabel and Boland, 2007). Terfestatin A was a gift H. Nozaki (described in Yamazoe et *al.* 2005). Unless stated otherwise, all chemicals were obtained from Boehringer-Mannheim (Germany), MBI Fermentas (USA), Merck (Germany), Roth (Germany) or Sigma (Munich, Germany).

GFP-transformed lines	
35s::GFP-FABD2	Visualizes f-actin; see Voigt et al. 2005a
35s::GFP-FYVE	Visualizes endosomes containing PI3P rich membranes; see Voigt et al. 2005b
35s::pts1-GFP	Visualizes a peroxisomal import signal; courtesy of B. Bartel
35s::mit-GFP	Visualizes a mitochondrial protein; see for example Logan and Leave 2000
PIN1p::PIN1-GFP	Visualizes PIN1 auxin efflux facilitator; courtesy of R. Chen
PIN2p::PIN2-GFP	Visualizes PIN2 auxin efflux facilitator; courtesy of R. Chen
DR5::GFP_{rev}	Visualizes an IAA inducible reporter construct; courtesy of J. Friml
GUS-transformed lines	
PIN2::GUS	Visualizes promoter activity of PIN2; courtesy of C. Luschnig
PIN2::PIN2-GUS	Visualizes putative PIN2 auxin efflux facilitator; courtesy of C. Luschnig
BA3::GUS	Visualizes an IAA inducible reporter construct; courtesy of Y. Oono
pro3DC::GUS	Visualizes an ABA and stress inducible reporter construct; courtesy of C. Rock
Arabidopsis mutants	
PLDζ2^{+}mutant	PLDζ2 gain of function mutant; courtesy of G. Li
PLDζ2^{-}mutant	PLDζ2 loss of function mutant; courtesy of G. Li
agr1-2	Mutant with strongly reduced PIN2 protein content; courtesy of R. Chen
eir1-4	Mutant with knocked out PIN2 protein; courtesy of C. Luschnig
pex5/7	IBA resistant mutant with peroxisomal defects; courtesy of B. Bartel
pex6	IBA resistant mutant with peroxisomal defects; courtesy of B. Bartel
pxa1	IBA resistant mutant with peroxisomal defects; courtesy of B. Bartel
ped1	IBA resistant mutant with peroxisomal defects; courtesy of B. Bartel
NOA1	Mutant with reduced ability to produce nitric oxide; courtesy of N.M. Crawford
Maize mutant	
lrt1	Mutant lacking lateral roots; courtesy of F. Hochholdinger
rum1	Mutant lacking lateral and crown roots; courtesy of F. Hochholdinger
lrt1-rum1	Mutant lacking lateral, adventious. and crown roots; courtesy of F. Hochholdinger
semaphore	Mutant lacking a negative regulator of KNOX1; courtesy of M. Scanlon

Table 2.1. List of mutants and transgenic lines used for this thesis

2.2. Stably transformed GUS and GFP-fusion protein expressing Arabidopsis lines

For description of *PIN2p::PIN2-GFP* see Shin *et al.* (2005) and for description *PIN1p::PIN1-GFP* see for example Vieten et *al.* (2005). The auxin response element $DR5_{rev}$-GFP line was used under the same conditions as described by Friml and coworkers (Friml et *al.* 2003). The *PIN2p::GUS* line

was characterized by Malenica et *al.* (2007) and Shin et *al.* (2005). *PIN2p::PIN2-GUS* line visualizing PIN2 protein in plant tissues was described by Sieberer et *al.* (2000).

For monitoring the actin cytoskeleton, the ABD2-GFP line was used. Endosomes and vesicles were visualized with the 2xFYVE-GFP line. Both were made and described by Voigt et *al.* 2005 (a, b). In vivo monitoring of peroxisomes and mitochondria were done with pts1-GFP and mit-GFP respectively (see Woodward and Bartel 2005b and Logan and Leave 2000 respectively).

2.3. Histochemical ß-Glucoronidase (GUS) staining

Seedlings of stably transformed promoter-GUS plants were stained for ß-Glucoronidase activity. Samples were vacuum infiltrated for 10 min with substrate solution (100 mM sodium phosphate buffer, pH 7.0, 10 mM EDTA, 0.1% Triton X-100, 0.5 mM potassium ferricyanide, 0.5 mM potassium ferrocyanide, and 1 mM 5-bromo-4-chloro-3-indolyl glucuronide) and incubated at 37°C for 2h up to 8h. The stained seedlings were cleared in absolute ethanol, passed through a graded ethanol series diluted with H_2O. The seedlings were kept in H_2O and transferred to microscope slides and mounted using an anti-fade mounting medium containing *p*-phenylenediamine. Roots were examined using a Leica MZ FL III binocular equipped with a CCD camera.

2.4. Indirect immunofluorescence labeling

Apical root segments (~7mm) encompassing the major growth zones were excised and placed in 3.7% formaldehyde in stabilizing buffer (SB; 50 mM PIPES, 5 mM $MgSO_4$ and 5 mM EGTA, pH 6.9) for 1 h at room temperature. Following a short (15min) rinse in SB, the root segments were dehydrated in a graded ethanol series diluted with phosphate buffered saline (PBS). Subsequently they were embedded in Steedman's wax and processed for immunofluorescence (for details see Baluška et *al.* 1997). To enable efficient penetration of antibodies, sections were dewaxed in absolute ethanol, passed through a graded ethanol series diluted with PBS, and then kept in PBS for 20 min. After that, sections were transferred to PBS containing 2% BSA for 15 min at room temperature and incubated with antibodies.

The following primary antibodies were used: Actin monoclonal antibody (actin-C4 clone from ICN) diluted 1:100, catalase monoclonal antibody (from Sigma) diluted 1:100, JIM5 monoclonal antibody (Baluška et *al.* 2002) diluted 1:20, anti-RGII polyclonal antibody (Baluška et *al.* 2002) diluted 1:100, anti-PIN1 polyclonal antibody (courtesy of K. Palme, Uni Freiburg) diluted 1:40, anti-IAA polyclonal antibody (courtesy of M. Strnad, Palacký University) diluted 1:20. All primary antibodies were diluted in PBS and buffers were supplemented with 1% BSA.

Sections were incubated in primary antibody for 1 h at room temperature. After rinsing in PBS, the sections were incubated for 1 h either with FITC/TRITC-conjugated anti-rat IgGs, anti-mouse IgGs or with anti-rabbit IgGs, each raised in goat and diluted 1:100 in appropriate buffer containing 1% BSA. A further rinse in PBS (10 min) preceded a 10 min treatment with 0.01% Toluidine Blue to diminished autofluorescence of root tissues. The sections were then mounted using an anti-fade mounting medium containing *p*-phenylenediamine (Baluška et al. 1997). Sections were examined with an Axiovert 405M inverted microscope (Zeiss, Oberkochen, Germany) equipped with epifluorescence and standard FITC/TRITC excitation and barrier filters.

2.5. Double immunofluorescence labelling:

After labelling of IAA with TRITC-conjugated anti-rabbit IgGs samples were postfixed for 45 min with 3.7% formaldehyde prepared in PBS, followed by a second blocking step with PBS containing 2% BSA for 15 min at room temperature. The subsequent labelling procedure followed the standard protocol.

2.6. Sucrose Density Gradient, Aqueous Two-Phase preparation, DRM-purification and Immunoblotting:

Root tissue was collected from 4d old treated or untreated plants (maize or arabidopsis) and ground in TE-buffer: 10 mM TRIS (pH 7.2), 1mM EDTA and 20% sucrose (w/v), 1 mM DTT and protease inhibitors in the form of "Compressed, EDTA-free" tablets (One tablet is recommended for the inhibition of proteases present in a maximum of 20 g of tissue extract.) at 4°C. 2-3 ml buffer were used were used per 1g fresh weight. All following steps were done on ice at 4°C. The homogenate was cleared by spinning at 2,500xg for 5 min. The pellet was discarded and the supernatant was separated into the cytosolic and microsomal fractions by centrifugation at 100,000xg for 45 min at 4°C. The cytosolic supernatant was discarded and the microsomal pellet was resuspended in 2ml TE-buffer for the sucrose density gradient centrifugation or in 330/5 buffer (330mM Sucrose, 5 mm potassium phosphate [pH 7.8]) for the two-phase separation.

2.6.1. Sucrose Density Gradient centrifugation:

A 20% to 60% sucrose step gradient was prepared in TE-buffer by layering five 2ml steps over each other (see also Dhonuske et *al.* 2006). The resuspended microsomal fraction was layed on top of the gradient and samples were centrifuged for 18 hours in a SW41 swinging bucket rotor at 35,000rpm at 4□C. After the run, twelve 1ml fractions were collected from the top of the gradient. The sucrose concentration in each fraction was determinded using a refractometer. In addition, the protein concentration of each fraction measured with the Bradford method.

2.6.2. Aqeous Two-Phase System:

The aqueous two-phase partitioning method was performed according to the batch procedure described by Larson et *al.* (1987). Phase separations were carried out in a series of 10-g phase systems with a final composition of 6.2% (w/w) dextran T500, 6.2% (w/w) polyethylene glycol 3350, 330mM sucrose, and 5 mm potassium phosphate (pH 7.8), 3mM KCl, and protease inhibitors. Three successive rounds of partitioning yielded final upper and lower phases. The combined upper phase was enriched in plasma membranes vesicles and the lower phase contained intracellular membranes. The final upper and lower phases were diluted 5- and 10-fold, respectively, in ice-cold Tris-HCl dilution buffer (10mm, pH 7.4) containing 0.25M sucrose, 3mM EDTA, 1mM DTT, 3.6mM l-Cystein, 0.1mM MgCl, and the protease inhibitors. The fractions were centrifuged at 100,000*g* for 60min. The pellets were then resuspended in TE buffer and used further or the protein content was measured after Bradford.

2.6.3. Separation of detergent soluble and insoluble components of the plasma membrane:

Samples were split and one half was treated with 1% Triton X-100 for 30 minutes on ice (4°C), the second half was sonicated without addition of Triton X-100. After treatment, samples were mixed with TE-buffer containing 60% sucrose (w/w) to yield a final sucrose concentration of 48%, 2ml were overlaid with a continuous sucrose gradient (15-45%) and centrifuged for 24 hours in a SW41 swinging bucket rotor at 35,000rpm at 4□C. Protein content was determined in the resulting low density Triton X-100 insoluble membrane fractions and the high density plasma membrane fractions.

2.6.4. Immunoblotting:

Membrane protein samples obtained from the previous step were precipitated with methanol and chloroform by mixing 500µl of a sample with 500µl MetOH and 125µl chloroform in an Eppendorf tube and vortexed. After a microfugation for 10min at 13.000 rpm and 4°C the upper phase of the resulting two-phased sample was discarded. Another 500µl MetOH was added to the lower phase and microfuged a second time for 10min at 13.000 rpm and 4°C. The resulting pellets was dried completely and resuspended in 1x SDS-PAGE sample buffer (final protein concentration of 1µg per µl). Each sample was loaded onto a 15% SDS-PAGE gel, electrophoretically separated and western blotted onto nitrocellulose.

All working steps of the immunoblotting procedure were carried out at room temperature. The nitrocellulose was washed in TBS buffer (10mM TRIS (pH 7.4), 150mM NaCl) and then blocked with 4% BSA in TBS for 1h. After five minutes washing in TBS the blots were incubated in the

primary antibody (1:1000 or 1:2000) in TBS for 1h, washed again three times in TBS with 0,05% Tween 20 (TTBS) and incubated in the secondary, alkaline phosphatase-conjugated antibody diluted at 1:10.000 in TBS. After incubation for 1 h blots were washed three times with TTBS. Positive bands were detected by the BCIP-NBT (Sigma Chemical) staining reaction. The staining reaction was stopped with 1% acetic acid in water.

2.7. Microscopic dye staining protocols

Staining of cytoplasmic calcium with Fluo3-AM: Loading of Ca^{2+}-sensitive Fluo3-AM in roots was carried out as described by Zhang et *al.* 1998.

Labeling with the endocytosis tracer FM4-64: Roots were incubated for 10 min with 5µM FM-dye at 4°C to slow down endocytosis and then washed before observation. To monitor the red fluorescent dye, 488 nm excitation and 620 nm or 710 nm emission filters were used.

Nitroblue tetrazolium staining of root hairs: To visualize the subcellular sites of superoxide production in root hair tips, staining was carried out as described by Carol et *al.* (2005).

2.8. Nitric oxide labelling and measurements in root apices

Detection of NO was achieved by the specific fluorescent probe 4,5- diamino-fluorescein diacetate (DAF-2 DA; Calbiochem, USA). Briefly, roots were incubated with 15µM DAF-2 DA for 30min and washed before observation. As a negative control a treatment with 10µM of the NO-scavenger cPTIO was included (see for example Correa-Aragunde et *al.* 2004).

2.8.1. Monitoring of nitric oxide accumulation in roots:

Roots were incubated in the dark for 30min. at 25°C in 10mM Tris HCl (pH 6.5) containing 10µM DAF-2DA added from a 10mM stock in DMSO (Sigma). Then the roots are washed three times in fresh buffer to remove excess fluorophore, mounted in buffer on microscope slides, and then examined immediately under a confocal laser scanning microscope (Leica TCS-4D). For the detection of the green fluorescing DAF-2 a 495nm excitation filter and a 515nm emission filter were used.

Dihydrorhodamine 123 is an uncharged and nonfluorescent peroxynitrite indicator that can passively diffuse across membranes, where it is oxidized to the cationic form of rhodamine 123, which exhibits green fluorescence (Szabó et *al.* 1995). Roots are incubated in the dark for 10min at 25°C in 10mM Tris HCl (pH 6.5) containing 10µM Dihydrorhodamine 123 and then examined with an Axiovert 405M inverted microscope equipped with epifluorescence and standard FITC excitation and barrier filters.

2.8.2. Semiquantitative measuring of nitric oxide in root extracts:

Roots were incubated in the dark for 30min at 25°C in 10mM Tris HCl (pH 6.5) containing 10µM 4,5-diaminofluorescein diacetate (DAF-2DA) added from a 10mM stock in DMSO (Sigma). The supernatant was captured in a 1ml cuvette for fluorimetric measurement and roots were frozen in liquid nitrogen, homogenized in 1ml buffer, incubated for 15min and spun down. The resulting supernatant was collected in a 1ml cuvette and measured with a fluorometer at 488nm excitation and 515nm emission.

2.9. ROS measurements of root extracts

2.9.1. Determination of O_2^- by measuring nitro blue tetrazolium (NBT) reducing activity:

Measurement of NBT (Sigma) reduction, a method used for the determination of O_2^-, was described by Doke (1983). About 3-5 roots were immersed in 3ml 0.01M potassium phosphate buffer (pH 7.8) containing 0.05% NBT and 10mM NaN_3 (Sigma) for 1h. After removing the roots the mixture was heated at 85°C for 15min and cooled. The NBT reducing activity of the roots was expressed as light absorbance at 580nm h^{-1} per 1g of fresh weight. The effect of SOD on the reduction of NBT by the roots was determined by adding SOD (100µg ml^{-1}) to the reaction solution from which NaN_3 was omitted. Results are shown as relative values.

2.9.2. Assay of hydrogen peroxide concentration:

Hydrogen peroxide was measured as described by Capaldi and Taylor (1983). Roots were ground in 5% trichloroacetic acid (TCA, 2.5ml per 0.5g root tissue) with 50mg activated charcoal at 0°C, and centrifuged for 10min at 15,000 x g. The supernatant was collected, titrated with 4N KOH to pH 3.6 and used for H_2O_2 assay. The reaction mixture contained 200µl of root extract, 100µl of 3.4 mM 3-methylbenzothiazoline (MBTH, Sigma). The reaction was initiated by adding 500µl of horseradish peroxidase solution (90 U per 100ml) in 0.2M sodium acetate (pH 3.6). Two minutes later 1400µl of 1N HCl was added. Absorbance was read out at 630nm after 15min. Results are shown as relative values.

2.9.3. Assay for the determination of hydroxyl radical secretion by root tissue:

Secreted hydroxyl radicals were measured by the method described by Tiedemann (1997). 2-Deoxyribose (DOR) (Sigma) was used as a scavenger and molecular probe for $HO^{\cdot}$ radicals. DOR was slightly sensitive to degradation by $HO^{\cdot}$ Radicals, which resulted in the accumulation of thiobarbituric acid-reactive degradation products. 5-10 roots were immersed in 1ml of 1mM DOR incubated at room temperature in the dark for 45min. Then 0.5ml of the incubated DOR solution was added to a preheated mixture of 0.5ml thiobarbituric acid (TBA)

(Sigma) 1% w/v in 0.005 M NaOH and 0.5ml trichloroacetic acid (TCA) (Sigma) 2.8% w/v, and immediately boiled for 10min. Absorbance was measured at 540nm. The results are given as absorbance units per g, of fresh weight and shown as relative values.

2.10. Enzyme activity assays

2.10.1. Assay of NADPH-oxidase activity:

The activity of NADPH-oxidase was assayed by its ability to reduce XTT (Sigma), following a modified protocol after Sagi and Fluhr (2001). The reaction mixture contained Tris-HCl buffer (pH 7.4), 100µm $CaCl_2$, 350µM XTT, and 20µl of plasma membrane enriched protein fractions (see chapter 2.8.2.). The reaction was started by the addition of 1mM NADPH and absorbance measurements at 470nm were performed every minute (Sagi and Fluhr 2001). XTT reduction was determined at 470 nm in the presence and absence of 50 units CuZn-SOD. The results are given as relative value (absorbance of sample with CuZn-SOD divided by sample without CuZn-SOD).

2.10.2. Preparation of enzyme extracts:

Root tissue of 0,5g was homogenized in 5ml of 50mM phosphate buffer pH 7,0 containing 1N NaCl, 1% PVP (Sigma) MW 40.000, 1mM ascorbate (Sigma) at 4°C. The supernatant was collected after a centrifugation at 15.000 x g for 15min.

2.10.3. Assay of SOD activity:

The activity of SOD was assayed by measuring its ability to inhibit the photochemical reduction of NBT using the method of Beauchamp and Fridovich (1971). The 3ml reaction mixture contained 50mM phosphate buffer (pH 7.8), 13mM methionine, 75µM NBT, 2µM riboflavin, 1mM EDTA and 20µl enzyme extract. Riboflavin was added last and the reaction was initiated by placing the tubes 30cm below a 15W fluorescent lamp. The reaction was started by switching on the light and was allowed to run for 10min. Switching off the light stopped the reaction and the tubes were covered with black cloth. Non-illuminated tubes served as control. The absorbance at 560nm was recorded. The volume of enzyme extract corresponding to 50% inhibition of the reaction is considered as one enzyme unit. Results are shown as relative values.

2.10.4. Assay of ascorbate peroxidase (APX) activity:

APX activity was determined spectrophotometrically by the decrease in absorbance at 265nm (ε=13,7 mM^{-1} cm^{-1}) using the method of Nakano and Asada (1981). The reaction mixture contained 50mM potassium phosphate buffer (pH 7.0), 5mM ascorbate, 0.5mM H_2O_2 and 20µl enzyme extract. The reaction was started by the addition of H_2O_2. The rates were corrected for

non-enzymatic oxidation of ascorbate by the inclusion of reaction mixture without enzyme extract. Enzyme activity is expressed in µmol ascorbate min^{-1}. Results are shown as relative values.

2.10.5. Assay of Catalase (CAT) activity:

CAT activity was determined by consumption of H_2O_2 using the method of Dhindsa et *al.* (1981). The reaction mixture contained 50mM potassium phosphate buffer 7.0, 16mM H_2O_2 and 20µl plant extract. The consumption of H_2O_2 was monitored spectrophotometrically at 240mm (ε=45,2 mM^{-1} cm^{-1}). Enzyme activity was calculated from the slope of the absorbance change over time (ΔA) divided by the molar absorption coefficient (ε) and expressed in µM H_2O_2 min^{-1}. Results are shown as relative values.

2.11. Measurement of the conversion of IBA to IAA

The conversion of IBA to IAA was measured by Prof. J. Ludwig-Müller (University Dresden) using a radiometric assay. Five weeks old plants were incubated with a [indole-$^{13}C_9$]-IBA (^{139}IBA) for 16 h. Duplicate measurements were performed on wild type, *ped1*, *pxa1* and *NOA1* plants.

Concentration of labeled IBA was calculated in the tissue as ng / mg fresh weight. For IAA determination a [indole-$^{13}C_6$]-IAA (^{136}-IAA) standard was added, because a ^{139}- labeled IAA was not available. This might cause a slight underestimation of the conversion of IBA to IAA in each sample.

2.12. RNA isolation and reverse transcriptase-PCR

Total RNA was isolated from the excised root of 7-d-old seedlings using RNeasy Plant Mini kit (Qiagen) and treated with on-column DNase digestion according to the manufacturer's instruction. The corresponding cDNAs were synthesized and amplified by the PCR using primers for the indicated genes as follows: *IAA1*, 5'-ggattacccggagcacaag and 5'-ggagctccgtccatactcac; *IAA19*, 5'-gagcatggatggtgtgccttat and 5'-ttcgcagttgtcaccatctttc; and *UBIQUITIN* (*UBI*), 5′-gatctttgccggaaaacaattggaggatggt and 5′-cgacttgtcattagaaagaaagagataacagg. The amplified products (*IAA1*, 208 bp after 24 cycles; *IAA19*, 141 bp after 27 cycles ; *UBI*, 206 bp after 25 cycles) were analyzed by 3% agarose gel electrophoresis.

2.13. Microscopy, Image Processing and Cytofluorimetric Measurement

Confocal microscopy was carried out with either a Leica TCS 4D or a Nikon Eclipse C1si Spectral Imaging Confocal Microscope. The Leica TCS 4D was equipped with an argon/krypton

mixed gas laser and excitation/emission filter combinations for FITC/GFP and TRITC/FM-dye detection. The Nikon Eclipse C1si Spectral Imaging Confocal Microscope acquires high resolution data over a spectral range of 400-750nm, in a single scan. Samples were examined using 40x oil immersion and 63x water-immersion objectives. The red fluorescent dye FM4-64 was excited by the 488 nm laser line and emission was filtered between 620 and 710 nm. Serial confocal optical sections were taken at different step sizes ranging from 0.5 to 2µm. Projections of serial confocal sections and final image processing were done with Adobe Photoshop 7.

For growth and curvature measurements seedlings were observed directly on the Petri dishes with a binocular (ICS Leica, Germany) using Discus imagesoftware (Carl H. Hilgers, Königswinter), or the Petri dishes were placed on a standard PC scanner. Analysis and measurements were made with the open source software Image-J (http://rsb.info.nih.gov/ij/).

3. Results:

3.1. Cellular basis of auxin efflux

3.1.1. Antibody-studies in *Zea mays*

3.1.1.1. Characterization of the IAA-specific antibody

A number of structurally related indoles and IAA metabolites may be present in plant tissues. Antibody specificity is, therefore, a crucial point in the immunocytochemical assay of IAA. The IAA-N1 antibody used in this thesis work was produced in M. Strnad´s lab and subsequent ELISA tests indicated that the antibody is specific (Data presented in Schlicht et *al.* 2006).

Several controls were performed in order to confirm the specificity of the IAA antibody at the level of immunolabelling: (1) labelling with the preimmune rabbit IgG instead of IAA antibody (data not shown), (2) labelling with the IAA antibody immunodepleted with an excess of IAA for 24 h (Fig. 3.1A), (3) labelling with the IAA antibody in the presence of an excess of NAA, IBA, and 2,4D, respectively, for 24 h (Figs. 3.1B-D), (4) labelling only with the anti-rabbit IgG, omitting the first antibody step (data not shown). Labellings with the IAA antibody of root apices treated with different concentrations of IAA showed an increase in the fluorescence signal corresponding with the increase in IAA concentration (Fig. 3.1E). All these cytological controls unequivocally confirmed the specificity of the IAA antibody, as documented already by our co-operation partner at the biochemical level (Schlicht et *al.* 2006).

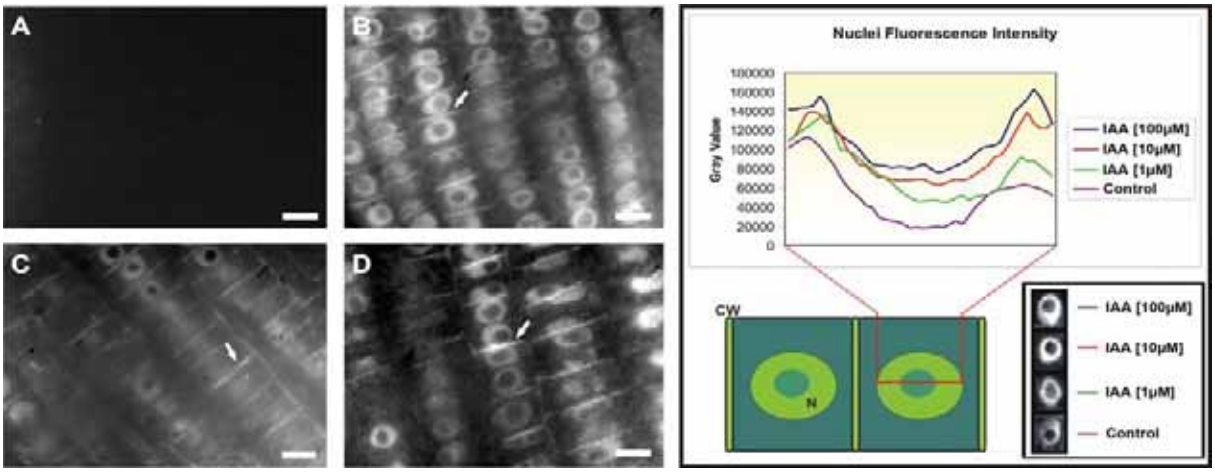

Figure 3.1. IAA labelings in maize root apices: antibody specificity.
A/ Labeling with the IAA antibody immunodepleted with an excess of IAA for 24 h.
B-D/ Labeling with the IAA antibody incubated with an excess of 2,4D (**B**), 1-NAA (**C**) or IBA (**D**) for 24 h. White arrows indicate auxin-enriched end-poles (cross walls).
E/ Comparison of the fluorescence intensities of transition zone cells after treatments with different IAA concentrations. average intensities of transition zone cells of 5 roots per treatment are represented. For the comparison, root sections labeled with the same antibody concentration were used. The images were recorded with the same exposure settings. (CW, cell wall; N, nucleus).
Bars: (B) 18 µM, (C) 12 µM, (D) 10 µM.

3.1.1.2. IAA immunolocalization in cells of control, BFA-, IAA-, and TIBA-treated maize root apices and *Arabidopsis thaliana* root apices

Untreated maize roots showed the most prominent signal in cells of the root apex, especially in the transition zone (Fig. 3.2A) and in the quiescent centre (Fig. 3.2B). In these cells, a prominent auxin signal was visible in the nuclei and at the polar cross-walls, (Fig. 3.2A, D, E), which mark the apical and basal end poles of the cells. In BFA-treated roots, IAA was still localized within nuclei while a slightly weaker signal was scored at the polar cross-walls (Figs. 3.2C, F, G). Additionally, BFA-induced compartments are enriched with auxin (Fig. 3.2G).

At higher magnification the signal at the cell end-poles was resolved as a cloud of closely apposed spots at which IAA co-localized with PIN1 (Fig. 3.3A). This co-localisation was obvious also in BFA-treated cells when endocytic BFA-induced compartments were positive for PIN1 (Fig. 3.3B), IAA, and recycling cell wall pectins recognized by the JIM5 antibody (Fig. 3.3C). In control roots, all cell end-poles in the transition zone were enriched with auxin while nuclei were also labelled (Fig. 3.4A). In TIBA treated roots, IAA was more enriched within nuclei while a strong signal was scored also in the cytoplasm and at some cross-walls (Fig. 3.4B). Exposure of root apices to external IAA resulted in an increased signal in the cytoplasm, and both nuclei and cell ends showed strong immunofluorescence (Fig. 3.4C). Importantly, BFA-treated wild type roots showed IAA-enriched BFA-induced endocytic compartments (Fig. 3.4D). These compartments were smaller in roots pretreated with TIBA and auxin (Figs. 3.4E, F).

The IAA-labelling patterns in Arabidopsis roots were slightly different than in maize root apices. All together the fluorescent signal was weaker and the nuclear labelling was less pronounced. Instead, stronger cytoplasmic signal with many spot-like structures were visible (Fig.3.5). Auxin transporting tissues of Arabidopsis roots showed signal at end poles like already in maize monitored (Fig.3.5B, C).

The labeling of IAA in Arabidopsis root tips revealed a maximum of fluorescence intensity in the root tip (Fig.3.5D), only weakly resembling the maximum of the well established DR5-construct (see also Fig.3.22 or 3.27). The cells of the quiecent center, surrounding of the apical meristem and the lateral root cap cells showed the strongest signal intensity (Fig. 3.5D) The behavior of this maximum in response to inhibitors is quite different to the DR5 signal. Terfestatin A, a inhibitor of auxin induced transcriptional activity, shifted the antibody detected maximum to the central root cap, but disposes DR5 signal at the root tip (Fig. 3.5E, compare with Fig. 3.27 or see Yamazoe et al. 2005). A treatment with auxin transport inhibitor NPA alleviated the maximum in the root cap and increased the meristematic located IAA, which is detected by the antibody (Fig. 3.5F). Consequently, an IAA treatment increased signal in the complete root tip (Fig. 3.5G).

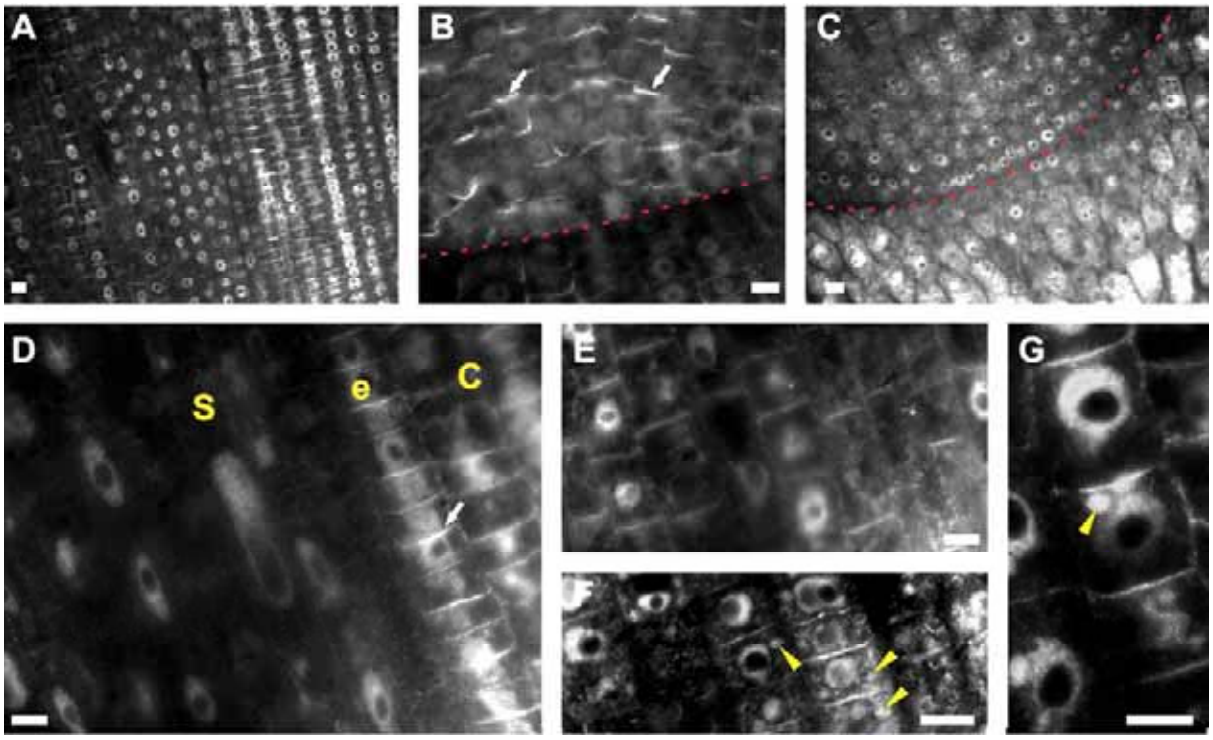

Figure 3.2. IAA labelings in maize root apices: sub-cellular and cellular distributions.
A, B, D and E/ In the untreated root, IAA enriched cross-walls (end-poles) are prominent in stele cells of the transition zone (**A**) and the whole quiescent centre (QC) (**B**).
C, F and G/ In BFA-treated root tips (2 h), IAA labeling of end-poles vanishes in the stele while the nuclear labeling gets more prominent. BFA treatment shifts IAA signal into BFA-induced compartments.
D/ In cells of the cortex, intensity of the cross-wall labeling gets weaker while labeling of nuclei increases. Yellow arrowheads point on auxin-enriched BFA-induced compartments.
Red Line in (**B**) and (**C**) marks the border between meristem and root cap. (S, stele; e, endodermis; C, cortex) Bars: 10 μM.

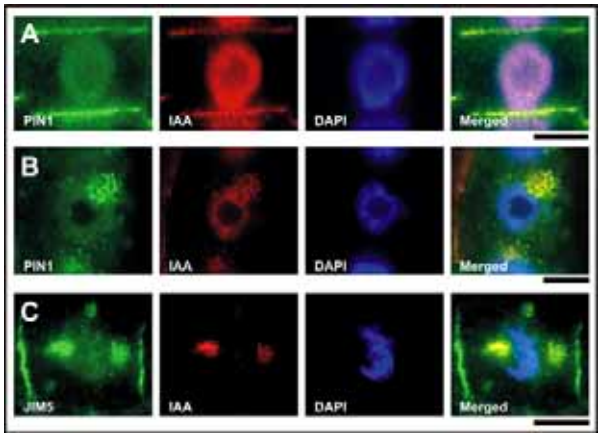

Figure 3.3.
PIN1-IAA colocalization in control and BFA-treated root apices.
A/ In untreated roots, co-localization of PIN1 with IAA in distinct patches at the end-poles is obvious.
B and C/ After 2 h of BFA exposure, PIN1, IAA, and JIM5-positive cell wall pectins co-localize in patch-like structures within endocytic BFA-induced compartments. Bars: 10 μM.

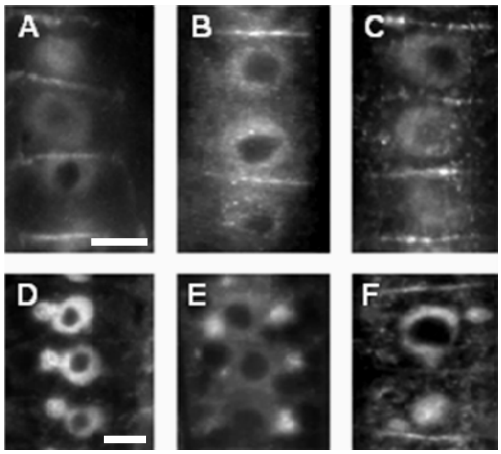

Figure 3.4.
IAA labelings at the end-poles and within nuclei.
A/ Control. **B**/ 2 hrs of TIBA-treatment.
C/ 2 hrs of IAA-treatment. **D**/ Wild-type after 2 hrs of BFA treatment. **E**/ 2 hrs of TIBA followed by 2 hrs of BFA treatment. **F**/ 2 hrs of IAA followed by 2 hrs of BFA treatment. Bars: (**A–C**) and (**F**) 10 μM; (**D and E**) 8 μM.

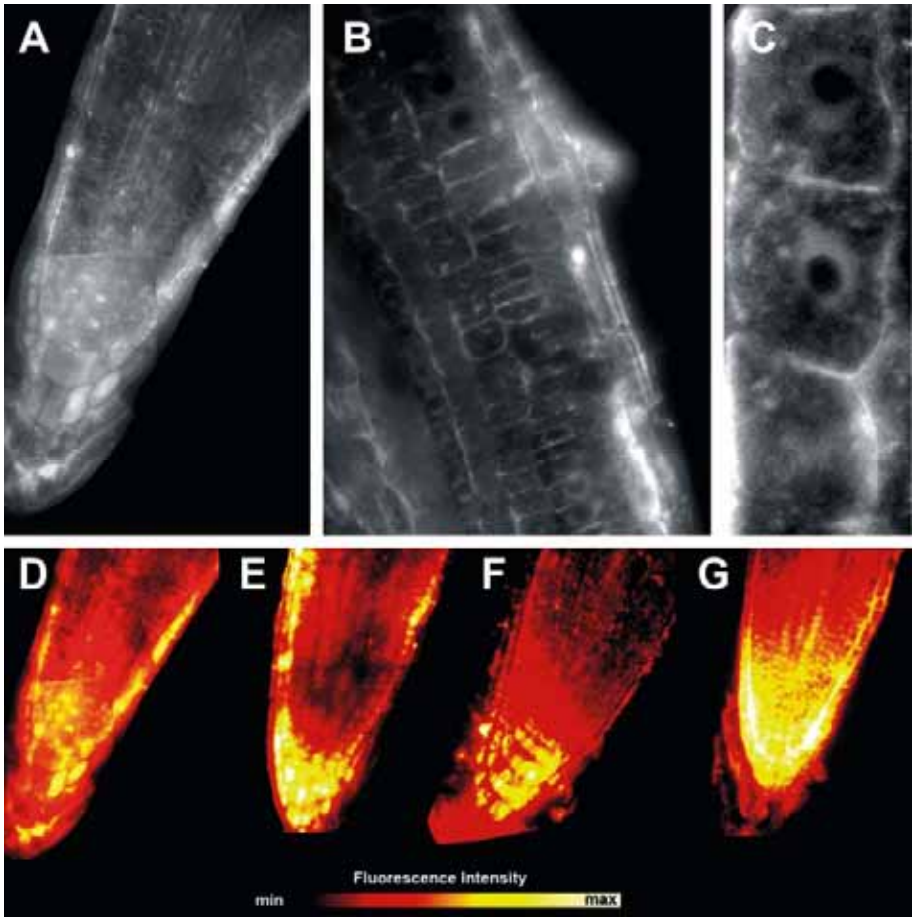

Figure 3.5.
IAA labelings in *Arabidopsis thaliana* root apices
A/ Overview of the root tip. Prominent signal in the root cap and quiescent center and striking weak signal in columnella cells. Note: Figure A is composed of several microscopic pictures.
B/ Rhizodermis, outer cortex and lateral root cap cells show antibody signal mainly at cross walls.
C/Endodermal cells show signal at polar cross walls, cytoplasma and nuclei, but prominent spot like structures are also visible in the cells.
D-G: Intensity of IAA labelings in *Arabidopsis thaliana* root apices
D/ Overview of the root tip. Visualization of fluorescence intensity shows an auxin-maximum quite similar to the known auxin signaling maximum of the DR5-reporter.
E/ Overview of a Terfestatin A (2h with 10µM) treated root tip. No visible quenching effect on the IAA maximum but a distinct shift to the central root cap.
F/ Overview of a NPA (2h with 10µM) treated root tip shows an alleviated IAA tip maximum in the root cap and an increase in the meristem.
G/ Overview of IAA (2h with 1µM) treated root shows elevated intensity of the IAA labelling at the root tip maximum.

3.1.1.3. **BFA treatment shifts PIN1 from the plasma membrane into endosomes**

PIN proteins are showing rapid vesicle recycling. A maize specific PIN1 antibody was used, which was tested on western blots. The maize antibody showed one specific band around 70kDA (Fig. 3.6F). Immunofluorescent labelings with the maize PIN1 antibody showed, that after 2 h TIBA and after 10 min BFA treatments, when auxin transport was inhibited, PIN1 protein was almost exclusively located at the plasma membrane of the apical cell end pole Figs. 3.6A-D). Only after 2h duration of BFA-treatment the PIN1 signal was shifted into the BFA-induced compartments (Fig. 3.6E). TIBA pretreatment prevented this accumulation of PIN1 within the endocytic BFA-induced compartments (Figs. 3.6C). Biochemical analysis using sucrose density gradients and aqueous two-phase system also showed that PIN1 was strongly present at the plasma membrane after the 10 minutes BFA treatment. However, after two hours of BFA treatment, a shift from the PM protein fractions into endosomal protein fractions took place (Fig. 3.6F,G). This shift can be prevented by TIBA and IAA pre-treatments, which are known to inhibit the endocytosis of PIN1 in *Arabidopsis* root cells (Katekaar and Geissler 1980; Geldner et *al.* 2001).

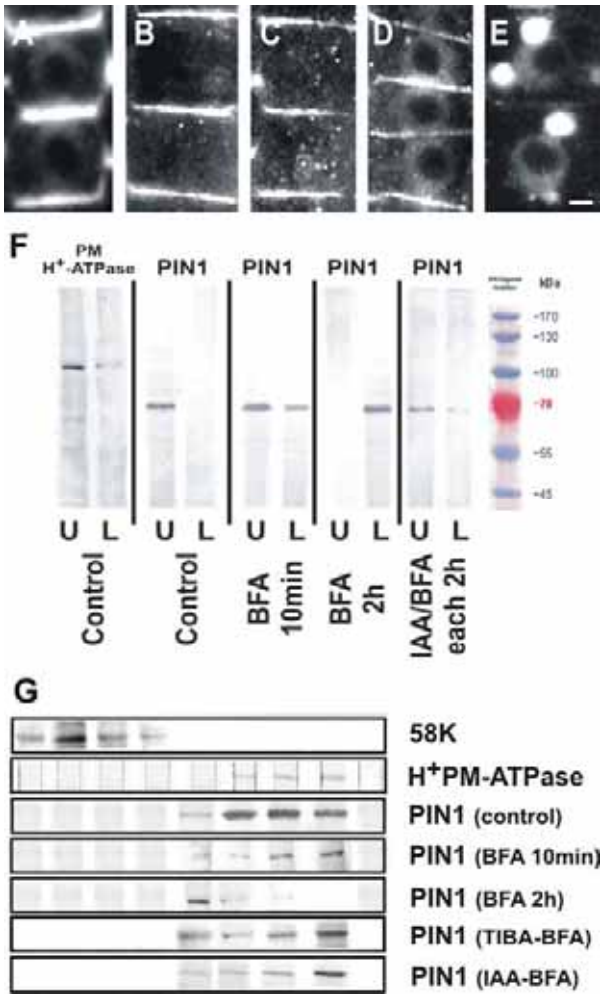

Figure 3.6. PIN1 antibody
A-E/ PIN1 localization in cells of the transition zone in wild type roots
Control, untreated (**A**), 2 hours of TIBA treatment (**B**), TIBA/BFA treatments combined, 2 hours of TIBA followed by 2 hours of BFA (**C**), BFA-treatment for ten minutes (**D**), BFA-treatment for 2 hours (**E**); Bars: 10 μM.
F/ Aqueous Two-Phase System reveals that BFA induces shift of PIN1 from the plasma membrane-enriched upper phase (U) into the endomembrane enriched lower phase (L). Pretreatment with IAA inhibits this BFA-induced shift.
G/ Sucrose density gradient analysis of PIN1 localization reveals that BFA induces shift of PIN1 from the plasma membrane into the endosomal fractions, but not to the Golgi apparatus fractions. Pretreatment with TIBA and IAA inhibits this BFA-induced shift. Comparison of treatments with fractions of matchable sucrose density. Sucrose density of fractions increases from left to right.
58K is cis-golgi marker and serves as example of lower density fractions of the gradient

3.1.1.4. **BFA and different PAT inhibitors deplete F-actin from polar cell ends**

BFA had an obvious effect on the actin cytoskeleton of the root apex cells Instead of a strong and continuous labeling of the actin filament bundles and a strong labeling of the end-poles, the fluorescent label became sketchy along the bundles and weakened at the cell ends indicating a partial disruption and break down of the actin cytoskeleton (Figs. 3.7A, B; see also Paciorek and Friml 2006).

In fact, all PAT inhibitors tested in this study, as well as Latrunculin B, depleted F-actin at the cell end poles and more or less disintegrated the F-actin cables interconnecting the opposite end poles of the cells (Figs. 3.7A-H). Moreover, all inhibitors induced a shift in the positioning of the nuclei towards the basal cell pole (Figs. 3.7B-G). Latrunculin B induced a conspicuous accumulation of G-actin within the nuclei (Fig. 3.7H) which is a phenomenon not further addressed in this study.

To monitor effects of the auxin transport inhibitors and Latrunculin B on recycling of vesicles an immunofluorescence labeling of cell wall pectins was performed, because pectins recycle between the cell wall and the endosomes (Baluska et *al.* 2005). After BFA-treatment pectin was located within the BFA-induced endocytic compartments, thus showing the same behavior as PIN1 (Fig. 3.8). The size of these compartments reflects the recycling rate of cell wall pectins. The data revealed that two hours of pre-treatment with latrunculin B (Fig. 3.7F), as well as with all PAT inhibitors tested, resulted in smaller BFA-induced compartments than those scored after BFA treatment alone (Figs. 3.8G, H, L, M, N).

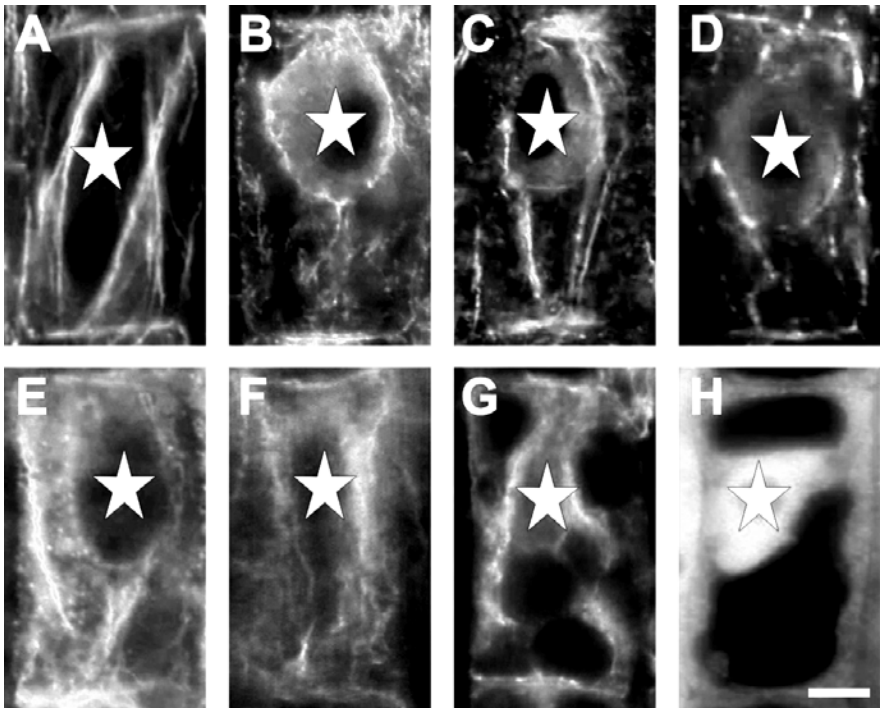

Figure 3.7.
F-Actin arrangements in cells of the transition zone.
A/ Control. **B**/ BFA treatment. **C**/ TIBA treatment. **D**/ NPA treatment. **E**/Flurenol treatment. **F**/ Chlorflurenol treatment. **G**/ Chlorflurenolmethyl treatment. **H**/ Latrunculin B treatment. Note the depletion of F-actin from end-poles and disintegration of F-actin cables while nuclei are shifted from their original central position towards the basal cell pole. Bar: 8 μM.

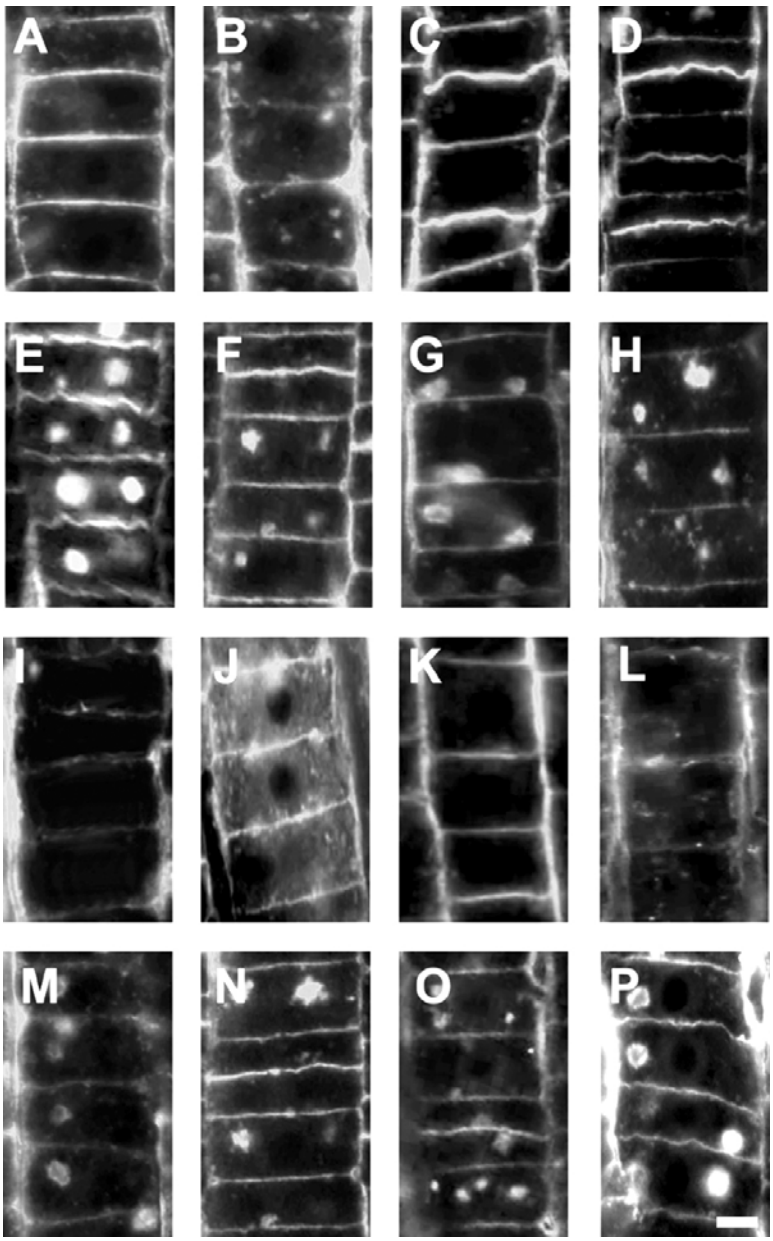

Figure 3.8. Labeling of the recycling pectin RGII in cells of the transition zone.
A/ Control wild-type roots. **B**/ Latrunculin B-treated roots. **C**/ TIBA-treated roots. **D**/NPA-treated roots. **E**/BFA-treated roots. **F**/ Latrunculin B/BFA-treated roots. **G**/ TIBA/BFA-treated roots. **H**/ NPA/BFA-treated roots. **I**/Flurenol-treated roots. **J**/ Chlorflurenol-treated roots. **K**/ Chlorflurenolmethyl- treated roots. **L**/ Aluminium-treated roots. **M**/ Flurenol/BFA-treated roots. **N**/ Chlorflurenol/BFA-treated roots. **O**/ Chlorflurenolmethyl/ BFA-treated roots. **P**/ Aluminium/BFA-treated roots.
Note that BFA-induced compartments are smaller in cells of roots pretreated with PAT inhibitors. All treatments were done for two hours, the combined treatments consisted of two hours of PAT inhibitors followed by two hours of BFA. Bar: 8 μM.

3.1.1.5. **Immunolabeling in maize mutants with auxin related phenotype**

The maize mutant *semaphore1* is impaired in the negative regulation of KNOX1-genes and is characterized by reduced PAT which is the reason for the pleiotropic phenotype of this mutant (Scanlon et *al.* 2002). The *rum1* mutant is deficient in the initiation of seminal and lateral roots from the primary root (Woll et *al.* 2005) and shows strongly reduced polar auxin transport capacities. The *lrt1* mutant (Hochholdinger and Feix 1998) which shares some phenotypical similarities with *rum1*, including the missing initiation of lateral roots, has wild type like PAT rates (Santelia et *al.* 2005). The double mutant *rum1-lrt1* shows a novel phenotype and has reduced PAT just like *rum1* (Woll et *al.* 2005). Immunofluorescent labeling revealed that the polarized root cell organization of mutants with reduced PAT is strongly disturbed.

The actin cytoskeleton in transition zone cells of *semaphore1* (Fig. 3.9F), *rum1* (Fig. 3.9P) and *rum1-lrt1* (Fig. 3.9U) mutants showed changes which have strong similarity to those observed after treatments with diverse PAT inhibitors (see Fig. 3.7). Moreover, auxin failed to accumulate at the cross-walls in those mutants (Fig. 3.9G, Q, V). The *lrt1* mutant showed neither significant disturbances of the actin cytoskeleton nor a reduced IAA-labeling (Fig. 3.9K, L). Exposure of *semaphore1* roots to BFA revealed that mutant cells had smaller BFA-induced compartments indicating decreased vesicular recycling rates (Fig. 3.9J). Moreover, BFA-treated cells of *rum1* and *lrt1 / rum1* double mutants completely lacked any BFA-induced compartments (Figs. 3.9T, Y).

In conclusions, disturbances of vesicle recycling, irrespective of whether this is induced by inhibition of polarized secretion by BFA or by PAT inhibitors, appear to be a consequence of the disintegration and depletion of the actin cytoskeleton at the polar cross walls.

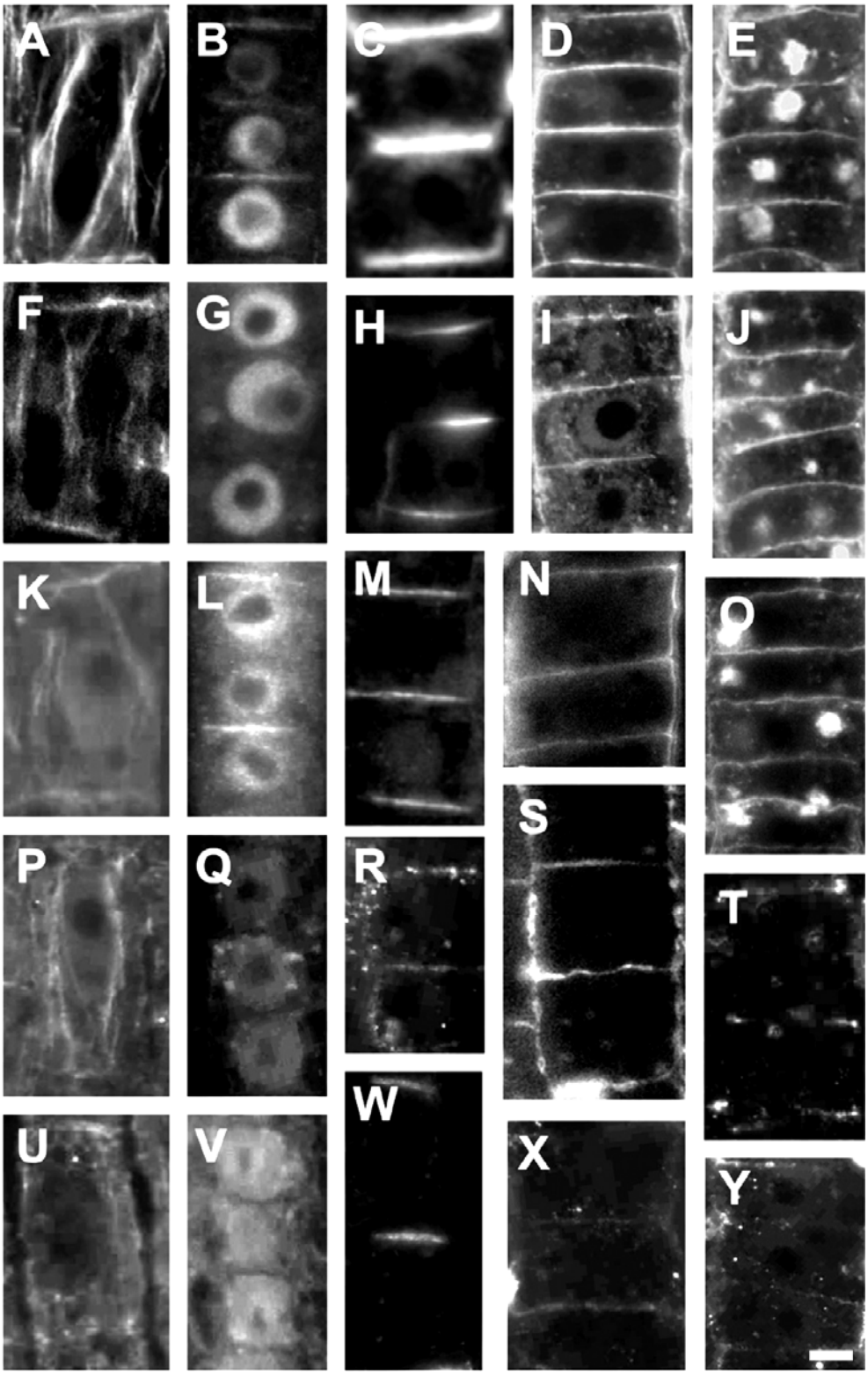

Figure 3.9
Actin, IAA, PIN1, and RGII labelings in root apices of wild-type and maize mutants.
Actin (**A, F, K, P, U**), IAA (**B, G, L, Q, V**), PIN1 (**C, H, M, R, W**), and RGII (**D, I, N, S, X**) and RGII after two hours of BFA-treatment (**E, J, O, T, Y**) labelings in stele periphery cells of the transition zone the wild-type (A–E), *semaphore1* (F–-J), *lrt1* (K–O), *rum1* (P–T), and *lrt1/rum1*(U–Y) mutants. Note the depletion of F-actin and IAA from the cellular end-poles, which is correlated with small size of BFA-induced compartments (E, J, O, T, Y) but PIN1 shows still a signal on the end-poles. The only exception is the *lrt1* mutant which is, in contrast to all other mutants, also not affected in PAT. Bars: A, C, F, K, N, P, S, U and X, 8 μM; B, D, E, G, H, I, J, L, M, O, Q, R, T, V,W and Y, 10 μM.

3.1.2. Phospholipase D affects the auxin signaling maximum of DR5 in root apices

Phosphatidic acid (PA) generated via PLD activity is essential for the positioning of the DR5-typical auxin signaling maximum at the distal portion of the root apex transition zone, which is the most active part of the whole plant body with respect to polar auxin transport. DR5::GFP transgenic lines (Fig. 3.10) show a maximum of auxin induced gene activity at the root tip and this maximum was increased after treatment with PA (Fig. 3.10C), whereas it disappeared after the inhibition of PLD with 0.4% 1-butanol (Fig. 3.10D). 0.4% of tert-butanol, which cannot inhibit PLD activity, has no effect on DR5 expression (Fig. 3.10E). Noteworthy, the PLD inhibitor 1-butanol and the PLD product PA were canceling each other with respect to DR5::GFP activation (Fig. 3.10F).

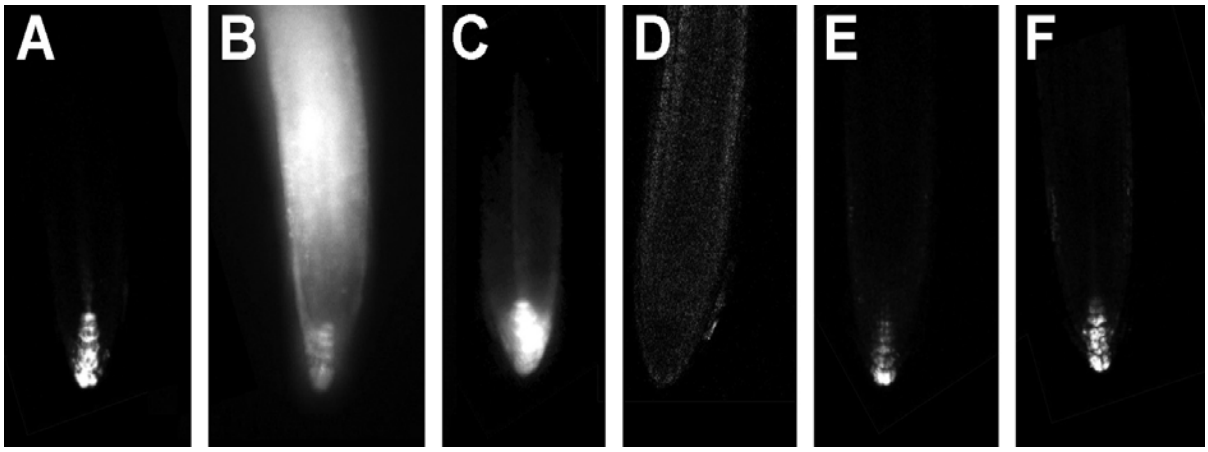

Figure 3.10
DR5::GFP$_{rev}$ expression in root apices
Treatments of 4 hours are sufficient to show the effect of PLD activity on IAA signaling in root tips.
A/ untreated Control. B/ IAA treatment (1µM). C/ Phosphatidic acid treatment (10µM). D/ 1-butanol treatment (0.4%). E/ tert-butanol treatment(0.4%). F/ Double treatment of phosphatidic acid (10µM) and 1-butanol (0.4%)

3.1.3. Phospholipase D activiy targets recycling and not localization of PIN1-GFP

Loss of Phospholipase D function either by mutation or by 1-butanol treatment leads to reduced auxin transport (Li et al. 2007). Treatment with PA (Fig. 3.11B) or 1-butanol (Fig. 3.11C, D) had no effect on PIN1 localization. 1-butanol inhibits PLD action and depresses endocytosis. PA, the signaling product of PLD activity, strongly increases endocytosis (Li et al. 2007). Interestingly, both chemicals reduce BFA-compartment formation (Fig. 3.11F, G). The size of the BFA-induced compartments reflects the recycling rate of PIN1. This indicates that PA not only increases endocytosis but stimulates exocytosis. Therefore, altering PLD activity modifies auxin transport rates by changing PIN recycling.

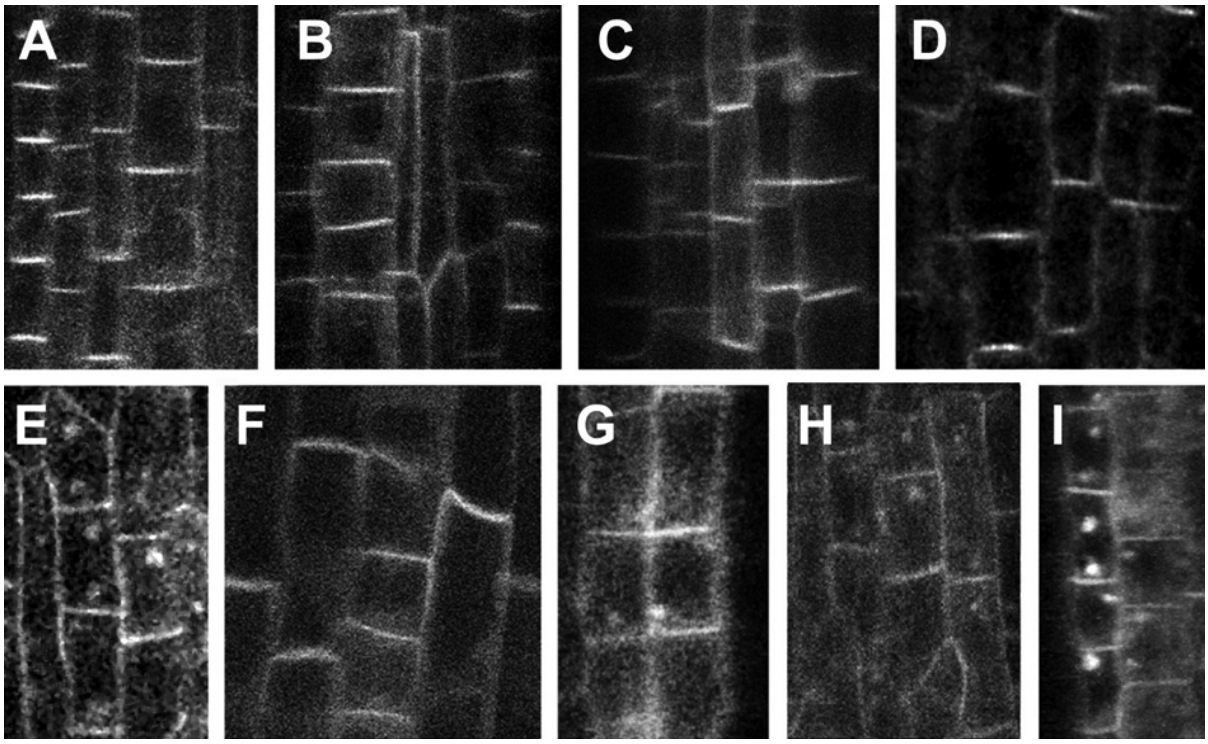

Figure 3.11.
PIN1-GFP recycling rate and not localization is dependent from PLD activity
A/ In untreated control roots PIN1-GFP is localized at the apical plasma membrane. **B/** Phosphatidic acid treatment (10µM) for 1h shows no visible effect on the PIN1-GFP localization. **C/** 1-butanol treatment (0, 4%) for 1h shows no visible effect on the PIN1-GFP localization. **D/** t-Butanol treatment (0,4%) for 1h shows no visible effect on the PIN1-GFP localization. **E/** Treatment with BFA (35µM) for 30min induces PIN1-GFP positive BFA-compartments. **F/** Treatment with phosphatidic acid (10µM) for 1h followed by a BFA treatment (35µM) for 30min. The phosphatidic acid pretreatment prevents formation of BFA-induced compartments.
G/ Treatment with 1-butanol (0, 4%) for 1h followed by a BFA treatment (35µM) for 30min. The pretreatment prevents formation of BFA-induced compartments. **H/** Treatment with tert-Butanol (0, 4%) for 1h followed by a BFA treatment (35µM) for 30min. The pretreatment shows no visible effect on the BFA-induced compartments. **I/** Double treatment with phosphatidic acid (10µM) & 1-butanol (0, 4%) for 1h followed by a BFA treatment (35µM) for 30min. Simultaneous applied pretreatments do not disturb the formation of BFA-induced compartments.

3.1.4. PIN proteins are enriched in detergent resistant fractions of the plasma membrane

The distinct localization of PINs at polar domains of the plasma membrane, i.e., membranes of the end poles, points to the operation of a polar sorting mechanism.

In order to address the nature of the sorting mechanism that directs PINs to polar membrane domains and to determine if PIN proteins are preferentially associated with lipid rafts, the plasma membrane of root apex tissue was analyzed. Triton X-100 treatment at 4°C of purified plasma membranes yielded a detergent resistant membrane fraction (DRM), which should contain lipid raft components and a detergent soluble fraction, which should contain the remainder of the plasma membrane. Testing immunoblots with antibodies directed against PINs1-4 showed that all four PINs were retrieved from the DRM fraction (Fig. 3.12) and hence are lipid raft components. However, only PIN1 and PIN2 were as tightly associated with the DRM as the genuine DRM-marker H^+ PM-ATPase, whereas PIN3 and PIN4 show only a slight enrichment in the DRM fraction.

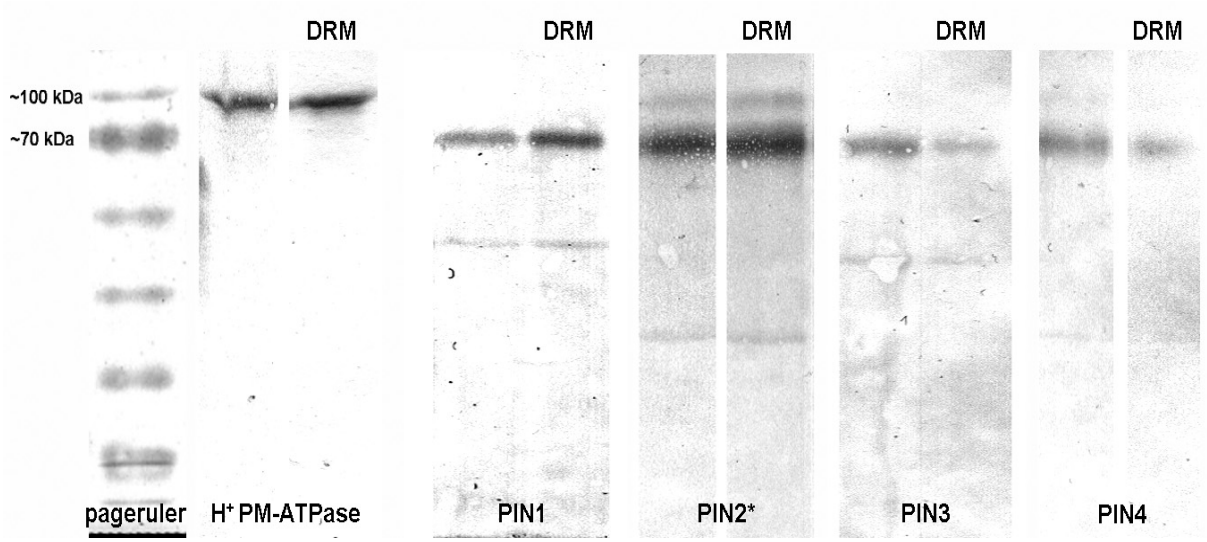

Fig. 3.12.
PIN proteins are enriched in detergent resistant membranes
Detergent resistant parts (DRM, right lanes) and complete fractions (left lanes) of enriched plasma membrane extracts of root apices (first cm of root tip from 100-200 roots per antibody) from Arabidopsis wild type and the PIN2::PIN2-GFP transgenic line were compared. All lanes were loaded with 15µg of protein content.

3.2. D'orenone blocks polarized tip-growth of root hairs, modifies root architecture and interacts with auxin actions

3.2.1. D'orenone blocks tip-growth of root hairs but stimulates root system density

Root hair tip-growth depends on the intracellular concentration of Auxin. From the following experiments it is concluded that the apocarotene inhibitor D'orenone interacts with this process. D´orenone rapidly blocked tip-growth of root hairs. This effect started at nanomolar levels (400 nM) and involved not only the rapid inhibition of polarized tip-growth of existing root hairs and but also the formation of new root hairs. Higher concentrations (4-400 µM) completely stopped root hair growth (Fig. 3.13A & B) without negatively affecting growth of the primary root in the range of 1-40 µM (see below). At higher concentrations, however, the density of lateral roots was slightly increased.

Of all tested compounds (Fig. 3.13), only D'orenone was effective at concentrations as low as 400 nM. Other apocarotenoids, such as all-trans retinal or all-trans retinoic acid, were much less active or not active at all. For example, retinal (4 µM) affected the relative growth rate of root hairs but required a ten-fold higher concentration to achieve an effect comparable to that of D'orenone (Fig. 3.13A). Lower concentrations of retinoic acid (1-4 µM), a bioactive signal molecule in animal systems (Chambon, 1996; Liou et *al.* 2005), had no visible effect on the growth of root hairs (data not shown). The activity of D'orenone decreased, when the conjugation of the double bond with the keto group was abolished by reducing the

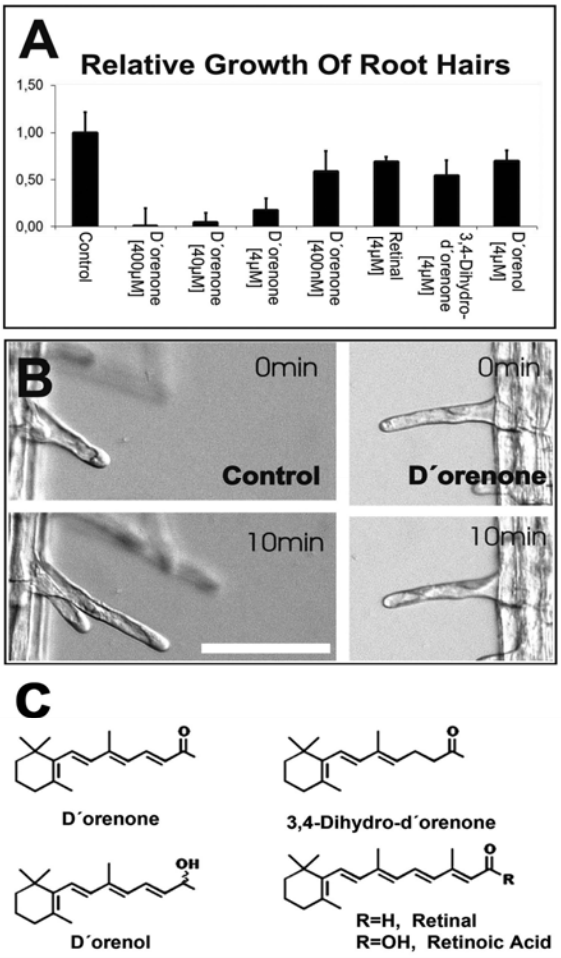

Fig. 3.13. D'orenone blocks tip-growth of root hairs but stimulates root system density.
A/ Relative growth rates of root hairs during short time treatments with different concentrations of D'orenone. (Means of five different plants from the first 30 min). Treatments with retinal, D´orenol and 3, 4-Dihydro-d´orenone along the same protocol show weaker effects than treatment with D'orenone.
B/ Comparison of bright field pictures from a DMSO mock-treated root hair and a root hair treated with D'orenone (10 µM). Note prominent cytoplasmic cap at the tip of the fast growing control root hair. Bar = 100 µm.
C/ Chemical structure of D´orenone and its analogues.

C(3)=C(4) double bond of the side chain (Schachtschabel and Boland, 2007). Activity also decreased upon reduction of the keto group to an alcohol. Both, the resulting 3,4-dihydro-conformation and the hydroxy-derivative of D'orenone displayed only weak inhibitory activity when tested on growing root hairs (Fig. 3.13A). Thus, already minor changes in the stereochemistry and polarity of the molecule are sufficient to reduce its biological activity.

At concentrations higher than 5 µM, D'orenone also transiently affected the root gravity responses of *Arabidopsis thaliana*. Although roots responded to gravistimulation in the presence of D´orenone, careful analysis revealed that consecutive gravistimulations caused subtle disturbances (Fig. 3.14B). For instance, after the third rotation of root apices relative to the gravity vector, a reduction of gravity-oriented growth response was monitored only in the D'orenone-treated root apices (Fig. 3.14D). Moreover, D'orenone rescues the root agravitropic phenotype of a PIN2 mutant with reduced PIN2-protein level but fails to completely stop root hair tip growth in this mutant (see below). D'orenone also promoted root system complexity by increasing the lateral root density (Fig. 3.22C).

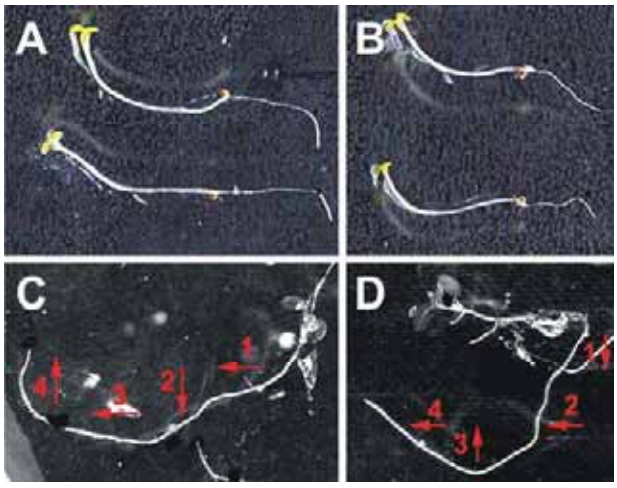

Fig. 3.14.
Gravistimulated roots during D´orenone treatment still perceive direction of gravity, but the growth behaviour shows a reduced sensitivity of the root. Repetitions of gravistimulation from different directions reveal the reduced answer to the gravity signal.

A/ 90° gravistimulated seedlings on ½ MS Medium mock treated with added DMSO as solvent.
B/ 90° gravistimulated seedlings on ½ MS Medium treated with added 1µM D´orenone dissolved in DMSO
C/ Multiple gravistimulated seedlings on ½ MS Medium mock treated with added DMSO as solvent.
D/ Multiple gravistimulated seedlings on ½ MS Medium mock treated with added 1µM D´orenone dissolved in DMSO.
Arrows indicate direction of gravity vector. Numbers count the repetition of gravity direction change.

3.2.2. Effects of D'orenone on cytoarchitecture, F-actin, ROS, calcium and endosome gradients

Treatment with 10 µM D'orenone led to a rapid disintegration of the F-actin- and vesicle-rich 'clear zone' at the tip of root hairs, and at the same time tip growth was inhibited. Dynamic vacuoles protruded up to the very tips of the root hairs after exposure to 10 µM D'orenone (Fig. 3.15). Experiments with FABD2-GFP plants (Voigt et *al.* 2005a) revealed that after about 15 minutes of exposure to D´orenone, the F-actin meshwork at the tip disintegrated. Only some longitudinal F-

actin cables, connecting to the root hair base, remained (Fig. 3.15). Higher concentrations (>10 µM) did not result in faster or stronger effects. Exposure to lower concentrations of D'orenone caused the same effects, however, it required more time - up to 40 min (data not shown).

ROS forms a tip focused gradient in the root hair due to the activity of NADPH-oxidase and this is an essential precondition for polarized tip growth (Foreman et *al.* 2003; Rentel et *al.* 1994; Carol et *al.* 2005). Labelling with the $O_2^{\cdot-}$-sensitive dye NBT revealed that treatment with D'orenone blocks the formation of the tip-focused ROS gradient (Fig. 3.16A). However, the ability of plasma membrane resident NADPH-oxidase to produce ROS is not instantaneously blocked. The enzymatic activity of NADPH-oxidase decreased only after treatment with D´orenone for more than 30 minutes (Fig. 3.16C). This delay indicates that the NADPH-oxidase is not a primary target of D´orenone action.

Loading the roots with the cell-permeable Ca^{2+} dye Fluo3-AM revealed, that D'orenone also eliminated the tip-focused Ca^{2+}-gradient (Fig. 3.16B) and finally, the apical accumulation of endosomes made visible in the 2xFYVE-GFP transgenic line was also lost (Ovecka et *al.* 2005; Voigt et *al.* 2005b) after D'orenone treatment (Fig. 3.17).

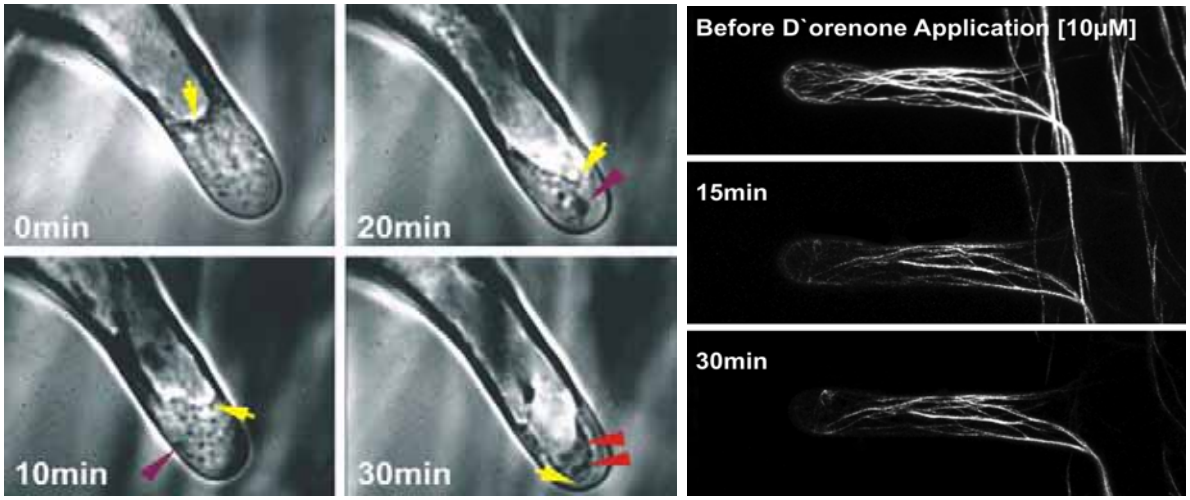

Fig. 3.15.
Left/ Dynamic vacuoles protrude as far as the very tips of the growth ceasing root hair after exposure to D'orenone at 40 µM. Yellow arrows mark the tonoplast;
Purple arrowheads mark enlarged endosomes, which are often inside of vacuoles (red arrowheads).
Right/ Effect of D'orenone (10 µM) on FABD2-GFP-labelled actin bundles in growing root hair. The F-actin meshwork at the tip disintegrated and only some longitudinal F-actin cables, originally from the hair base, remain preserved.

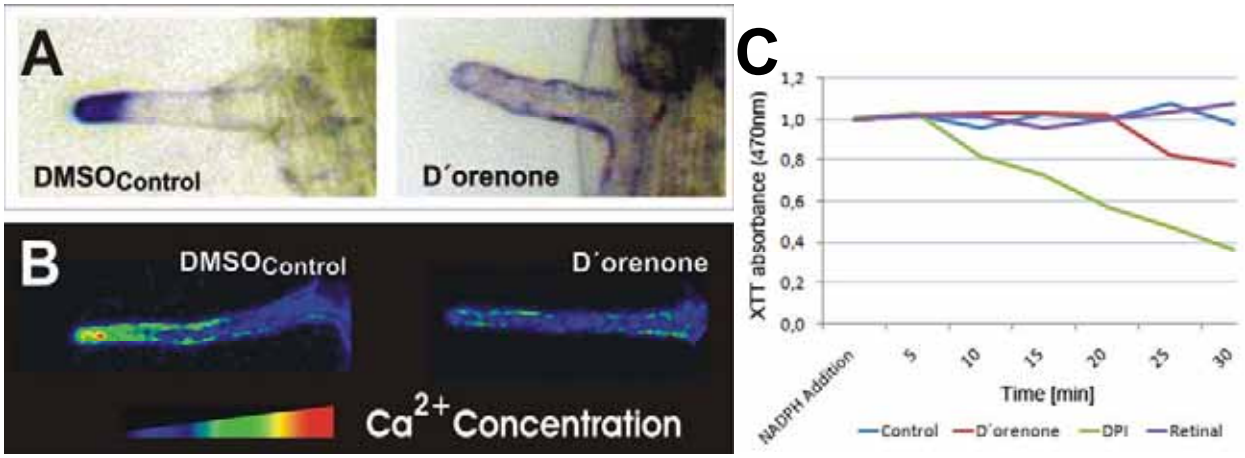

Fig. 3.16.
A/ NBT-staining of mock treated (left) and D'orenone-treated (10 µM) root hair showing ROS production. D'orenone blocks the formation of ROS and results in the loss of the tip-focused ROS gradient.
B/ Fluo3-AM-staining of mock treated (left) and D'orenone-treated (10µM) growing root hairs showing the distribution of cytosolic Ca^{2+}.
C/ NADPH-oxidase dependent ROS production decreases in plasma membrane extracts of D'orenone-treated (10 µM) roots after 25min treatment time. In contrast DPI treatment inhibits immediately NADPH-oxidase activity.

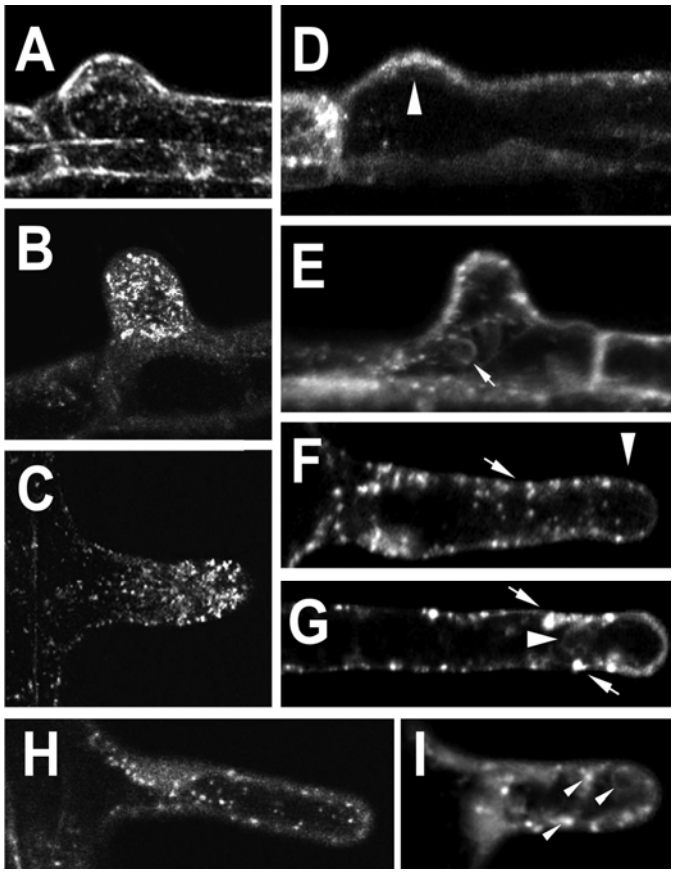

Figure 3.17.
2xFYVE-GFP localization in growing root hairs. **A-C**/ Growing stages of DMSO mock treated control root hairs. **D-G**/ Growing stages of D'orenone-treated (10 µM) root hairs. During root hair formation, FYVE-labeled early endosomes are recruited to the bulging site (**A**). In tip-growing root hairs, abundant and motile small endosomes accumulate within the growing hair tip (**B** & **C**). During the first 40 min of the D'orenone treatment, only a few FYVE-positive early endosomes were recruited to the bulging site (arrowhead in **D**). In tip-growing root hairs, endosomes are enlarged and aggregated. The 'clear-zone' in the growing hair tip disappears (arrowhead in **F**). Depletion of endosomes from the hair tip is often associated with the emergence of FYVE-labeled MVB-like structures (arrowhead in **G**) and enlarged endosomes (arrows in **F** & **G**).
The root hairs in stages, which show under control conditions a tip orientated enrichment of FYVE-positives endosomes, show also a depletion at the tip (**H**) and bigger FYVE-positive aggregates after wortmannin treatment (33µM) (**I**).

3.2.3. D'orenone increases PIN2 abundance and enlarges PIN2 expressing tissue domains

D'orenone increased the abundance of PIN2 protein in roots (Fig. 3.18). In order to find an explanation for this effect, GUS lines visualizing both PIN2 transcripts and PIN2 proteins (introduced in Sieberer et *al.* 2000) were analyzed. While PIN2 transcript localization was not changed significantly in response to D´orenone (Fig. 3.26A), PIN2 protein was found over a larger root apex area than in untreated plants (Fig. 3.18B), covering both the apical meristem and the transition zone. This expansion of PIN2 protein expressing tissue domains was confirmed using the GFP-PIN2 line (Fig. 3.20). In the D'orenone-treated root apices, the PIN2-GFP signal vanished from the lateral root cap and a new, rather diffuse signal appeared prominently in transition zone cells (Fig. 3.20C). Although the overall PIN2 polarity at the cell periphery was maintained at this location, there was an additional signal in small subcellular compartments and at the tonoplast (Fig. 3.20E, F).

This change of PIN2 recycling activity is supported by the finding that double treatment with D'orenone and BFA caused the formation of the PIN2-GFP-positive BFA-induced compartments only after much longer treatment periods (> 1 hour instead of typical 20 – 30 minutes; Fig. 3.20K, L). Western blotting showed increased protein levels of PIN2. This high PIN2 level is quite resistant to the protein biosynthesis inhibitor CHX after D´orenone treatment (Fig. 3.20G). In contrast, PIN1 remained unaffected (compare Fig. 3.27I).

In order to address auxin signalling, transcription of IAA inducible genes (RT-PCR of the IAA1-mRNA, Fig 3.19) and expression of the DR5-reporter gene (Fig. 3.20A) were compared in control and D´orenone exposed roots. While transcription of IAA1 is not affected (Fig. 3.19), the auxin-responsive reporter $DR5_{rev}$-GFP, which responds to gravistimulation (Friml et *al.* 2002b; Ottenschläger et *al.* 2003,) was strongly activated in the root apex after exposure to D'orenone, starting 30 minutes after the begin of treatment (Fig. 3.20A). Experiments with gravistimulated roots pre-exposed to D'orenone showed a somewhat higher expression of the $DR5_{rev}$-GFP reporter on the lower root side; but on the upper root side an unusually prominent signal of the DR5 reporter was also observed (Fig. 3.20).

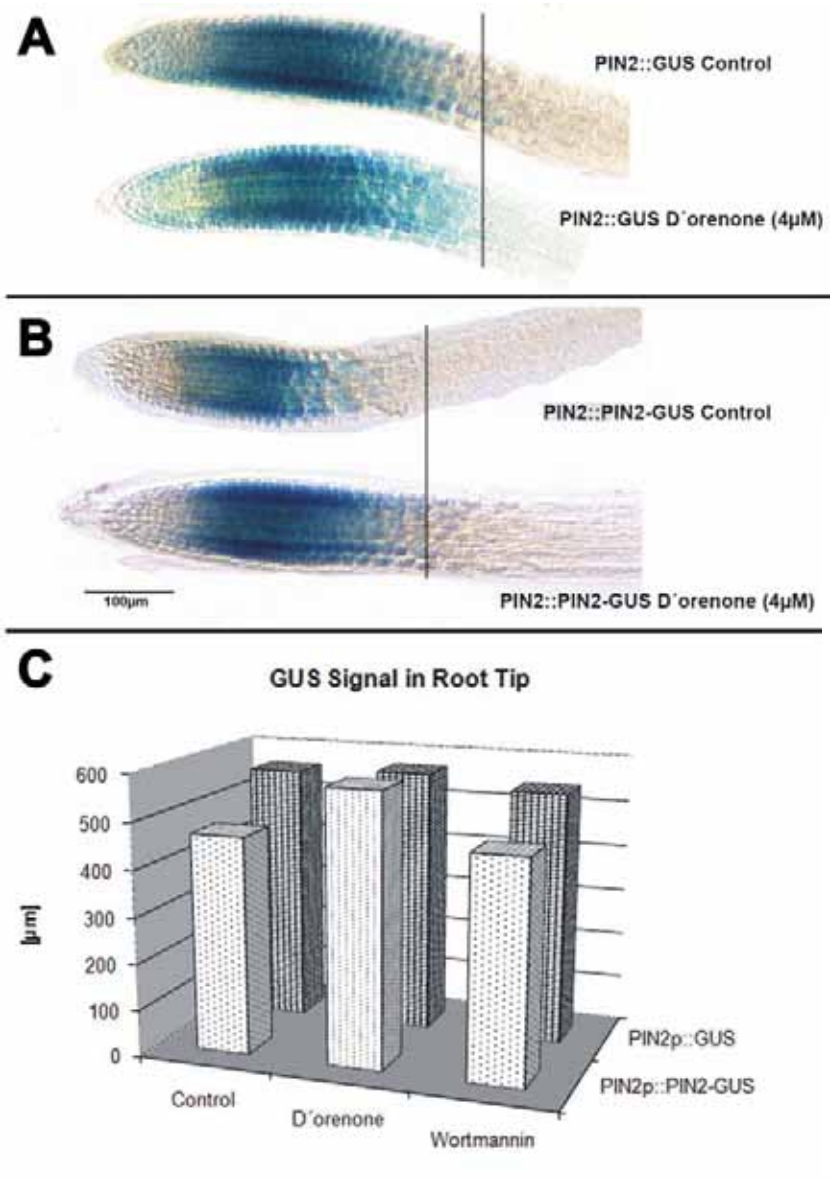

Fig. 3.18.
D´orenone affects PIN2 proteins but not transcripts.

A, B/ PIN2::GUS and PIN2::PIN2-GUS expression in root apices. The GUS signal in the apex of control and D´orenone (4µM) exposed rootd shows no significant responses of PIN2 promoter transcipt (PIN2::GUS) localization to D´orenone treatment (**A**) while PIN2-GUS protein (PIN2p:PIN2-GUS) was found in larger root apex domain after the D´orenone treatment (**B**).
C/ Diagram comparing the PIN2::GUS (proteins) and PIN2::PIN2-GUS (transcripts) expression domains in the control root apices as well as in the D´orenone and Wortmannin treated root spices.

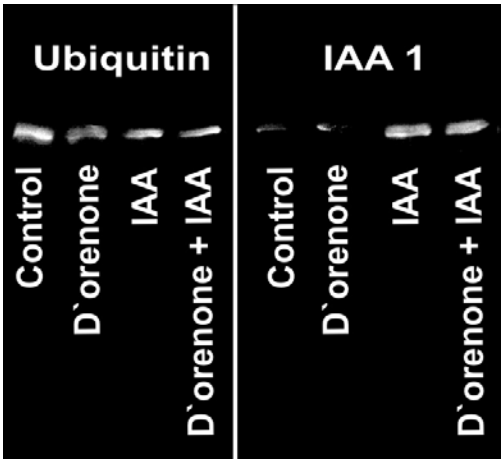

Fig.3.19. RT-PCR against auxin inducible IAA1 gene
Treatment for two hours with 1µM IAA or/and D´orenone (10µM)

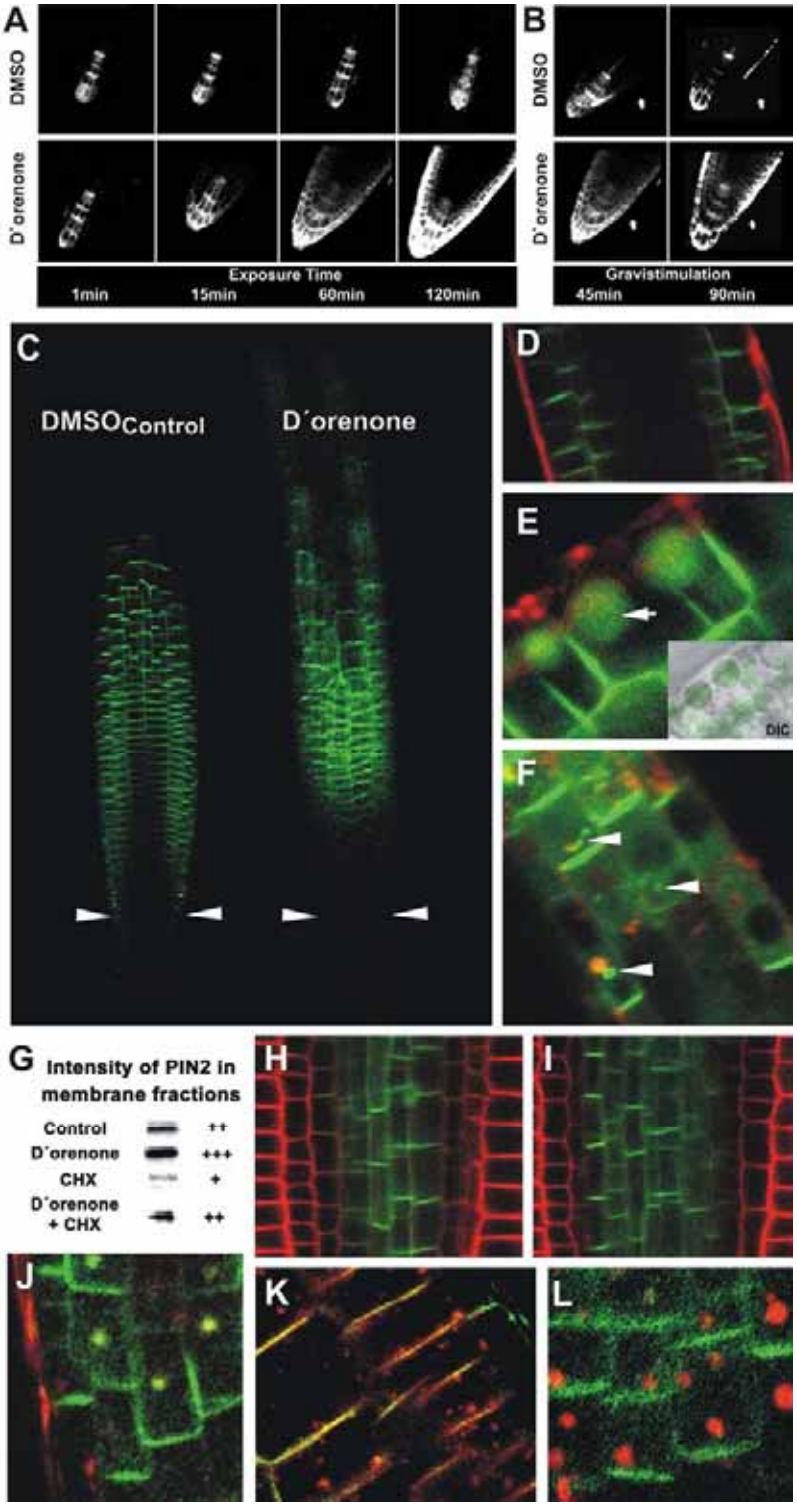

Fig.3.20.
D'orenone interacts with PIN2

A-B/ *DR5::GFP$_{rev}$ expression in root tips.*
The GFP signal in the apex of control roots (A upper panel) and after gravistimulation (B) (90 min, arrow indicates the lower part of the root apex). 10 μM D'orenone activates DR5::GFP$_{rev}$ expression in the whole root cap and lateral root cap cells (A, lower panel). Gravistimulation of the D'orenone exposed root apices (10 μM , 90 min, arrow indicates the lower part of the root apex) shows DR5::GFP$_{rev}$ signal also on the upper side of the root apex (B).
C-F/ *PIN2-GFP localization in green and localization of endocytic tracer FM4-64 in red.* **C/** Overview of control root tip and overview of the D'orenone-treated (10 μM) root tip. In the D'orenone-treated root apices, nearly all PIN2-GFP signals vanished from the lateral root cap (arrowheads), whereas new signals for PIN2–GFP appeared prominently in transition zone cells. Root tips of the controls show typical polar localization of PIN2-GFP at the plasma membrane of the cross poles (**D**). Besides the polar localization of PIN2 at the PM, treatment with D'orenone (10 μM) induces a diffuse cytoplasmic PIN2-GFP signal (**F** arrow heads) along with PIN2-GFP positive tonoplast and vacuoles (**E arrow**). Western blots of membrane fractions labelled with Anti-PIN2 reveals a more distinct band in extracts of D´orenone treated roots (4μM for 2h) (**G**). Treatment with protein biosynthsis inhibitor CHX diminished signal intensity, whereas double treatment with D´orenone and CHX shows only a light effect (**G**).
H-I/ *PIN1-GFP localization in green and localization of endocytic tracer FM4-64 in red.*
PIN1-GFP shows typical polar localization at the plasma membrane. cross poles of stele cells are clearly labelled (**H**). D´orenone has no influence on subcellular localization of PIN1-GFP (**I**). **J-L/** *PIN2-GFP localization in green and localization of endocytic tracer FM4-64 in red.* Treatment with the secretion inhibitor brefeldin A (BFA) at the concentration 35 μM revealed the PIN2-GFP positive BFA-induced compartments are already formed after 30 min (**J**). Pretreatment with D'orenone (10 μM) for 30 min revealed that BFA-induced compartments are formed slower (compare **K** with results from 30 min of BFA treatment and **L** with 1 h BFA treatment). Only after a longer treatment period of 1 hour are bigger BFA compartments monitored. Interestingly, only the endocytic tracer FM4-64 is found in the compartments.

3.2.4. Auxin rescues the root hair phenotype in D'orenone treated roots

Root hairs of plants treated simultaneously with auxin (30 nM) and D'orenone (4 µM) showed comparable growth rates to root hairs of controls (Fig. 3.21A,C). Moreover, the pretreatment of roots with external auxin resulted in roots insensitive to externally applied D'orenone (Fig. 3.21B). Therefore, it appears that auxin rescues the D'orenone-induced block of root hair tip growth (Fig. 3.21). On the other hand external auxin was not able to rescue the wortmannin-induced inhibitory effects on root hairs and root apices (Fig. 3.21A), demonstrating that either targets or mode of binding of D'orenone and wortmannin are not identical.

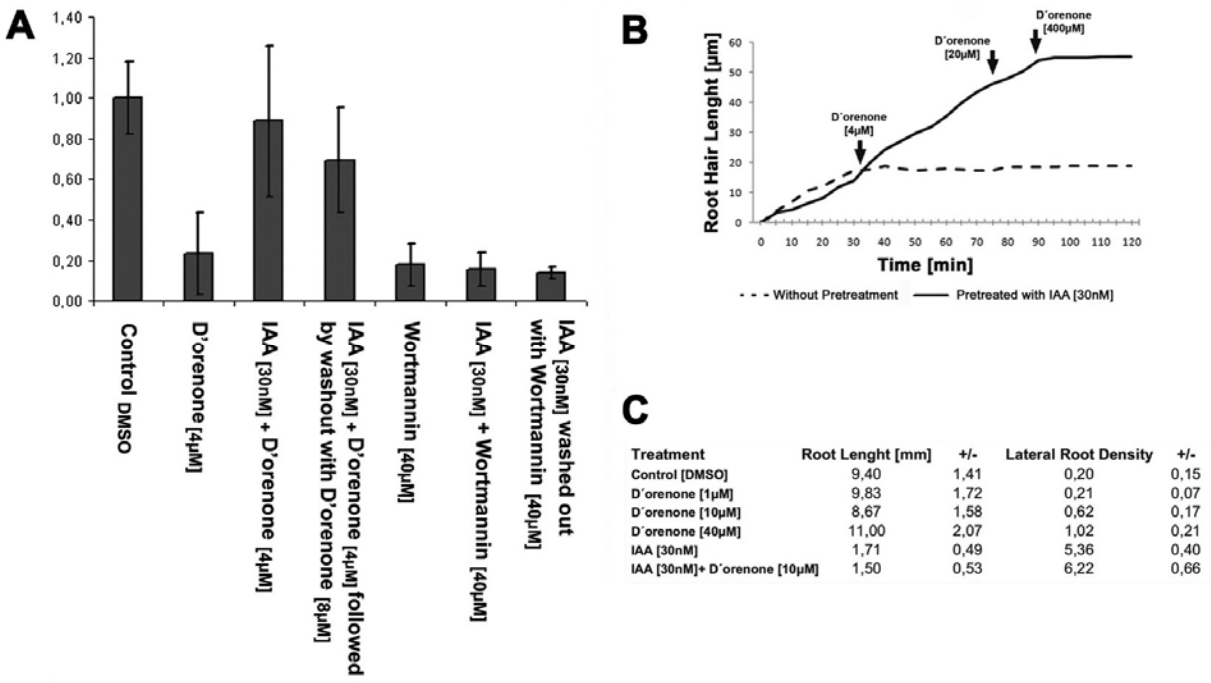

C

Treatment	Root Lenght [mm]	+/-	Lateral Root Density	+/-
Control [DMSO]	9,40	1,41	0,20	0,15
D´orenone [1µM]	9,83	1,72	0,21	0,07
D´orenone [10µM]	8,67	1,58	0,62	0,17
D´orenone [40µM]	11,00	2,07	1,02	0,21
IAA [30nM]	1,71	0,49	5,36	0,40
IAA [30nM]+ D´orenone [10µM]	1,50	0,53	6,22	0,66

Fig. 3.21.

Auxin rescues the root hair phenotype in D'orenone treated roots.

A/ The external addition of auxin (IAA, 30nM) rescues the D'orenone-induced root hair phenotype (D'orenone, 4µM). Root hairs of double treated plants show comparable growth rates to control root hairs. External auxin also makes the roots more resistant to additionally applied D'orenone (first 4µM followed by 8µM). Wortmannin (40µM) induced stop of root hair growth is not rescued by external applied auxin (30nM). These data are mean values of at least 10 hairs.

B/ Pretreatment with external auxin (30nM) makes root hairs more resistant to additionally applied D'orenone (first 4µM followed later by 20µM and 400µM).

C/ D´orenone has no significant effects on growth of primary roots. However, at concentrations of 10µM or higher, D´orenone increases slightly the number of lateral roots. These data are mean values of at least 25 plants. The root lengths are measured in mm and the lateral root density values are mean number of lateral roots per mm.

3.2.5. D'orenone rescues the agravitropic phenotype of PIN2 mutant roots

All above data indicate that D'orenone manipulates the root hair growth via its effects on polar auxin transport and PIN2 protein. To provide the final genetic evidence for this scenario, roots of two *pin2* mutant lines (*agr1-2* and *eir1-4*) were analyzed after exposure to D'orenone. The *agr1-2* mutant is not a null line, i.e. some PIN2 protein is still found in this mutant.

D'orenone rescued agravitropic phenotype of roots of the *agr1-2* mutant line (Fig. 3.22A). Importantly, D'orenone did not block completely the root hair tip growth in the *agr1-2* mutant line (Fig. 3.22B), indicating that the PIN2 protein is nessecary for the D´orenone mediated stop of the root hair growth. On the other hand, in the *pin2* null mutant line (*eir1-4*), without any PIN2 protein left, root growth was agravitropic after D´orenone treatment. In addition, cytoarchitecture and growth rates of root hairs was not affected by D´orenone in this line (Fig. 3.22C), showing clearly the PIN2 dependance for the D´orenone induced root hair phenotype.

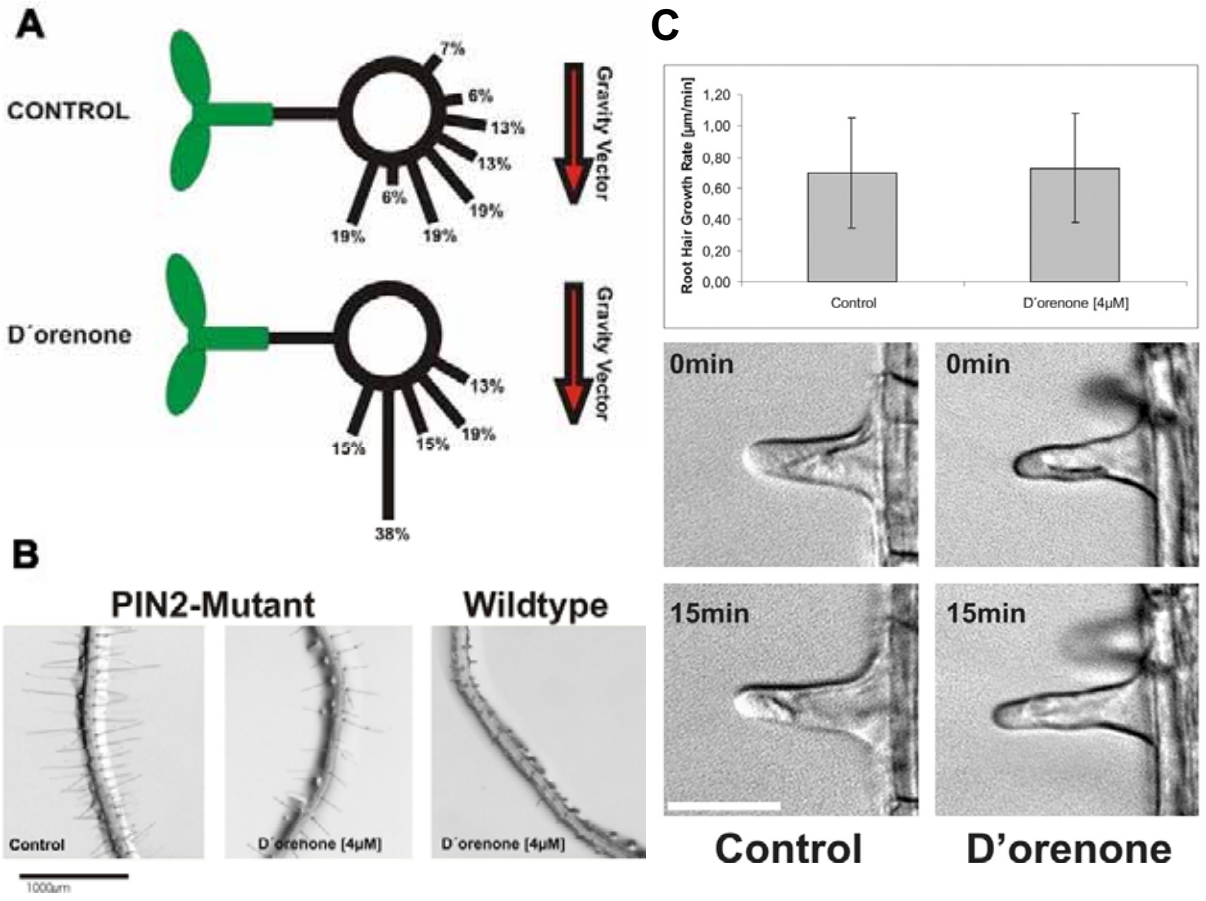

Fig. 3.22. D'orenone rescues agravitropic phenotype of leaky PIN2 mutant roots and has no effect on PIN2 null mutant root hair growth.

A/ PIN2-mutants lines with less PIN2 protein than wildtype are agravitropic. D'orenone rescued agravitropic phenotype of PIN2 mutant roots (The data are of at least 25 plants per experiment.).

B/ D'orenone does not block completely root hair tip growth in the PIN2 mutant in contrast to wild type roots.

C/ Treatment with D'orenone (4µM) shows no visible effects on the root hair growth rate and root hair cytoarchitecture in the *pin2* null mutant line (*eir1-4*). (The data are of at least 45 root hairs.)

3.3. Auxin modifies root architecture via ROS (reactive oxygen species) production

3.3.1. Indirect activation of auxin-induced transcription activity by IBA

Indole butyric acid shows only weak activity in most auxin growth assays. The only exceptions are the ability to induce lateral (Zolman et *al.* 2000) and adventitious roots (Nordström et *al.* 1991) more strongly than other auxins at comparable concentrations (reviewed in Woodward and Bartel 2005a).

To understand the activity of IBA, several tests for typical auxin transcription activity were conducted. First, the two reporter constructs BA3::GUS and DR5::GFP_{rev} were checked, which are reliable tools to follow auxin signalling in roots. Both reporters are driven by a promoter containing an auxin response element that activates transcription after exposure to auxin (constructs were originally presented by Oono et *al.* 1998 and Friml et *al.* 2003 respectively).

The appearance of a strong BA3::GUS labelling of the transition zone was detected after a 6h treatment with 1µM IAA (Fig.3.23B). But no BA3::GUS was monitored after treatment with 1µM IBA (Fig.3.23C). A similar behaviour was seen with the more sensitive DR5::GFP_{rev} reporter. Compared to the IAA-induced reporter signal the IBA-induced GFP signal only weakly detectable in the root tip (Fig. 3.23D I and II).

Terfestatin A (Trf A) a root specific auxin signalling inhibitor disturbs the TIR^{scf} proteasome complex and disables the IAA induced transcription of naturally occurring Aux-IAA proteins and of the synthetic DR5-reporter (Fig. 3.23D III and see also Yamazoe et al. 2005).

A co-treatment with Trf A prevented IAA or IBA induced activation of the DR5::GFP_{rev} reporter (Fig. 3.23D III and IV), indicating that IBA-signalling involves the same TIR^{scf} complex for its transcriptional regulation.

To distinguish whether IBA shows auxin transcriptional activity directly via a weaker affinity to the TIR^{scf} complex or indirectly via a conversion to IAA, semi-quantitative RT-PCRs were performed to determine the transcript levels of IAA1 and IAA19 in wild type and mutants.

Like the artificial reporter, both transcripts were induced by IBA. But longer treatments or higher concentrations of IBA were needed, compared to the IAA induced activity (Fig. 3.23E).

Three Arabidopsis mutants *pex5-7* (Fig. 3.23E), *pxa1 and pex6 (*data not shown) with defects of ß-oxidation and IBA-insensitivity were also tested. All mutants showed a normal behaviour upon IAA treatments with a strong activation of the IAA1 and IAA19 transcripts, however, after IBA treatment no transcriptional activation was detectable. This indicates , that a ß-oxidation-like conversion from IBA to IAA is needed for an IBA induced transcriptional activity of Aux/IAA genes.

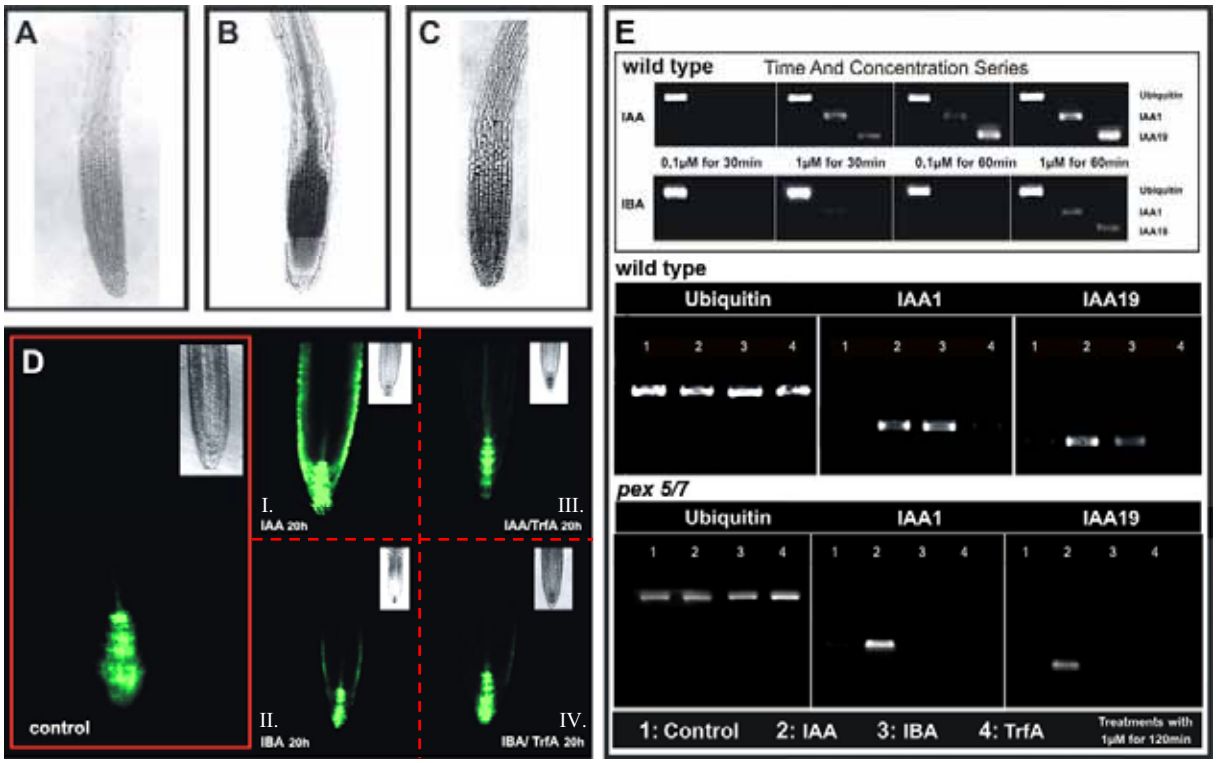

Fig. 3.23.

Auxin induced transcription activity

A-C/ BA::GUS auxin response line. No visible promoter activity of the auxin inducible gene in untreated root apices (A). Treatment with 10µM IAA for 6h induces strongly GUS activity in transition zone and stele tissue (B). Treatment with 10µM IBA does not induce promoter activity (C).

D/ DR5::GFP auxin response line. Strong promoter activity in columella cells in root tip of untreated plants. Root tips treated with 1µM IAA show activation in outer cortex and stele cells (**I**). This activation is prevented by co-treatment with 10µM Terfestatin A (Trf A) (**III**). IBA (1µM) can also induce the DR5 promoter but slightly weaker (**II**). Again, this activation is prevented by Trf A (**IV**).

E/ RT-PCR of auxin inducible genes (IAA1 and IAA19) from cDNA of roots. Both transcripts are expressed in root apices after IAA treatment. Transcripts are detectable after 30 minutes treated with 1µM or after 1 hour with 0, 1µM IAA. System was adjusted with ubiquitin expression for semi quantitative comparison. IBA is able to induce transcripts starting with one hour treatment time and a concentration of 1µM.

Comparison of transcription activity of IAA1 and IAA19 after two hours treatment with 1µM of IAA or IBA in wild type and *pex 5/7* mutants. In the IBA resistant mutant *pex 5/7* IBA fails to induce transcripts.

3.3.2. Measurement of IBA to IAA conversion

In co-operation with Prof. Dr. Ludwig-Müller (Dept. Of Botany/TU Dresden) a protocol to measure IBA to IAA conversion was developed. 2 weeks old Arabidopsis plants were incubated with radioactive ^{139}IBA for 16h and harvested. To determine the conversion rate from a mass spectrograph, a labeled standard (^{136}IAA) was added. The ^{139}- label in the IAA peak was calculated on the basis of the standard. Then based on this value conversion of IBA to IAA in each sample was measured (Table I)

Wild type plants show an average conversion rate of 55, 8% of ^{139}IBA in this system, the IBA-insensitive mutant *pxa1* has a rate of 8% and the *ped1* mutant which exhibits a partially impaired ß-oxidation and is slightly less sensitive to IBA shows a rate of 16%.

The Arabidopsis mutant *AtNOA1* has a greatly diminished ability to generate endogenous nitric oxide compared to wild type. The mutant has up to 80% lesser NO production after exposure to different environmental changes (Guo et *al.* 2003). The *NOA1* mutant shows a comparable conversion rate (55, 2%) to the wild type.

Arabidopsis Line	**fresh weight [mg]**	**Labeled IBA [ng / mg fresh weight]**	**Labeled IAA [ng / mg fresh weight]**	**conversion IBA → IAA [%]**
Wild Type	68,03	0,61	0,29	55,8
ped1	60,7	1,14	0,10	8,5
pxa1	40,8	0,32	0,05	16
AtNOA1	46,7	0,72	0,41	55,2

Table I.
IBA to IAA conversion ***(Data are a courtesy of Prof. Dr. Ludwig-Müller)***

3.3.3. IAA localization and behavior of peroxisomes after an indole-butyric-acid treatment

One assay that could help to prove ß-oxidation-like conversion of indole-butyric-acid to indole-acetic-acid in peroxisomes is to immunolocalize IAA in the peroxisomes after the root tissue has been treated with IBA using the specific IAA antibody described above (see chapter 3.1.).

With this antibody big spot-like structures were recognized after IBA-treatment in addition to labelling of the nuclei and cross wall domains (Fig. 3.24A). Co-localisation experiments with antibodies against organelle specific proteins confirm, that these structures are peroxisomes. Clearly seen in maize root apices, the appearance of IAA-positive peroxisomes was limited to certain tissues at the border between root stele and root cortex, starting with cells behind the quiescent-center of the root apical meristem (Fig. 3.24C).

Co-localisation studies in Arabidopsis of IAA with catalase also confirmed an accumulation of IAA in peroxisomes after treatment with IBA. Importantly Arabidopsis mutants like *pxa1, pex6 and pex5-7,* which are showing an insensitivity towards IBA and in addition are impaired in ß-oxidation and other peroxisomal functions, were lacking almost completely IAA-positive peroxisomes after IBA treatments (Fig. 3.24).

It is noteworthy that both auxins (IAA and IBA) induced a peroxisomal proliferation which yielded bigger sprawled peroxisomal structures than the circular peroxisomes normally found in mock treated maize and Arabidopsis roots.

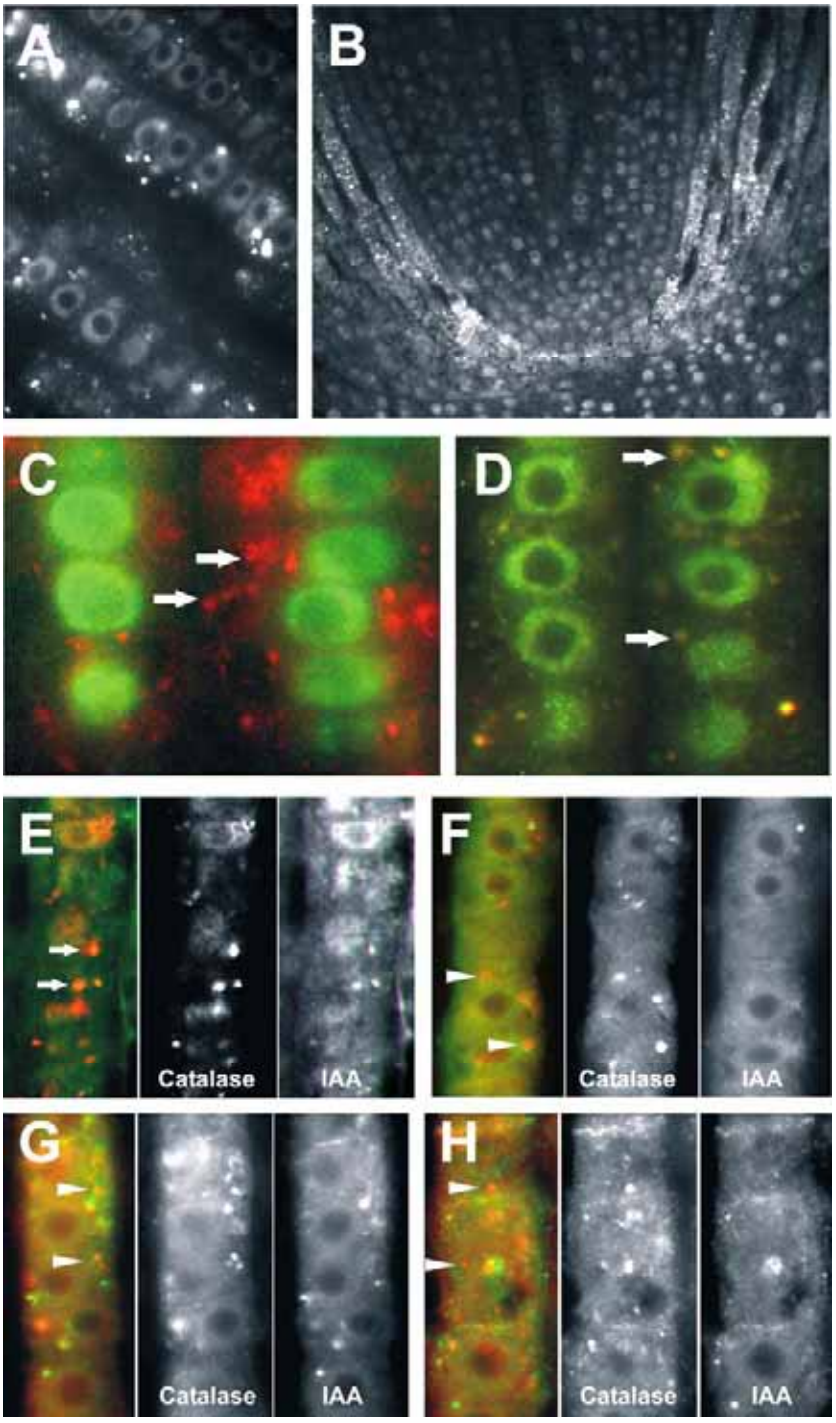

Fig. 3.24. Peroxisomal IAA localization after IBA-treatment

A-D/ IAA labeling in maize root apices. After an IBA-treatment spot-like structures positively recognised with the IAA antibody appear (**A**). IAA-positive structures are limited to certain tissues at the border between root stele and root cortex, starting with cells at the quiescent-center of the root apical meristem (**B**). The spot-like structures are peroxisomes. Co-labelling of IAA (green) and catalase (red) show that after an IBA-treatment (**D**) but not after an IAA-treatment (**C**) a co-localisation occurs, indicating a peroxisomal location of auxin after IBA exposure.

E-H/ IAA labeling in arabidopsis root apices. The nuclei labelling is less pronounced, compared to maize labelings. Instead, stronger cytoplasmic signal with many spot like structures are visible.

E/ After IBA-treatment bigger and more pronounced spots appear (white arrows). They are positive for IAA (green) and catalase (red). Mutants *pxa1* (**F**) and *pex5/7* (**H**) which are highly resistant to IBA, show no co-localisation of IAA (green) and catalase (red). Catalase positive peroxisomes are highlighted by white arrowheads. The mutant *pex6* which responds to IBA at higher concentrations shows IAA negative (arrowheads) but also few IAA positive peroxisomes (**G**)

Monitoring of peroxisomes in vivo with a *pts1*-GFP Arabidopsis line (*pts1* is a peptide sequence which targets Proteins to peroxisomes) revealed that proliferation of peroxisomes in root tissues was already prominent after one hour of auxin exposure (Fig. 3.25).

Experiments with the red fluorescent endocytic tracer FM4-64 showed a partial co-localisation with *pts1*-GFP after auxin treatment, implicating an involvement of recycling endosomal vesicles in the peroxisomal proliferation. The most prominent and easiest to follow example were epidermal cells (Fig. 3.25D), but this effect was also seen in the other types of root cells. The tips of root hairs are perfect to monitor this co-localisation. The tip is quite small and peroxisomes and endosomes follow swiftly the cytoplasmic streaming. Tracking movement of both revealed that indeed a fraction of both co-localised after an auxin treatment (Fig. 3.25E-H). The strong red halation of FM4-64 labelled plasma membrane and *pts1*-GFP peroxisomes located nearby leads to the appearance of false positive spots. To minimize this error, only spots which were showing co-localisation during movement were considered as truly connected (shown in blue).

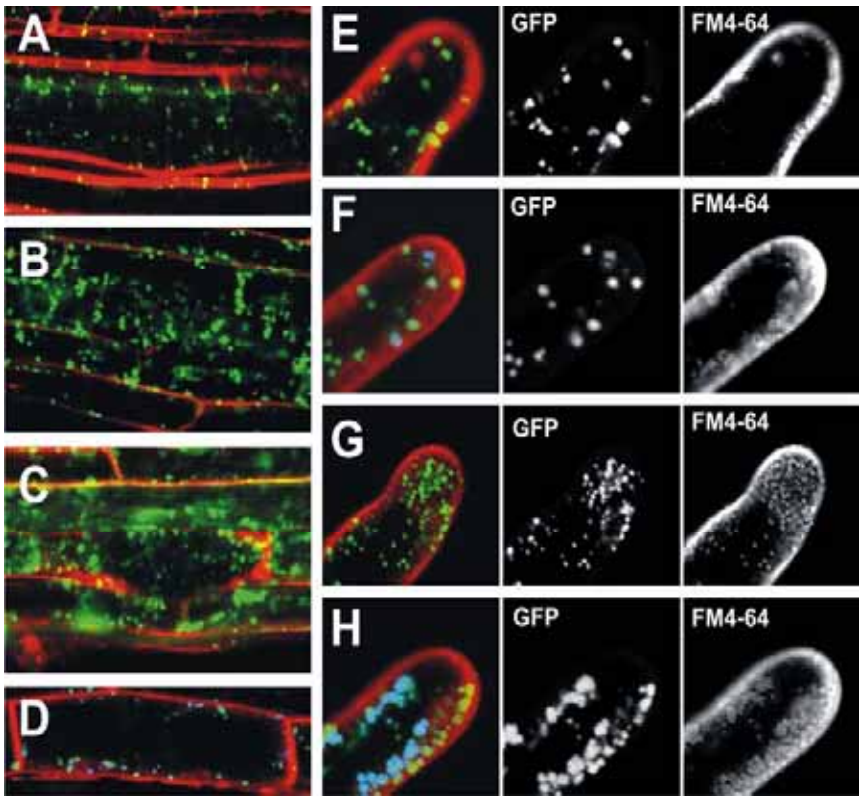

Fig. 3.25.
Peroxisomes (*pts1*-GFP) and endosomal membranes (red) co-localize after auxin-treatment
A-C/ *pts1*-GFP at emerging lateral roots in untreated control (**A**) and in 1µM IAA (**B**) and 1µM IBA (**C**) treated plants (auxin treatment of 1 hour). Auxin treatment induces strong proliferation of *pts1*-GFP positive peroxisomes.
D/ Single optical section of epidermal cell after IBA treatment (1µM). *Pts1-GFP* is seen in green and FM 4-64 in red. Collocation is shown in blue
E-H/ / *pts1*-GFP at FM 4-64 labeled root hair tips. Single optical section (**E**) projection of image stack representing the complete tip (**G**) show no co-localization of GFP and dye.
Root hair tips of 1µM IAA treated roots show a partial overlapping of FM4-64 and pts1 positive spots (**F**; indicated in blue) in single layer image. Stack images show proliferation of peroxisomes. The peroxisomal structures appear not only enlarged because of the proliferation effects but also due to movements along the z-axis of the stack, giving summation of size. FM-dye positive peroxisomes are shown in blue.

3.3.4. IBA-to-IAA conversion promotes RNS formation

An indirect effect of IBA, i.e., by its conversion to IAA, could explain the slow response of transcriptional activation and the weak inhibition of primary root growth upon IBA treatment. Nevertheless, this scenario can not explain the fact that IBA is effective in boosting lateral root formation. Several lines of data indicate the feature of IAA to induce these roots by using reactive NO as downstream signals (Correa-Aragunde et al. 2004). The NO specific dye Diaminofluorescein–2 Diacetate (DAF-2DA) was used, to test if IBA induces RNS in a comparable manner as IAA does it.

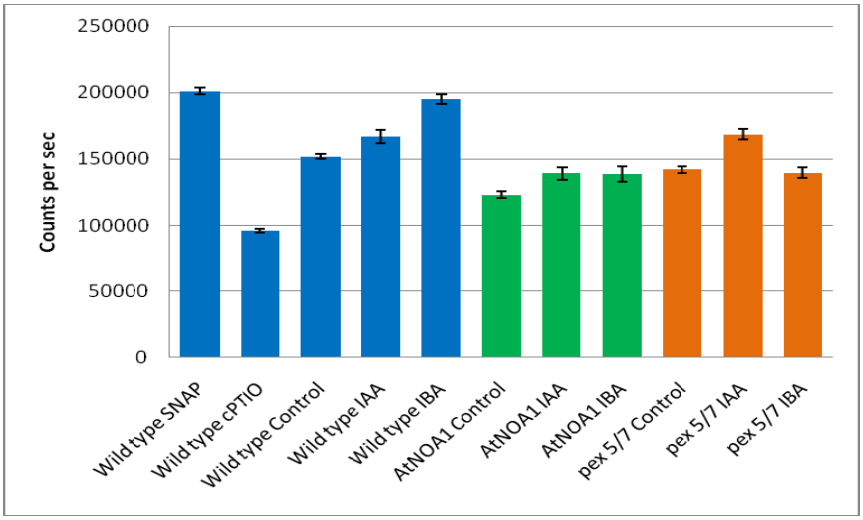

Fig. 3.26. Measured fluorescence intensity at wavelength 515nm of DAF-2T by a fluorometer
To adjust system of inducible/dynamic nitric oxide measurement (photons per second) two extracts treated with both the NO-Donor SNAP (1µM) and the NO-scavenger cPTIO (10µM) were used. Wild type measurements are shown in blue. The measurements for the NO deficient mutant *NOA1* and peroxisomal/developmental mutant *pex5/7* are displayed in green and orange respectively.
IAA (1µM) builds up an increase of fluorescence about 10%in wild type and both mutants. IBA (1µM) induces the light signal much stronger in wild type (~23%). *NOA1* shows after IBA treatment the same proportion of NO rise as after IAA treatment. In the IBA resistant mutant *pex5/7* is no induction of nitric oxide by IBA gaugeable.
Before extraction for each 25 plants were exposed to SNAP, cPTIO auxin or mock treated for 2h.

DAF-2DA emits a green fluorescence in living cells under physiological conditions. Once inside the cell the diacetate groups on the DFA-2DA reagent are hydrolyzed by cytosolic esterases thus sequestering the reagent inside the cell. Production of RNS converts the non-fluorescent dye, DAF-2, to its fluorescent triaole derivative, DAF-2T. The resulting fluorescence can be monitored by confocal microscopy (Foissner et *al.* 2000) or semi-quantified by a fluorometer under stable pH conditions of pH 6, 5.

The fluorescence measurements of 2h treated Arabidopsis roots showed both auxins boost RNS production and IBA even promoted RNS production much more strongly than IAA (Fig. 3.26).

Furthermore, the mutants *pex5-7* (Fig. 3.26)*, pex6 and pxa1 (data not shown)* were enabled to produce additional RNS after an IAA treatment but not after an IBA treatment.

Both auxins induced nitric oxide production in the *AtNOA1* mutant, although on a lower level than in wild type plants. The IAA-induced ratio of NO-production in showed more or less the same ratio to untreated controls was nearly the same as in wild type roots. While IBA still induceed a rise of detectable NO, the ratio to untreated roots was clearly lesser than compared with wild type roots.

A slight adaptation of the DAF-2DA labelling protocol allowed monitoring of the sub-cellular distribution of nitric oxide sources. Besides a strong diffuse cytoplasmic signal near the plasma membrane several strongly fluorescent moving spots were detectable (Fig. 3.27). Since DAF-2DA has fluorescein as chromophore the fluorescence spectrum of the emitted light is distinguishable from the GFP-spectrum. The maximum intensity peaks of DAF-2DA (515nm) and GFP (509nm) differ by ~7nm. New generation spectral confocal microscopes can separate the two signals. Thus, the usage of different Arabidopsis GFP-lines allowed the identification of NO producing spots in untreated and auxin treated roots (Fig. 3.27). The GFP fluorescence is somewhat lower at a pH of 6,5 than at neutral pH but this pH allows to just visualize the rather low DAF-2T fluorescence of nitric oxide production in untreated cells. At higher pH´s the specifity of the dye is abolished and the stronger GFP-signal could more easily outshine the DAF-2T signal *(data not shown)*. A handicap of this method, treatments which are strongly enhancing NO production (e.g. SNAP treatment with ≥10µM concentration) will lead to the opposite effect of DAF-2T fluorescence outshining the GFP-signal. Loading the cells with the optimal amount (15µM) of DAF-2DA is important for the success of this labelling technique. Otherwise, this method is only limited by the ability of tissues to take up DAF-2DA and the photostability of DAF-2T.

In untreated cells the bulk of the DAF-2T spots were identified as mitochondria and FVYE-GFP positive endosomes. Interestingly, after auxin treatment peroxisomes appeared as the third major source of NO (Fig. 3.27). They were only insignificant NO sources in untreated control cells.

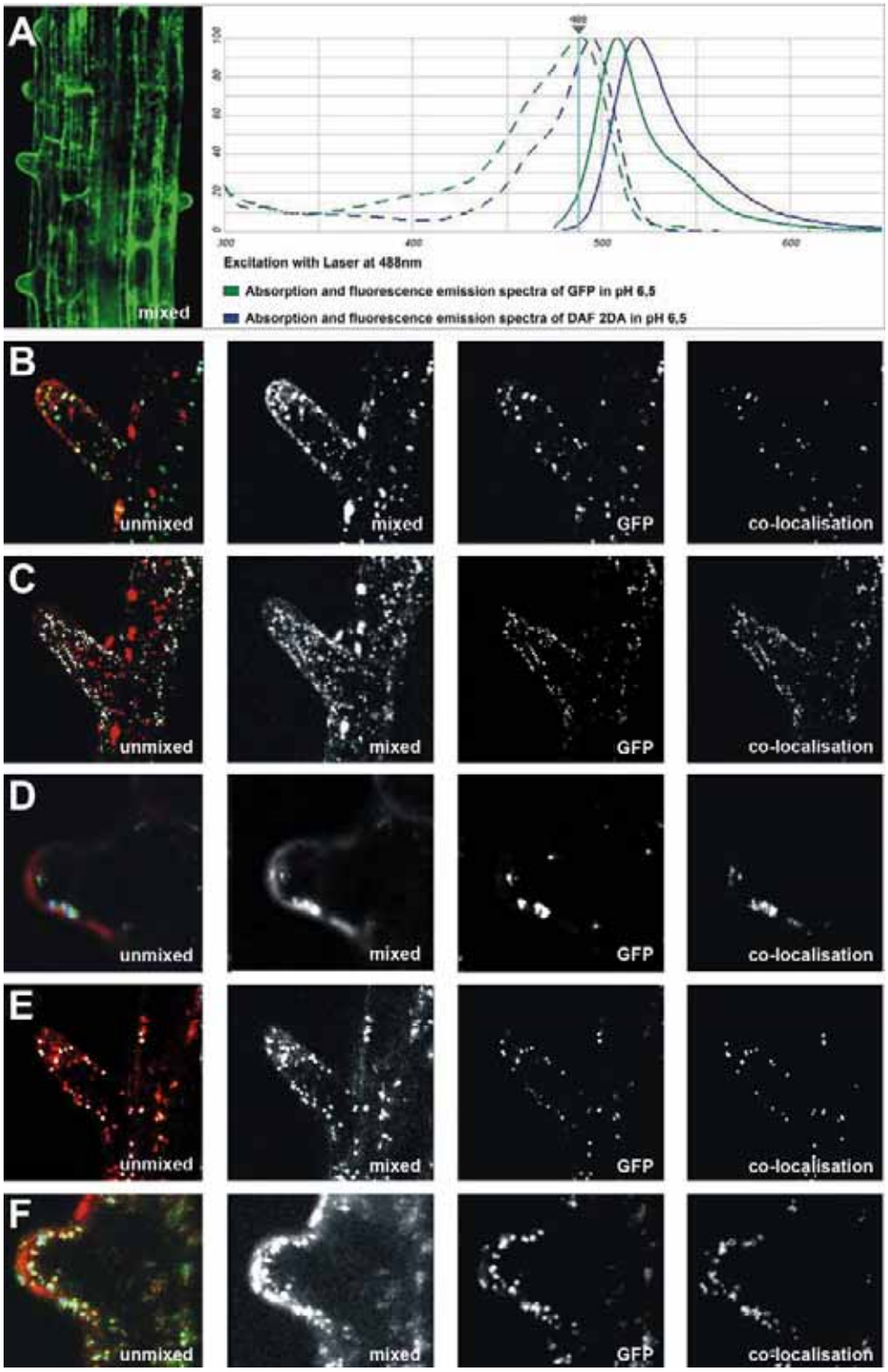

Fig. 3.27. Cellular localization of DAF-2T

A/ Green DAF-2T labeling pattern in root cells consists of diffuse cytoplasmic signal often near the plasma membrane and moving intracellular spots (left). Normalized fluorescence spectra of DAF-2 and GFP are quite similar but not identical (right).

B-F/ DAF-2T staining of GFP lines monitored with a spectral-confocal microscope. After unmixing of GFP and DAF signal GFP is shown in green, DAF in red and co-localization of both in blue/white. Mito-GFP a mitochondrial marker shows a strong co-localization with DAF-2T in growing root hairs (**B**). The endosomal marker FYVE-GFP shows also a strong co-localization with DAF-2T in growing root hairs (**C**). Several DAF-2T positive spots which are not endosomes are visible. *Pts1-GFP* shows only a partial co-localization with DAF-2T in growing root hairs (**D**). The spot-like structures of peroxisomes show an increased co-localisation with DAF after IAA treatment (**E**).A extremely strong co-localisation of pts1-GFP and DAF-2T is monitored after an IBA treatment (**F**).

3.3.5. IBA promotes NO-pathways for lateral root formation (LRF)

To examine if IBA promotes lateral root formation by promoting RNS production a simple growth assay was performed (Fig. 3.28).

Both auxins at a concentration of 1µM promoted lateral root formation (LRF) in Arabidopsis wild type roots. The root specific auxin signalling inhibitor Terfestatin A reduced LRF of wild type plants in the presence of either IAA or IBA (see also Yamazoe et *al.* 2005). Though, the driving force of IBA is much less hindered than the effect of IAA. This suggests a partially IAA-independent mode for LRF by IBA.

Treatments with the NO-donor SNAP induced the formation of additional lateral roots similar to both auxins. A double treatment of the auxins with the nitric oxide scavenger cPTIO led to a decrease of LRF.

ß-oxidation defective mutants had a very low rate of LRF, which could be tripled by the addition of IAA, however not by IBA. Both auxins were ineffective in promoting LRF in the *AtNOA1* mutant.

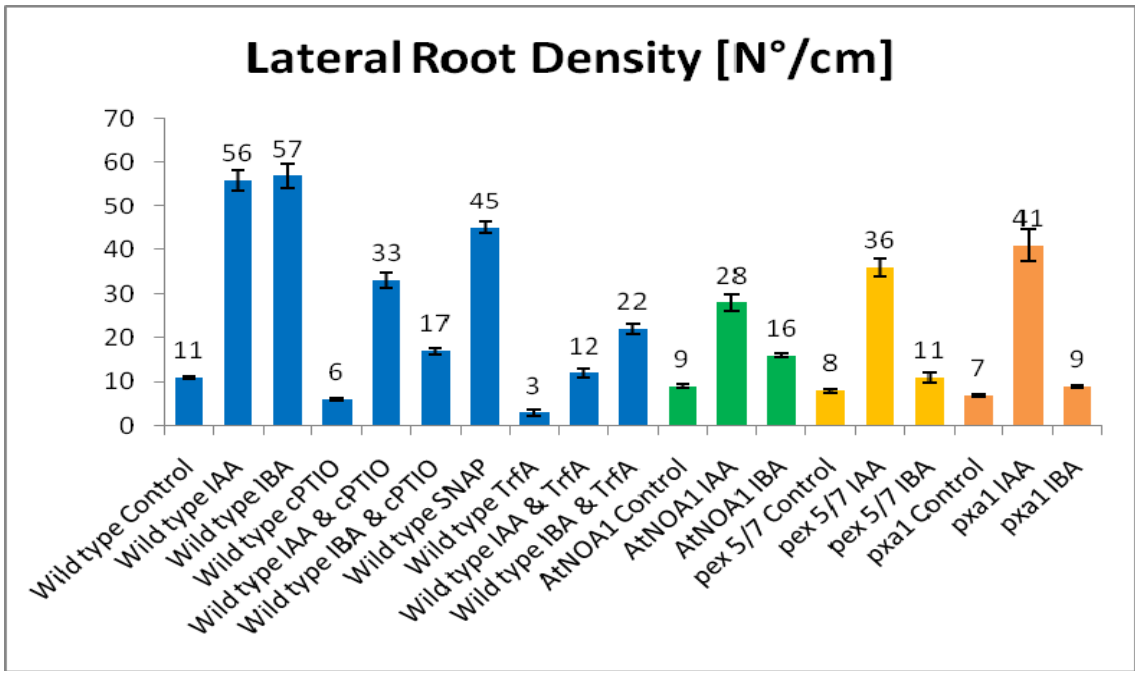

Fig. 3.28.
Mean average of lateral roots from 25 plants (DAG 4) per sample were measured and the number of lateral roots per centimeter of primary root was calculated. NO-Donor "SNAP", NO-scavenger "cPTIO" and auxin signaling inhibitor "Terfestatin A" (Trf A) were used with a concentration of 10µM and the auxins were used with a concentration of 1µM. Wild type measurements are shown in blue. The measurements for the NO deficient mutant *NOA1* and peroxisomal/developmental mutants *pex5/7* and *pxa1* are displayed in green, orange and yellow respectively.

3.3.6. **IBA and IAA promote different ROS populations**

Measurements of ROS production of root extracts from plants with or without auxin pretreatment revealed big differences with respect to the type of ROS that was induced by either IAA of IBA (Fig. 3.29A). IAA reduced the level of $O_2^{\cdot -}$,increased the level of OH^- moderately, whereas the H_2O_2-level was increased enormously. On the other hand, IBA increased the levels of both $O_2^{\cdot -}$ and OH^- moderately, and the rise of the H_2O_2-level less pronounced. Activity assays of ascorbate peroxidases, catalases and superoxide dismutases (SOD) yielded complementary results (Fig. 3.29B). IAA had a negative effect on ascorbate peroxidases, catalases, whereas IBA affected them only moderate, but was stronger inhibiting SOD. The peroxynitrite specific dye 1,2,3-Di-Hydro-Rhodamine showed a stronger and faster increase of signal intensity after auxin treatments. Taken the higher $O_2^{\cdot -}$ and NO level after IBA treatment, it was not surprising that the 1,2,3-Di-Hydro-Rhodamine labeling was stronger after incubation with IBA than with IAA (Fig. 3.29C).

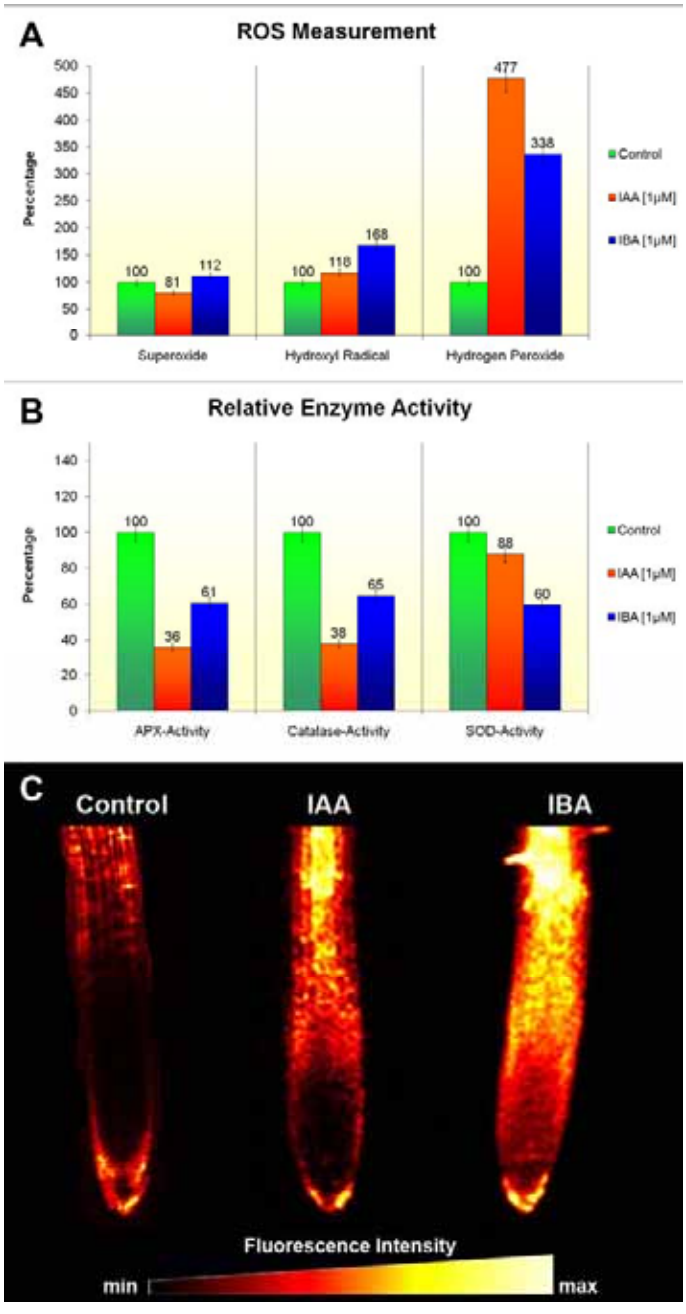

Fig. 3.29.
Auxin induced ROS production
A/ Relative ROS-Measurement in root extracts of control and auxin treated plants. Before extraction, about 20 plants were incubated for one hour with an auxin or mock treated.
B/ Relative enzyme activity in root extracts of control and auxin treated plants. Before extraction, about 20 plants were incubated for one hour with an auxin or mock treated.
C/ Fluorescence intensity of peroxynitrite specific dye 1, 2, 3-Di-Hydro-Rhodamine monitored with a confocal microscope.

3.3.7. **Stress-and ABA-response reporter is activated by auxin**

To verify if ROS production after auxin treatments reflects a stress situation GUS labelings with two stress and ABA responsive reporter lines were performed. The pro3DC::GUS line is a well documented and reliable tool to visualize transcriptional changes by different ROS-producing stresses (Chak et *al.* 2000). Pro3DC::GUS expression in root apices is activated by treatment with IAA and IBA. The staining pattern is similar for both auxins but differs from the pattern induced by ABA. (Fig. 3.30).

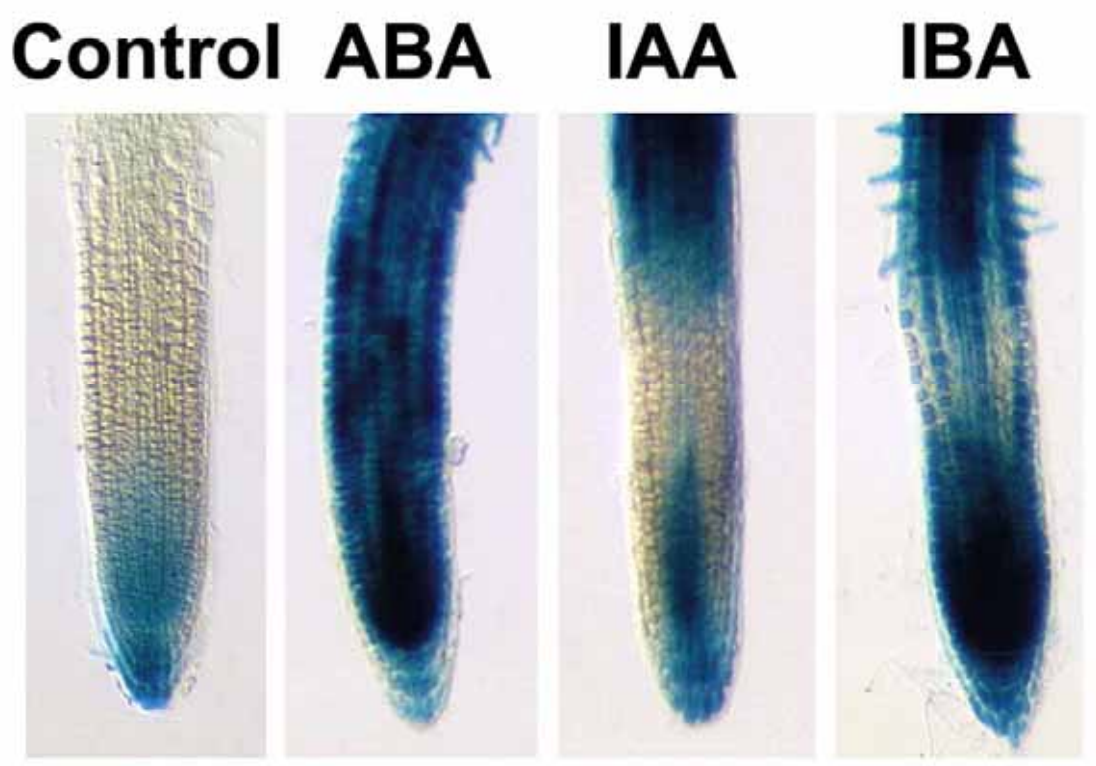

Fig. 3.30.
ABA-response element reporter
Five days old plants were incubated for one hour with 1µM auxin or 1µM ABA. Shown are typical examples of the treatments.

3.3.8. The maize mutant *lrt1* and IBA

The lateral rootless (*lrt1*) *Oryza sativa* (rice) mutant is insensitive to auxin (IAA, IBA and 2, 4-D) with respect to root elongation. The only auxin that can restore lateral root initiation in the mutant is IBA (Chhun et *al.* 2003).

The analogous maize mutant *lrt1* shows a similar behavior (Fig. 3.31). It was insensitive to IAA and NAA, whereas treatment with 1µM IBA resulted in a qualitative rescue of the lateral root phenotype. The IBA-induced lateral roots were stunted and grouped closely together, giving rise to small clusters with several lateral roots (Fig. 3.31).

Interestingly, a co-treatment with the NO production inhibitor c-2-Phenyl-4,4,5,5-tetra-methylimidazoline-1-oxyl 3-oxide (cPTIO) inhibited the rescuing effects of IBA. Moreover a co-treatment with the NO donor S-Nitroso-N-acetyl-DL-penicill-amine (SNAP) increased the quality of the rescue immensely. Treatment with SNAP alone resulted only in a partially rescue with about 60% of all individual mutants showing stunted lateral roots, delayed by one or two days.

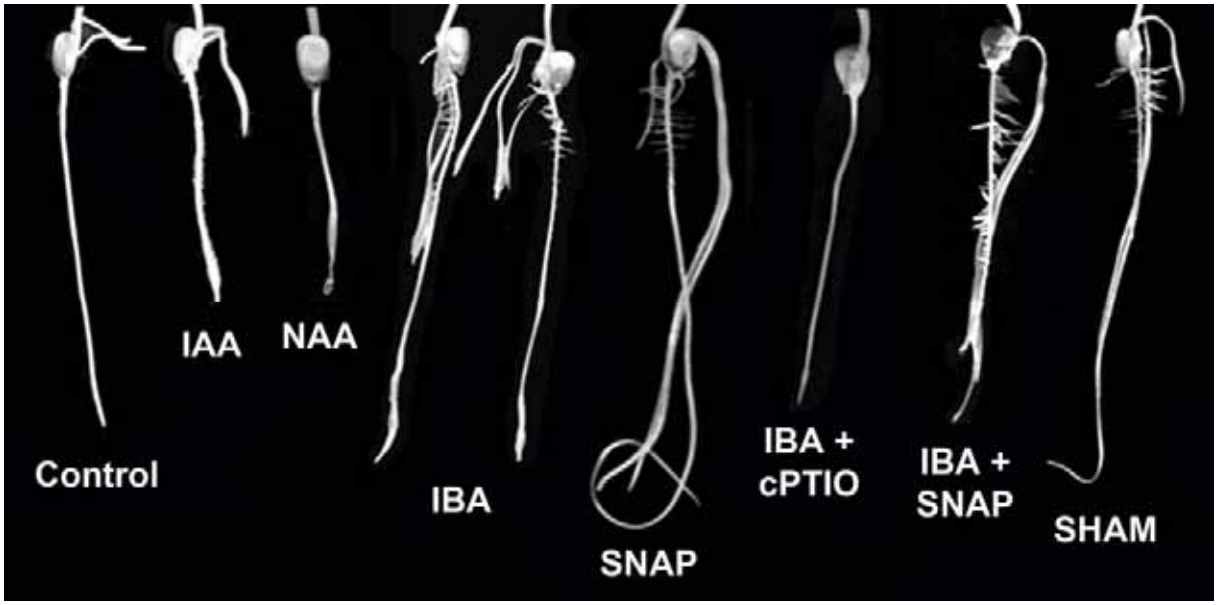

Fig. 3.31.
The maize mutant *lrt 1*
One week old maize plants were incubated for 48 hours with 1µM auxins and/or 10µM inhibitors. Shown are typical examples, N = 25. Note that the plant representing the SNAP treatment is 11 days old.

4. Discussion

4.1. A New Model of Cellular Auxin Transport

Active efflux (pumping out) of auxin was hypothesized to be mediated by putative auxin carriers inserted in polarly localized plasma membrane domains. About ten years ago, the first of these carriers has been identified in several laboratories and subsequent localization of the carrier protein and its analysis in auxin transport-defective mutants confirmed almost all expectations, i.e. the polar plasma membrane localization of the carrier fit the measured direction of PAT. Numerous papers have been published since on both efflux carriers of the PIN family and influx carriers of the AUX family (for recent reviews see Teale et *al.* 2006; Blakeslee et *al.* 2005; Sieberer et *al.* 2005; Vieten et *al.* 2007; Bandyopadhyay et *al.* 2007). All this has been interpreted as the final evidence for the chemiosmotic theory. It is an interesting phenomenon that this theory is now generally accepted; despite the fact that several published observations contradict several of the predictions made by this theory (e.g. Geldner et *al.* 2001).

4.1.1. Several aspects of PAT contradict the classical chemiosmotic theory

Importantly, this theory predicts that the localization of PINs in the plasma membrane is tightly linked with the activity of polar auxin transport (PAT) at the plasma membrane. Both pharmacological and mutant approaches document, that this is not the case. The classical chemiosmotic theory (Fig. 4.1.) cannot explain the rapid PAT inhibition induced by Brefeldin A (BFA) within a few minutes (Delbarre et *al.* 1996; Mancuso et *al.* 2005; Delbarre et *al.* 1998), when the auxin transporters are still at the plasma membrane (Paciorek et *al.* 2005). Moreover, the most likely BFA target is an ARF-GEF protein, which is necessary for PIN1 recycling. A genetic modification of this protein results in a BFA resistant mutant with undisturbed PIN1 localization after the secretion inhibitor treatment (Geldner et al. 2003). The chemiosmotic theory completely ignores vacuoles and endosomes as possible compartments participating in PAT.

Published papers do not critically address these issues and the concept of the classical chemiosmotic theory has remained unchallenged. Several circumstances, the availability of a new, specific auxin antibody, the Steedman's wax embedding technique and the recently characterized maize mutants impaired in PAT have made it possible to reinvestigate several key aspects of polar auxin transport in this work. As a consequence, several new observations have been made, which are incompatible with the classical chemiosmotic theory of PAT. First, auxin is enriched within the endosomal membrane compartment at the auxin

transporting end-poles of cells active in PAT, but not in cells impaired in PAT, either due to inhibitors or as a result of genetic lesions. Next, in maize mutants affected in polar transport of auxin (*semaphore1, rum1 and lrt1-rum1*), PIN1 localizes abundantly to the end-poles but as judged from the immunolocalization results presented here, auxin is depleted from the end-poles. At the same time F-actin is also missing and BFA-treatment does not induce BFA-compartments in these mutants. In addition, biochemical analysis like the 2 phase portioning and sucrose gradients (see Chapter 3.1.1.3) confirmed the obtained cytological data that PIN1 is still at the plasma membrane after 10 minutes of BFA treatment, when auxin efflux is already strongly inhibited (Delbarre et *al.* 1996; Delbarre et *al.* 1998). Similar evidence is provided by forcing wild type roots to grow against the gravity vector due to placing them into thin glass capillaries. Such roots get progressively thinner and because the number of dividing cells decreases in the apical meristem due to a possible inhibited supply of auxin, which apparently can not be transported effectively against the gravity vector. Nevertheless, PIN1 in these root apices is localized properly at the cross-walls but apparently does not support auxin transport. Preliminary observations have shown, that under these conditions, BFA-induced compartments do not form, indicating that these cells do not accomplish rapid recycling of PIN1 (Markus Schlicht, Alina Schick, Dieter Volkmann, and František Baluška, data unpublished).

Moreover, three classes of PAT inhibitors, clearly separable by their chemical structure (TIBA, NPA, morphactins, see also Schneider 1970), all deplete F-actin from the end-poles and inhibit endocytosis/vesicle recycling at the same time (see Chapter 3.1.1.4). A substantial portion of the polar transport of auxin in root apices is driven by vesicle-mediated secretion regulated by the PLDζ2 activity and its product phosphatidic acid (PA). In the Arabidopsis *PLDζ2* mutant and after 1-butanol treatment, auxin fluxes in root apices measured by an IAA-sensitive microelectrode are strongly suppressed despite undisturbed PIN localization (Mancuso et *al.* 2007). Results obtained here from the study of phospholipase Dζ2 mutants and over-expressing lines (Li et *al.* 2007) as well as results obtained by the application of its signaling product, PA, support the auxin immune-localization data, that vesicular recycling and secretion, and not just the mere presence of PINs at the plasma membrane, are essential for polar cell-cell auxin transport. The *PLDζ2* mutant shows strongly reduced auxin fluxes in root apices and Brefeldin A has almost no additional negative effect on polar auxin transport in the *PLDζ2* mutant, which also fails to form BFA-induced compartments. All this is suggesting that the BFA-sensitive portion of the polar auxin transport needs PA produced by the activity of PLDζ2 (Mancuso et *al.* 2007). The tissue area, where *PLDζ2*-Expression is observed, corresponds exactly to the root apex region,

which is relevant for the PLDζ2/PA-driven vesicular secretion of auxin (Li et *al*. 2007; Mancuso et *al.* 2007). Four PINs (isoforms 1, 2, 3 and 4) are expressed in this zone of the root and three PGPs (isoforms 1, 4, and 21). This is the highest number of IAA transporters ever scored for any part of the plant body (Bandyopadhyay et *al.* 2007) It is also this region, in which the basipetal transport in the epidermis links up with the acropetal transport in the stele (Blilou et *al.* 2005). Previous results and in vivo recordings show that this particular root region has by far the highest rate of auxin transport (Mancuso et *al.* 2005; Santelia et *al.* 2006; Bouchard et *al*. 2006), so it is unique from the perspective of polar auxin transport.

There are several important conclusions with respect to the PLDζ2 activity and the role of PINs in polar auxin transport. Recycling of PINs is essential for the undisturbed polar auxin transport in root apices and this is in agreement with the observations of Geldner and coworkers (Geldner et *al.* 2001; 2003). Recycling of both PIN2 (Li et *al.* 2007) and PIN1 depends on the vesicular secretion driven by PA the product of PLD activity. The auxin transport not sensitive to manipulation of PA levels is accomplished in all probability via PGP-type ABC transporters, which are abundantly expressed in the root apex (Santelia et *al.* 2006; Bouchard et *al.* 2006; Bandyopadhyay et *al.* 2007).

4.1.2. Auxin response elements do not distinguish between IAA-signaling and polar auxin transport processes

Direct localization of IAA, using the new specific antibody, in cells of the root apex of maize failed to reveal the previously reported auxin maximum specific in cells of the quiescent centre and root cap statocytes, as shown with the DR5 promoter line of Arabidopsis (Sabatini et *al.* 1999; Friml et *al.* 2003; Ottenschläger et *al.* 2003). The IAA-labeling of Arabidopsis shows a maximum of IAA antibody fluorescence in the root tip, which is not identical to DR5 promoter line maximum. This discrepancy is not unexpected, because other auxin reporters visualize ‘auxin maxima’ at other locations. For instance, a second popular reporter the BA3 construct visualizes an ‘auxin maximum’ in those cells, which are embarking on rapid cell elongation (Oono et *al.* 1998; Armstrong et *al.* 2004). These conflicting observations indicate that these reporters just reflect particular signaling cascades feeding into the activation of different auxin-responsive transcription promoters, but they do not necessarily reflect a maximum of IAA-molecules. There are also several other problems associated with auxin-response reporters. For example, different auxins (IAA, NAA or 2,4-D) and several other substances like brassinolides can induce transcription of auxin response reporters (Nakamura et *al.* 2003; Nemhauser et *al.* 2004), and the root specific auxin signaling inhibitor Terfestatin A,

which causes, as one would expect, the disappearance of the DR5 root tip maximum (Yamazoe et *al*. 2005), leads only to a small dislocation of the auxin maximum, when looked at it with the auxin antibody (see chapter 3.1.1.2). So, with regard to these problems, it is surprising that in many publications the DR5-signal is taken as the true representation of Auxin distribution in plant tissue (e.g. Sabatini et al. 2003).

One should also consider the possibility, that a maximum activity of the expression of auxin-response reporters reflects a prolongation of IAA transit through the cells, i.e., in tissue regions, where Auxin becomes redirected (Bandyopadhyay et al. 2007), rather than reflecting a local rise in concentration.

All this makes it obvious that, in order to understand the nature of PAT, the direct localization of auxin with a specific antibody is essential. Unfortunately, those antibodies, which are available and currently in use, recognize auxin as well as auxin conjugates (Aloni et *al.* 2006b). The newly generated antibody used in this thesis work (see also Schlicht et al. 2006), which is mono-specific for IAA and does not recognize IAA conjugates, solves this problem. The data show, that a prominent cell compartment in root tissue, which accumulates auxin, is the nucleus. This is not surprising, particularly with regard to the auxin-responsive elements discussed above, but especially because of the nuclear auxin receptor TIR1, which is active in its auxin-bound form within nuclei, activating transcription of auxin-regulated genes (Dharmasiri et *al.* 2005; Parry and Estelle 2006). Further, actin-enriched cell-end poles and adjacent endosomal compartments are identified as auxin enriched domains in cells of the root apex. This finding has far-reaching consequences for the field of auxin research. Cellular end-poles conceptually characterized as “plant synapses”, (Baluška et *al.* 2003, 2005a) emerge as subcellular domains specialized for the transcellular transport of auxin along cell files. The currently popular version of the chemiosmotic theory is considering only the auxin pools, which are localized within the pH neutral cytoplasm and the acidic cell wall compartment (apoplast, for recent reviews and dispatches: Friml et *al*. 2003; Friml and Wisniewska 2005; Leyser 2005; Moore 2002; Blakeslee et *al*. 2005). This assumption ignores any possible contribution of acidic endosomes for the maintenance and regulation of PAT. The immunofluorescence data on auxin localization reveal that auxin is accumulated within endosomes, which communicate with the auxin-transporting cell-sites (Baluška et *al.* 2003, 2005a). In accordance with previous observations on the partitioning of endosomal components in BFA-induced compartments, PIN-proteins and auxin get also aggregated into BFA-induced compartments, which lends additional support to the concept that both are bona fide endosomal components. Importantly, the auxin-enriched endosomes may represent the elusive BFA-sensitive source of auxin from which auxin is secreted

out of cells via BFA-sensitive processes (Baluška et *al.* 2003). Auxin accumulating endosomes may also act as intracellular "auxin vacuum cleaners" (Baluška et *al.* 2005a; Samaj et *al*. 2006), which would effectively remove all free auxin from the orifices of plasmodesmata in order to prevent their "uncontrolled" diffusion from cell-to-cell. This function of auxin-accumulating endosomes would be particularly important during early embryogenesis, when plasmodesmata are known to allow free passage of signaling molecules, hormones and peptides, demonstrating that all embryonic cells are part of a single syncytium (symplast) (Stadler et *al.* 2005; Kim et *al*. 2005). Free and uncontrolled passage of auxin within this syncytium would be incompatible with the intricate local and polar auxin accumulations in early embryos (Friml et *al.* 2003). Cells of the root apex transition zone are unique also with respect to the actin organization. They assemble F-actin enriched plasma membrane domains at the end-poles, which serve as dynamic platforms for rapid endocytosis and high rate of vesicle recycling. Those tissues, which are active in PAT, such as the stelar cells accomplishing acropetal PAT and the cells of the epidermis and outer cortex performing basipetal PAT, are enriched in F-actin (Baluška et *al*. 1997, 2003, 2005a, b; Schlicht et *al*. 2006).

F-actin at the end-poles allows effective cell-cell communication based on secretory processes as is known from neuronal and immunological synapses (Baluška et *al.* 2003, 2004, 2005a, b). For instance, auxin that has been secreted into the cross-wall space has been reported to elicit electric responses in the adjacent cells (reviewed in Baluška et *al.* 2004). All this indicates that auxin acts, in addition to its hormonal and morphogen-like properties, as a neurotransmitter-like agent (e.g. Baluška et *al.* 2003). Other puzzling data also fall into place. For instance, the rapid blockage of PAT after cold exposure (Wyatt et al. 2002), which is known to block endocytosis in root cells (Baluška et al. 2002) and an almost immediate recovery of PAT after returning the plants to room temperature (Wyatt et *al.* 2002; Nadella et *al.* 2006). Another example, the finding that synaptic proteins occur in plants, like synaptotagmin and BIG, which are present in plant and animal genomes. BIG has similarity to the synaptic protein CALLOSIN/ PUSHOVER driving synaptic signal transmission at neuromuscular synapses, is essential for PAT in plants (Paciorek et *al.* 2005b; López-Bucio et *al.* 2005) and its action is related to endocytosis and vesicle recycling (Baluška et *al.* 2003, 2005a). Other puzzling facts are beginning to make sense now, namely the observation that high concentrations of extra cellularly applied auxin inhibit endocytosis, and BIG in a still unknown mode is important for this unexpected auxin action (Paciorek et *al.* 2005). BIG is relevant also for the endosomal BFA-sensitive secretion, because *lpr1* mutant, which is allelic to *BIG*, is phenocopied by treatment of wild-type seedlings with BFA (López-Bucio et *al.* 2005). Obviously, the classical chemiosmotic model has difficulties to explain the rapid blockage of the

auxin export after inhibition of vesicular secretion with BFA and monensin (Paciorek et *al*. 2005b; Wilkinson et *al.* 1994; Delbarre et *al.* 1996, 1998; Mancuso et *al.* 2005). Furthermore, it cannot explain rapid inhibition of PAT after cold exposure (Wyatt et *al.* 2002; Nadella et al. 2006) and after the application of actin polymerization inhibitors (Sun et *al*. 2004; Li et *al.* 2005). Delbarre et *al.* (1998) reported that auxin efflux from plant cells is blocked with agents affecting proton gradients and intracellular pH status. The latter authors interpreted these data only from the perspective of the classical chemiosmotic theory. However, these findings appear in a new perspective if one considers the accumulation of auxin within endosomes. Intriguingly, the activity of H+-pyrophosphatase AVP1 is involved in PAT (Hu et *al.* 2000) and this further supports the concept of secretion via endosomes as a major pathway for exporting auxin (Friml et *al.* 2005; Baluška et *al*. 2003, 2005a). Pyrophosphatases represent single-subunit H+ pumps, which generate an electrochemical gradient across delimiting membranes of small vacuoles and endosomes (Ratajczak et *al*. 1999; Rea and Poole 1999). Overexpression of AVP1 stimulates PAT, while *avp1-1* null mutants show a reduction of PAT (Li et *al.* 2005). Moreover, overexpression of AVP1 stimulates root growth (Li et *al*. 2005; Park et *al*. 2005) while null mutants develop severely disrupted roots. In addition to the vacuolar membrane, the AVP1 signal was found at punctated structures and, importantly, discontinuous sucrose gradient analysis revealed an association of AVP1 with the endosomal fraction (Li et *al.* 2005). There is no way at all of explaining all these observations with the classical chemiosmotic concept. The *Perspectives Science* article, commenting this paper suggested that AVP1 acidifies the putative X compartment (Grebe 2005). This corresponds nicely to the auxin-enriched endosomes reported here and summarized in the model (Fig. 4.1). Further support for this concept comes from the observation that VHA-a1 subunit of the vacuolar ATPase (V-ATPase), which acidifies endosomes, vacuoles and the trans-Golgi network (TGN) in plant cells, localizes to the early endocytic compartments in root cells of Arabidopsis (Dettmer et *al.* 2006). It will be important in the future to analyze PAT in the available V-ATPases mutants in Arabidopsis. The dwarf phenotype of the *det3* mutant (c subunit), which is due to lack of cell elongation (Schumacher et *al.* 1999), indicates that PAT requires both PPase and V-ATPase activities. Moreover, VHA-a1 subunit of the V-ATPase co-localizes with TGN SNAREs (Schumacher et *al.* 1999) and one of these (VTI1) is essential for basipetal PAT (Surpin et *al*. 2003). Intriguingly, PM-based PIN1 localizes properly in the polar manner (Schumacher et *al.* 1999) despite the fact that PAT is strongly affected in the VTI1 mutant, resembling the situation reported in the present study for maize mutants affected in PAT. The acidic nature of auxin and of endosomes implies that auxin relies on the continuous activity of putative vesicular transporters in order to be enriched within endosomes. The vesicular nature

of PIN2 was strongly indicated by a recent study using yeast and HeLa cells (Petrasek et *al.* 2006). In vitro mutation of PIN2 by changing Serine 97 to glycine resulted in a loss of PM localization and only a vesicular localization of PIN2 in yeast cells that accumulated auxin. It seems that PIN proteins are also functional inside the cell since yeast cells expressing the mutated version of PIN2 accumulate more auxin than control cells (Petrášek et al., 2006).

When interpreting these data, it is important to keep in mind that the endosomal interior originates from the extracellular space. This means that by transporting auxin into the endosomal interior with PIN2 efflux protein, it is removed from the cytoplasm.

4.1.3. Polar cellular localization of PIN proteins and hence PAT direction is maintained via recycling processes

The polar localisation of PINs at distinct subcellular domains corresponds with the direction of PAT, i.e., in case of a basipetal direction of transport, PINs are localized at the basal end of the cell (Gälweiler et *al.* 1998; Terasaka et *al.* 2005).

Changes of PIN localizations by different mutations or treatments from one cell pole to another, result in disturbances of PAT (e.g. Michniewicz et *al*. 2007). Evidence is growing that the dynamic recycling of PINs co-determines the polar positioning at the plasma membrane (Men et *al.* 2008; Kleine-Vehn et *al.* 2008). For example after cytokinesis, PIN2 localizes initially to both newly formed membranes but subsequently disappears from one by endocytosis, suggesting a recycling based mechanism for the establishment of asymmetric PIN localization (Men et *al*. 2008). Furthermore, it was shown that apical and basal PIN targeting pathways are regulated in part by BFA sensitive vesicle-trafficking regulators (Kleine-Vehn et *al.* 2008). The molecular target of BFA is a GDP/GTP exchange factor for small G proteins of the ARF class (ARF-GEF); in Arabidopsis it is named GNOM. PIN1 proteins constitutively cycle between endosomes and the plasma membrane in a GNOM-dependent manner (Geldner et *al.* 2001). Consequently, BFA disrupts the polarity of apical located PIN1. In epidermal cells of root tips PIN2 is located at the basal cell pole and recycles in a GNOM independent manner between sorting nexin 1 - defined endosomes and the plasma membrane (Jaillais et *al.* 2006). Consequently, BFA has no effect of PIN2 localization in those cells.

Disturbance of endocytosis by treatments targeting the actin cytoskeleton with inhibitors such as Latrunculin B (e.g. Schlicht 2004; Rahman et *al.* 2007) or else by the auxin transport inhibitors TIBA (Geldner et al 2001; Dhonuske et *al.* 2008) and NPA (Ruegger et *al.* 1997) also indicate a crucial role of endocytosis for maintaining polar orientation of PIN proteins after cytokinesis.

4.1.4. A possible role of lipid rafts for polar positioning of PINs

The cytoskeleton sorts PINs in a polar manner, but how the correct areas of the plasma membrane are marked for PIN accumulation is still unknown. Some recent publications indicate that the lipid composition in the plasma membrane plays a crucial role in this process (Men et *al.* 2008).

Lipid rafts are detergent insoluble membranes (Mongrand et *al.* 2004) with plant-specific lipid steryl-conjugates, free sterols and sphingolipids (Lefebvre et *al.* 2007). Lipid rafts in plasma membranes are hypothesized to play key roles in signal transduction and membrane trafficking (Morel et *al*. 2006; Lefebvre et *al.* 2007). Early endocytic sterol trafficking involves transport via actin dependent endosomes. Sterol-enriched endosomes are found in BFA induced compartments, suggesting a connection between endocytic sterol transport and polar sorting events (Grebe et *al.* 2003). Moreover, sterol-dependent endocytosis mediates polar localization of PIN2 (Men et *al.* 2008), as seen in the sterol-biosynthesis mutant *cpi1-1* (cyclopropylsterol isomerase1-1). This mutant has altered sterol composition and defects in PIN2 internalization causing PAT related defects such as reduced gravitropic bending.

Furthermore, the *smt1*^{orc} mutant, that lacks a sterol methyltransferase, displays several noticeable cell polarity defects; among other things, the polar initiation of root hairs is more severely randomized. Sterol methyltransferase is required for the appropriate synthesis and composition of major membrane sterols. In *smt1*^{orc} mutants, polar auxin transport is disturbed and expression of the auxin reporter DR5-GUS is aberrant. Consistently, the membrane localization of PIN1 and PIN3 proteins is disturbed, suggesting that a balanced sterol composition is a major requirement for cell polarity and auxin efflux (Grebe et *al.* 2003).

Preliminary results, shown here in Chapter 3.1.4, indicate that PIN proteins are located in detergent resistant membrane fractions (DRM-fractions), but in different quantity. PIN2 and PIN1 are very strongly enriched in lipid rafts, whereas only small amounts of PIN3 and PIN4 proteins are found. Moreover, several MDR/PGP ABC transporters (e.g. PGP1, PGP4, PGP19) are also located in lipid rafts (Murphy et *al.* 2002; Geisler et *al.* 2003; Terasaka et *al*. 2005; Bhat and Panstruga 2005; Morel et *al*. 2006; Lefebvre et *al.* 2007). PGP/ABC-transporter show auxin transport ability across the plasma membrane (e.g. Geisler et *al.* 2003) and can build complexes with PIN-proteins (shown in Arabidopsis for PIN1-PGP19 and PIN1-PGP1 respectively by Blakeslee et *al.* 2007). Heterologous systems of yeast and HeLa cells expressing plant PGPs and/or PINs show that PINs and PGPs form functioning

complexes with different auxin efflux/influx capacities depending on the binding partners (Blakeslee et *al.* 2007; Bandyopadhyay et *al.* 2007).

Both PGP and PIN gene expression and the distribution of the corresponding proteins are regulated by light and other factors (Geisler et *al.* 2003). It is also likely that specific PGP–PIN interactions occur in cells in which both components are expressed and that other additional factors, may regulate their interactions.

One such candidate is TWD1 (twisted dwarf 1) also named UCU2 (ultracurvata 2) an immunophilin-like protein, which can interact with PGP1 and modulates indirectly PGP1 efflux activity. TWD1 acts as a positive regulator of PGP mediated long-range auxin transport (Geisler et *al.* 2003; Pérez-Pérez et *al.* 2004; Bouchard et *al.* 2006).

The auxin transport inhibitor N-1-naphylphtalamic acid (NPA) display its ability to inhibit PAT by binding to auxin transporting complexes (e. g. Jacobs and Rubery 1988) and by disturbing the polar PIN positioning. Both PGP1 and TWD1 bind NPA unless they are present as a PGP1-TWD1 complex, which is less sensitive to NPA (Geisler et *al.* 2003; Bouchard et *al.* 2006).

NPA is a synthetic inhibitor, but naturally occurring flavonoids can bind and compete with NPA for the same protein domains (e.g. Peer et *al.* 2004). Flavonoids are plant-specific phenylpropanoid compounds, which can modulate the gravity response. Except for the competion to NPA for the same binding domains (NPA Binding Domains = NBDs) and the existence of mutants with altered flavonoid levels that show disturbed PAT (which can be rescued by externally applied flavonoids) neither the identity of specifically involved flavonoids nor their exact mode of action are known. Transport assays with PIN proteins indicate an indirect role of flavonoids on PIN expression, localization and trafficking (Peer et *al.* 2004; Peer and Murphy 2007).

Flavonoids have a brought spectrum of activity ranging from ROS scavengers to modulators of membrane fluidity. This makes it difficult to discern their role in PAT. But it is thought that flavonoids act as non-essential auxin transport inhibitors, which can modulate PAT by influencing NBD-proteins and such mediate alterations of auxin concentrations (Peer et *al.* 2004, 2006). Interestingly, flavonols are potent inhibitors of protein phosphatases and kinases. Taken into account that PIN localization is controlled by antagonistic phosphorylation/dephosphorylation by the AGC-kinase PID (PINOID) and a PP2A protein phosphatase, respectively (Friml et *al.* 2004; Shin et *al.* 2005; Michniewicz et *al.* 2007), a possible pathway for flavonol activity in polar PIN positioning seems to emerge.

In addition, a novel function of flavonols was shown recently, in that agravitropic root growth of PIN2 knockout mutants was rescued by low concentrations of flavonols that do not inhibit PAT. A laterally asymmetric distribution of PIN1 in the root cortex occurred and root growth followed the gravitropic vector after flavonol treatment in the mutant (Santelia et *al.* 2008).

PIN1 and PIN2 have redundant roles in size control of the root meristem and PIN1 can replace PIN2, when ectopically expressed and localized at the basal cell pole of epidermal cells (Wisniewska et *al.* 2006). Moreover, after flavonol treatment PIN1 showed the same localization at the basal cell pole as PIN2 in the epidermis and apical localization in cortex cells. It is important to note, that NPA is not able to induce asymmetrical PIN1 distribution and could not rescue gravitropic bending of PIN2 mutant. Moreover the flavonol permitted gravitropic bending in PIN2-mutants is still NPA sensitive (Santelia et *al.* 2008). This shows nicely that this flavonol activity is not linked to NBDs. PIN1 and PIN2 are redundant in function and are controlled by specific tissue expression and different interaction partners. Obviously, flavonols have the capacity to change these features.

A control of PID and PPA2 activity could at least partly explain this modulation activity of flavonoids. These two enzymes are antagonistically controlling polar sorting of PIN proteins in root tissues (Michniewicz et *al*. 2007). A loss of PP2A activity or a PID overexpression leads to an apical-to-basal PIN polarity shift in roots, as was shown for PIN1, PIN4 and PIN2 (in cortical cells). Interestingly, the basal localization of PIN2 in epidermal cells remained unaffected (Michniewicz et *al.* 2007) by any changes of the PID/PP2A phosphorylation balance.

Moreover, the flavonol accumulating mutants tt7 and 3 (*transparent testa7 and 3*) show increased PIN1 expression in cortex cells and increased expression of PIN4 but no difference of PIN2 expression (Peer et *al.* 2001). Level and composition of flavonols only modulate expression of the PINs, which are affected by PID/PP2A mediated polar positioning. Interestingly, PINOID is activated by PDK1 mediated trans-phosphorylation. The binding of plasma membrane located PID to PDK1, which is a component of the detergent resistant membrane fraction raises the possibility that PID could be recruited to lipid rafts and activated by PDK1 (Zegzouti et *al*. 2006).

In plants PGPs and TWD1 are located within lipid rafts and are targets of flavonoid action and several members of the PIN-family are more or less abundantly found in DRMs and their expression, polar localization and activity react strongly to altered lipid composition of the plasma membrane (Grebe et *al.* 2003; Men et *al.* 2008; Santelia et *al*. 2008). PIN1 subcellular localization

is sensitive to flavonoids, and tissue-specific PIN1 distribution is auxin responsive at the root tip. PIN2 localization and distribution are neither auxin nor flavonoid responsive, but PIN2 expression increases in the absence of flavonols (Peer et *al.* 2004).

The two most frequently occurring flavonols Kaempferol and Quercecitin accumulate in the root cap and the transition zone (Peer et *al.* 2001), strikingly similar to auxin signaling maxima shown with reporter constructs. The subcellular localization shows that a good part of flavonoids is associated with the plasma membrane at the cross walls.

Increasing evidence shows that PIN proteins are internalized into cells by at least two different pathways. Firstly, clathrin mediated endocytosis powers the constitutive route of basally located PIN1 and PIN2 uptake (Dhonukshe et *al.* 2007) to BFA sensitive GNOM-positive endosomes and secondly, the above mentioned sterol dependent endocytosis, which controls at least partly PIN2 internalization in a BFA insensitive manner (Men et *al.* 2008). Both pathways are likely connected.

In mammals clathrin mediated and lipid raft based endocytosis are two mutally excluding pathways. But it is important to note, that plant detergent resistant membrane fractions (DRM-fractions) possess a much more heterogeneous lipid composition than mammalian DRM fractions (e.g. Borner et *al.* 2005). This opens the possibility, as has been observed in yeast (Malinska et al. 2003), that in plants, several subclasses of lipid rafts exist.

Also protein classes, which are enriched in plant DRM fractions can be quite different from those in mammalian lipid rafts. GPI anchored proteins appear to be common components in plant and animal lipid rafts (Borner et *al*. 2005; Sangiorgio et *al.* 2004), however, proteomic analyses of plant DRMs have shown that several proteins of the clathrin depend endocytosis machinery are found in lipid rafts (Mongrand et *al*. 2004; Morel et *al.* 2006) In mammalian is the lipid raft mediated endocytosis clathrin independend (Nichols et *al.* 2001; Kirkham et *al.* 2005). Taken the results on PIN endocytosis, it appears that both, clathrin and sterol derived mechanisms (Dhonukshe et *al.* 2007; Men et *al.* 2008) are linked together in plants.

The question remains, how PINs are sorted in- or out of lipid raft domains? An important role will be played by their interaction-partners, such as PGPs and PINOID, which have been mentioned above. A recent publication shows even such a role for PGP19 to sort PIN1 in detergent resistant membrane fractions (Titapiwatanakun et *al.* 2008). Further studies will be necessary to shed light on the processes which govern correct sorting and positioning of PINs.

Taken together it may be concluded that lipid rafts emerge as signaling platforms, which play an important role in polar auxin transport and auxin related signaling. They are controlled by

flavonoids, which modulate PGP (PGP-TWD1) activity and may also regulate polar PIN localization via indirect recruitment into lipid rafts by the modulation of PID/PP2A activity.

4.1.5. An update of the classical chemiosmotic model for PAT

Considering all points of inconsistency discussed above with regard to the chemiosmotic model, there is an urgent need for the proposition of an updated, better fitting version of this concept to explain PAT. Besides acidic cell walls and neutral cytoplasm, the acidic endosome emerges as a new important player in the transcellular pathway of auxin transport. Regulated secretion out of cells via secretory endosomes, would then be accomplished by a quantal efflux of protonated auxin into the extracellular space. From there, it can either freely diffuse back to the same cell or into adjacent cell. In addition, adjacent cells could also import auxin through the activities of putative auxin transporters at the plasma membrane and/or via endocytosis of auxin molecules embedded within cell wall material like pectins and hemicelluloses. In accordance with this latter notion, it has been shown that the internalization of these cell wall molecules is particularly active at the auxin transporting end-poles (Baluška et *al.* 2002, 2005a; Samaj et *al.* 2004, 2005a; Dettmer et *al.* 2006). The "synaptic" nature (Baluška et *al.* 2003, 2005) of these end-poles has been strongly supported recently by showing that PIN1 localization to these sub-cellular domains is dependent on the contact between cells (Boutté et *al.* 2006). As soon as the cells lose their contact between each other, due to a long-term absence of microtubules, PIN1 rapidly redistributed from these domains to the whole plasma membrane (Boutté et *al.* 2006).

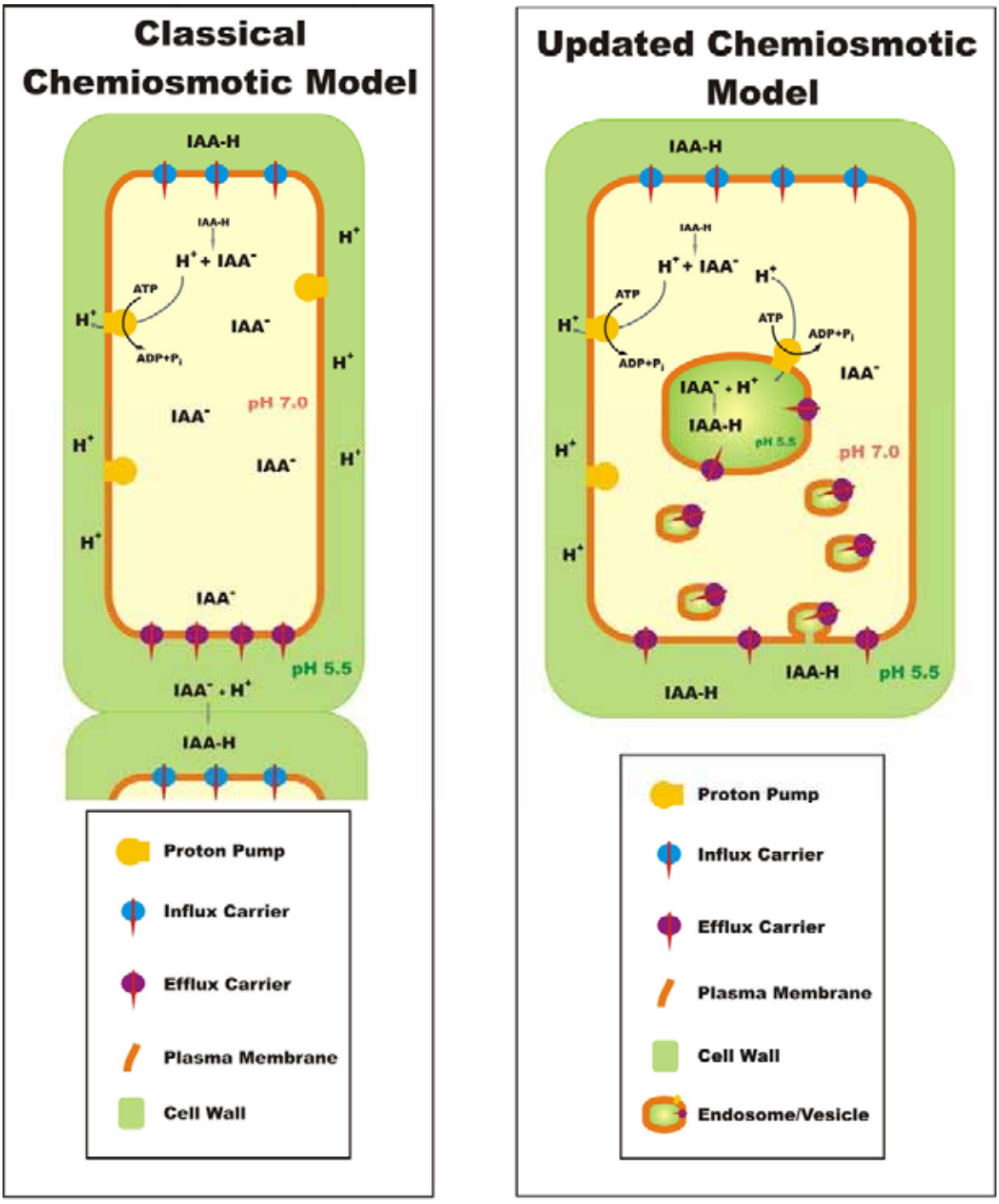

Fig.: 4.1. Classical and updated model of cellular auxin transport
The updated model postulates endosomes and vesicle recycling as essential parts of the auxin transport machinery.

4.1.6. Implications of auxin secretion

One of the most characteristic feature of polar auxin transport, which still awaits its biological explanation, is that the auxin transport in the root cap columella is tightly linked to gravity, i.e., its direction is always perpendicular to the gravity vector (Dolan 1998; Ottenschläger et *al.* 2003). Within a few minutes, a gravistimulated root apex curves downward after its auxin-secreting cell poles have shifted to the transversal position with respect to the gravity vector. PIN3-mediated auxin asymmetry starts to become detectable in the root cap within a few minutes (Friml et *al.* 2002a). Obviously, auxin is released out of root cells all the time towards the physical bottom facing the center of gravity, this is irrespective of the type of organ and of the preset polarity in this organ. In other words, internal genetic and epigenetic programmes, which are extremely robust so that single or even double-gene mutations are unable to change them, are prone to be easily overridden by physical information from the environment. One can explain this gravity-dependent secretion of auxin via differential stretch-stress reactions at the plasma membrane which is expected, due to protoplast settling within the casing of the wall, to have the highest values at the physical bottom and the lowest values at the physical top of cells (Baluška et *al*. 2005a, 2007). As high tension stress of the plasma membrane can be relieved by exocytosis, while on the other hand low tension stimulates endocytosis, the secretory model of auxin transport has the power to explain gravity dependent auxin transport. This unique feature of gravisensing at cell poles implies that the poles are inherently asymmetric not only molecularly but also mechanically. Importantly, epigenetic physical information, underlying the inherent mechanical asymmetry of the end poles, is at the heart of the plant synapse concept which describes auxin secretion in response to the gravity vector as the basic mechanis that provides flexibility to the shaping of the plant body (Baluška et *al.* 2005a, 2007).

Future studies should focus on both endosomes and regulated vesicular recycling in order to unravel critical and often neglected details of the polar transport of auxin across cellular boundaries in plant tissues. Vesicular secretion of auxin can be expected to be under tight control allowing quantal release of auxin after perception of specific stimuli. It can be expected that this feature will serve to feed extracellular auxin into various signalling channels, i.e., by manipulating levels of reactive oxygen species and nitric oxide as well as lipid signaling molecules (Joo et *al.* 2005; Lamattina et *al*. 2003; Lanteri et *al.* 2006, 2008) .

If the quantal release of auxin after an appropriate signal could be proven, it will have diverse consequences for the field of plant developmental biology. Among other aspects, vesicle recycling and secretion-based auxin efflux can be envisioned to act as the elusive flux sensor in the so called canalization theory (see also merks et *al.* 2007). This would then make new

hypotheses dispensable such as the travelling-wave hypothesis, which has recently been proposed in order to explain the dependency of cellular PIN1 expression from auxin maxima formation during vascular development in leafs (Merks et *al.* 2007).

The current status of auxin as a plant hormone seems to be based on a much too narrow perception of its multipurpose mobile signaling functions in the developmental or environmental context. It acts as plant hormone, morphogen, neurotransmitter-like elicitor and even transorganismic communicator molecule. It is used by fungi and bacteria such as Rhizobia and Mycorrhiza to establish symbiosis by manipulation of auxin flow and by using auxins as a means of communication (van Noorden et *al.* 2006; Ditengou et *al*. 2003).

4.2. D'orenone blocks polarized tip-growth of root hairs by interfering with the PIN2-mediated auxin transport network in the root apex

Highly polarized tip-growth of root hairs is relatively well understood and represents one of the best examples of polar cell growth inherently linked to signaling pathways via the dynamic cytoskeleton and endosomal vesicular trafficking (Baluška *et al.* 2000; Šamaj *et al.* 2004). Signal-mediated actin polymerization (Volkmann and Baluška 1999; Staiger 2000) is essential for tip-growth of root hairs; such growth stops immediately after exposure to latrunculin B (Baluška *et al.* 2000; Voigt et *al.* 2005a; de Ruijter et *al*. 1999). It is shown here, that after growing root hairs of Arabidopsis were exposed to D'orenone, their tip-growth stopped within just a few minutes and was associated with the disintegration of the vesicle-rich secretory 'clear zone' at the apex of the root hair. At the same time, the vacuoles protruded into the very tip and consequently tip growth was stopped. Further analysis revealed that D'orenone also targets other processes, which are essential for root hair tip growth, including actin polymerization, vesicle trafficking, as well as reactive oxygen species (ROS) and cytosolic free Ca^{2+}.

4.2.1. Root hair growth

To determine cellular target(s) of D'orenone, the actin cytoskeleton was analyzed, which is essential for tip-growth of root hairs (Baluška et *al.* 2000; de Ruijter et *al.* 1999). Indeed, the dynamic actin cytoskeleton proved to be extremely sensitive towards D'orenone: apical F-actin meshworks were lost within 30 minutes of treatment at a low concentration of D'orenone (10 μM) and only immobile actin bundels orginating from the hair base remained (see chapter 3.2.2.). Obviously, D'orenone affects the tip-focused actin polymerization machinery linked to signaling cascades (Šamaj et *al.* 2002, 2004; Huang et *al.* 2006) and partially mimics the effects of Latrunculin B, a potent inhibitor of actin polymerization (Baluška et *al.* 2000, 2001; Šamaj et *al.* 2002). This implies that putative D'orenone targets could be linked, directly or indirectly, to the actin polymerization machinery. In addition, D'orenone also mimics some effects of Wortmannin (Jaillais et *al.* 2006), an inhibitor of PI(3)K kinase, which blocks endocytosis and affects endosomes (for plant cells, see Lam et *al.* 2007).

The artificial dissipation of the tip-focused calcium gradient with the calcium ionophore A23187 has the same effect (Wymer et *al.* 1997) and disintegrates the vesicle-rich 'clear zone' (Preuss et *al.* 2006) in the same way as D'orenone does (see chapter 3.2.2.). The dynamic turnover of the actin cytoskeleton is controlled not only by Ca^{2+} but also by ROS generated by the plasma membrane protein NADPH oxidase. Both are essential for the polarized tip-growth (Foreman et *al*. 2003; Rentel et *al.* 1994; Carol et *al*. 2005). It is shown here (chapter 3.2.2) that

D'orenone inhibited the production of ROS, in contrast to the well-characterized NADPH oxidase inhibitor DPI (Foreman et *al.* 2003) delayed. Indicating that NADPH oxidases are only secondary targets of D´orenone. A recently released publication revealed an important secondary ROS-source in root hairs, PI(3)K kinases controlled endosomes (Lee et *al.* 2008). By a similar method, as presented here (results section 3.2.) This study uses a similar method for the co-localisation of a ROS sensitve dye with cell organelles as shown here (see chapter 3.3.4). A disruption of endosomal motility and membrane fusion processes by LY294002, an inhibitor of PI(3)K kinase, or root hair specific *FYVE* overexpression led to a reduced tip orientated ROS gradient in root hairs.

Growth of Arabidopsis root hairs stops within just a few minutes after the exposure to D´orenone which mimics some effects of the PI(3)K inhibitors wortmannin (Jaillais et *al.* 2006) or LY294002 (Lee et *al.* 2008). Other effects of wortmannin and LY294002 differ from the D'orenone-induced effects. I.e., both affect growth of root hairs and primary roots and both inhibit root gravitropism as well (see Jaillais et *al.* 2006, Joo et *al*. 2001, 2005). A further difference between D'orenone and PI(3)K kinase inhibitors is, that the application of exogenous auxin fully rescues all effects of D'orenone on root hairs, but not the effects of PI(3)K kinase inhibitor.

4.2.2. PAT influences root hair growth

At low concentrations (below 5 μM), D'orenone effectively blocked tip growth of root hairs but did not affect growth of the main root. Even at concentrations of up to 40 μM, D'orenone did not inhibit primary root growth significantly but, instead, promoted the formation of lateral roots. Moreover, D'orenone rapidly and prominently activates the DR5-promoter suggesting that this apocarotenoid interacts with auxin action at the root apex. As PINs localize dynamically to the plasma membrane and become rapidly internalized, which can be demonstrated by treatment with the vesicle recycling inhibitor brefeldin A (Geldner et *al.* 2001; Baluška et *al.* 2002; see also first part of this work). Moreover, vesicular trafficking of PIN2 is relevant for its proteasomal degradation (Sieberer et *al.* 2000; Abas et *al.* 2006) which leeds when prevented to an accumulation of PIN2 within multivesicular bodies (Jaillais et *al.* 2006, 2008; Jaillais and Gaude 2007).

Exogenous auxin fully rescues the D´orenone-inhibited root hairs, resembling the situation when overexpression of diverse auxin efflux transporters in trichoblasts imposes a block on the tip-growth of root hairs that can be overriden by exogenous auxin (Lee and Cho 2006; Cho et *al.* 2008). All this is in agreement with the model, originally proposed by Lee

and Cho, according to which the tip-growth of root hairs is tightly controlled by critical endogenous levels of auxin within the trichoblasts (Lee and Cho 2006; Cho et *al.* 2008). The most critical question in order to understand the D´orenone action is the identity of the molecular target(s) of this compound.

The obvious candidate is PIN2 as this is the auxin efflux transporter expressed and active in root hair trichoblasts driving basipetal auxin transport (Müller et *al.* 1998; Rashotte et *al.* 2000) toward the transition zone and distal elongation zone (Verbelen et *al.* 2006), where the auxin stream is redirected from the root periphery towards the central cylinder to join the acropetal auxin stream (Blilou et *al.* 2005). In support of this scenario, it is shown here (chapter 3.2.3) that D'orenone prominently increases PIN2 protein abundance and shifts the PIN2 domain from the transition zone into the elongation zone. In that respect, D'orenone resembles the effects of brassinosteroids (Li et *al.* 2002). Because PIN2 transcription is not affected, it may be concluded that D'orenone extends the half-life of PIN2 protein via a manipulation of proteasomal degradation (Sieberer et *al.* 2000; Abas et *al.* 2006). Indeed, PIN2 degradation is promoted in the upper side of gravistimulated roots, but slowed down in the lower side (Abas et *al.* 2006; Jaillais et *al.* 2006) and strong over-stabilization of PIN2 by mutation of the protein results in defective root gravitropism (Abas et *al.* 2006).

It is further shown (chapter 3.2.3) that an increase of PIN2 occurs in D'orenone exposed roots within vacuole-like compartments, resembling the increased vacuolar localization of PIN2 in the PIN2 over-expressing line (Abas et *al.* 2006). Similar vacuolar-like PIN2 localization was reported after treatment of roots with the phosphatidyl inositol-3-OH kinase inhibitor wortmannin (Jaillais et *al.* 2006) as well as the actin polymerization inhibitor latrunculin B (Rahman et *al.* 2007). This strengthens the hypothesis that D'orenone targets processes, which are related to PIN2 degradation, causing slower turn-over and increased protein levels of this auxin efflux carrier. Interestingly, D´orenone pre-treatment prevents fast transfer of PIN2 from the plasma membrane into BFA-compartments. Only longer BFA treatments are sufficent to relocate PIN2.

As sorting nexin 1 - defined endosomes are involved in both recycling and targeting of PIN2 for degradation (Jaillais et *al.* 2006, 2008; Jaillais and Gaude 2007), further studies will focus on this critical sorting platform of root cells, in order to understand how it integrates incoming sensory information to be fed into the regulatory circuits of adaptive behaviour.

Two mutant lines which differ in the stringency of PIN2 degradation helped to identify PIN2 as the potential D´orenone target. The *arg1-2* line, which represents a weak phenotype still possessing small amounts of PIN2, still reacts to some extend to D'orenone exposure and its

agravitropic behavior can be rescued by D´orenone. On the other hand, the *eir1* line, which is a strong phenotype completely lacking PIN2 protein is not sensitive to D'orenone. This provides crucial genetic evidence that PIN2 is a D'orenone target and this may well be the same in the case of roothair growth.

Overexpression of the ABC-transporter, PGP4, which shares the auxin transporting abilities with PIN2, leads to the inhibition of root hair growth, i.e. an overall length reduction (Cho et *al.* 2008). This could mean that PGP4 is another potential target of D´orenone. However, this and other components of PAT are clearly of secondary relevance as D´orenone targets.

D'orenone has been previously postulated as an early intermediate in the biosynthesis of trisporic acids which act as chemical signals between the (+)- and (-)-mating types of zygomycetes (Gooday 1978, 1983; Gessler et *al.* 2002; Schachtschabel et *al.* 2005; Schachtschabel and Boland, 2007). Even slight structural modifications of D'orenone result in a strongly reduced activity of the compound. In particular, the low activity of the 3,4-dihydro derivative is important, since this structural modification separates D'orenone from the entire group of structurally related fungal trisporates, which act as morphogenetic signals between the mating partners of zygomycetes.

It is tempting to speculate that this ketone or a closely related apocarotenoid could resemble or mimic a still unknown endogenous retinoid signal molecule that interacts with particular branches of the auxin signaling pathways (see also Bennett et *al.* 2006). This scenario would be consistent with the fact that primary root growth remains virtually unaffected, whereas root hair growth is clearly inhibited, concomittant with an increased amount of PIN2 protein and an enlarged and shifted PIN2 expressing tissue domain in the D'orenone-exposed root apices. It is interesting to note, that D'orenone is produced, along with other apocarotenoids already by cyanobacterial enzymes *in vitro* (*Synechocystis* spp.). Even higher plants seem to be able to generate D'orenone from certain apocarotenoids as has been recently shown for a carotene oxygenase from rice (Alder et *al.* 2008).

In conclusions, D´orenone is a hormone-like organismic signalling molecule, resembling closely hypothetical branching factors (Sieberer et *al.* 2006; Bennett et *al.* 2006), and/or as an inter-organismic signalling molecule for complex fungal/nematode – plant/root communication (Prusty et *al.* 2004; De Meutter et *al.* 2005: Bianco et *al.* 2006a,b; Curtis 2007). D'orenone has the potential to become a valuable tool, with which to dissect those integrated elusive processes that underlie the sensory-driven PIN2-mediated root growth in general (for salt stress see *Sun* et *al.* 2008; Li and Zhang 2008), and distinguish them from those processes controlling polarized tip-growth of root hairs (Šamaj et *al.* 2004).

In the root apex, D'orenone specifically interacts with PIN2-mediated auxin transport and signalling (see also Fig. 4.2). D'orenone holds the key for understanding how the integrated auxin signaling is linked to the complex auxin transport networks of the root apex.

How D´orenone influences PIN2 in roots, still remains to be answered. D´orenone alters expression and distribution of PIN2 and manipulates plasma membrane recycling rate. D´orenone action could be targeting PIN2 at the plasma membrane directly or by remodeling of lipid raft composition and/or localisation. In this scenario, the primary target of D'orenone could be the lipids of the plasma membrane themselves. D'orenone would then target primarily the plasma membrane fluidity (e.g. lipid rafts). This would secondarily affect signalling proteins embedded with, or associated with, the plasma membrane. This 'Top-Bottom' scenario implicates that the D'orenone-induced alterations to the actin cytoskeleton, endosomes, vesicle recycling and cytoarchitecture are downstream effects of the D'orenone binding to receptor (irrespective of this is single protein, lipid rafts, or the whole plasma membrane itself). Such a scenario would not be surprising considering the fact that carotenoids can be integrated into membranes and modulate plasma membrane fluidity (Subzynski et *al.* 1991). Polar carotenoids increase the structural order of lipid layers and thus decrease membranes fluidity. Apolar carotenoids (e.g. ß-carotenoids) are integrated between the two lipid layers and decrease their order. An increased fluidity is the consequence.

It could also be, that the putative receptor of D'orenone is some component of the actin cytoskeleton, endocytic vesicle recycling machinery, or embedded in membranes of endosomes, recycling vesicles, or tonoplast. In this 'Bottom-Top' scenario, the effects on signalling molecules (receptors, sources of second messengers, second messengers itself) is only a secondary effects due to alterations of some intracellular structures such as the cytoskeleton or internal membranes.

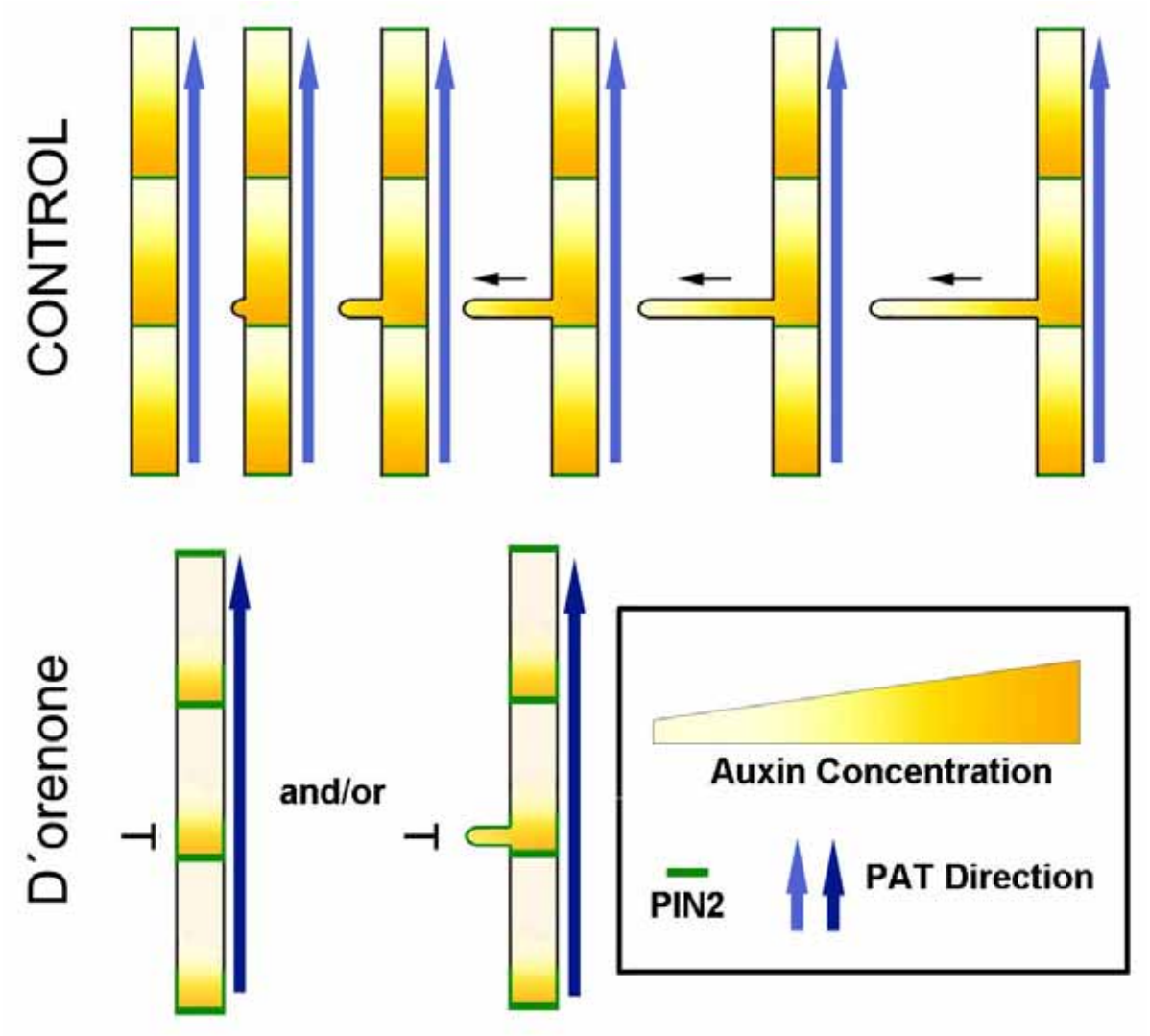

Fig.: 4.2.
D´orenone blocks polarized tip growth of root hairs by interfering with the polar auxin transport
The tip-growth of root hairs is tightly controlled by endogenous levels of auxin within the trichoblasts. Root hair growth (indicated by black arrow) takes place above a critical level of auxin. D´orenone increases intensity of expressed PIN2 and stimulates PAT (indicated by darker blue color of PAT direction arrow). Increased auxin export lowers endogenous level of auxin within the trichoblasts and averts formation of new root hairs and any existing root hair stops its growth respectively.

4.3. The Role of Redox-related Stress for Auxin Signaling

The ability of auxin to control processes like gravitropic bending is tightly linked with auxin induced ROS/RNS (e.g. Joo et *al.* 2005). Gravitropic curvature not only induces auxin accumulation at the lower root flank, but also nitric oxide and ROS (Hu et *al.* 2005; Joo et *al.* 2005). Moreover, NPA inhibits both PAT and nitric oxide formation (Hu et *al.* 2005) in root apices and a reduction of the ROS/RNS level alone is enough to impede gravitropic bending (Joo et *al.* 2005).

Because auxin influences virtually every aspect of plant growth and development, numerous papers on auxin responses have been published. Besides the well documented effect on the transcriptional level (Abel 2007), which shows the ability of auxin to switch on/off several genes, other effects occur, such as the activation of cGMP formation, MAP-kinase pathways and other redox level modifying signal chains (Mockaitis et *al.* 2000; Pagnussant et *al.* 2003, 2004; Lanteri et *al.* 2008). To measure the impact of only one of the mentioned aspects, genetic studies with DNA-chips and/or auxin related mutants are important tools. Such approaches uncovered many aspects of auxin biosynthesis (reviewed in Woodward and Bartel 2005a) and details of transcription regulation pathways of auxin inducible genes (Sawa et *al.* 2002; Pufky et *al.* 2003; Cluis et *al.* 2004; Himanen et *al.* 2004). But these kinds of approaches are not sufficiently specific to distinguish different pathways of non transcriptional auxin action. For example auxin transport mutants are difficult to separate from auxin signaling mutants (Bennett et *al.* 1996; Okada et *al.* 1991) or from mutants affected in downstream signalling components such as MAP-kinases. The same holds true for inhibitor studies which may reflect a complex impact on plant growth/behavior not necessarily linked to auxin action (e.g. Lam et *al.* 2007). A possible additional tool to distinguish transcriptional and redox-related auxin activity is the auxin derivative indole butyric acid. This auxin occurs in different plant species naturally (Epstein and Ludwig-Müller 1993) and its metabolism is linked to indole acetic acid. IAA can be converted to IBA and vice versa (reviewed in Woodward and Bartel 2005a).

4.3.1. Indole butyric acid (IBA) as tool to unravel auxin action

IBA is transported in a polar fashion (Poupart et *al.* 2005; Rashotte et *al.* 2003) and strongly promotes the formation of lateral roots (Zolman et *al.* 2000) and adventitious roots (Nordström et *al.* 1991). These are typical auxin activities, but IBA does not show a direct effect on transcriptional activity and influences cell elongation growth of the root only at higher concentrations. It can, of course, activate transcription of Aux/IAA genes, if it is converted to IAA. Growth of mutants with specific ß-oxidation defects is IBA insensitive and IBA is unable to activate transcription of Aux/IAA genes in such mutants. Moreover, as shown in chapter 3.3.1 these mutants show very low IBA to IAA conversion rates. All this is suggesting that IBA is converted to IAA in a process paralleling fatty acid ß-oxidation.

ß-oxidation of fatty acids in plants resides solely in the peroxisomes (Gerhardt, 1992; Kindl, 1993). IAA is found in peroxisomes of wild type roots after IBA treatment and this is not monitored in several peroxisomal mutants defective in IBA-response, supporting the assumption that the conversion of IBA to IAA is indeed peroxisomal.

Terfestatin A (Trf A) a root specific auxin signalling inhibitor disturbs the TIR^{scf} proteasome complex and disables transcription of Aux-IAA response proteins and of the synthetic DR5-reporter (Yamazoe et al. 2005). The blocking of auxin inducible gene transcription by Terfestatin A prevents the formation of lateral roots (LRF, see also Yamazoe et al. 2005) and neutralizes the positive LRF promoting effect of IAA. But inhibition of TIR^{scf}-complex controlled gene expression has only a moderate detrimental effect on IBA activity, pointing towards the existence of a second LRF promoting pathway in response to IBA (see chapter 3.3.5).

4.3.2. IBA-dependent NO-pathways induce lateral roots

During IBA-treatment a considerably amount of nitric oxide is generated (see also Kolbert et al 2007). This is not so in the IBA-insensitive mutants, indicating that ß-oxidation-like IBA conversion is responsible for the induction of the nitric oxide pathway. This is consistent with the finding that peroxisomes proliferate and emerge as the major nitric oxide source after IBA treatment. This is accompanied by a partial co-localization of FM 4-64 with peroxisomes, suggesting fusion processes between recycling endosomes/vesicles and peroxisomes. Endosomes appear together with mitochondria as the major source of organelle-based RNS production. But given the fact that peroxisomes are slightly weaker nitric oxide sources after IAA treatment than after IBA treatment, fusion of peroxisomes with the RNS producing endosomes is not a sufficient explanation for the strong nitric oxide formation inside of peroxisomes after an IBA-treatment. More likely is the scenario, that the IBA-to-IAA conversion is responsible for the stronger

peroxisomal nitric oxide signal. This would also provide a satisfactory explanation for the higher DAF-2T fluorescence after IBA treatment compared to IAA (chapter 3.3.4).

Consequently, the indole butyric acid impact on LRF is more susceptible to nitric oxide inhibition by cPTIO than the IAA effect. The Arabidopsis mutant *NOA1* has a diminished ability to produce nitric oxide in particular in stress conditions (Guo et al. 2003, 2005). The auxin promoting effect on lateral root formation is alleviated in the mutant. Similar to a cPTIO treatment, IBA-induced action is diminished more strongly than IAA-induced action. The *NOA1* mutant is not only quite resistant to IBA in the lateral root growth assay, but shows also a much weaker nitric oxide production ratio after indole butyric acid treatment compared to control. More important, the rate of conversion of IBA-to-IAA is not affected in the mutant.

NOA1, formerly known as *NOS1* was thought to be a plant NO-synthase (Guo et al. 2003) located in mitochondria (Guo et al 2005). However, sequence analysis revealed that *NOA1* shares nearly no homologies to animal NO-synthases (NOS), making a role as NOS in plants implausible. On the other hand, the *NOA1* protein produces nitric oxide from L-Arginine, which is a typical NOS feature. By now it is accepted that *NOA1* is an essential co-factor for a plant NOS-like enzyme. Interesting results revealed a NOS-like enzyme in peroxisomes of pea hypocotyls (Corpas et al. 2001, 2004). Moreover, peroxisomes and mitochondria can exchange material via a specialized vesicle transport (Neuspiel et al. 2007). This gives a possible pathway to unite all obtained conflicting data concerning peroxisomal or mitochondrial based NOS-like activity in plants.

By using a nitrate reductase (NR) mutant, a recent study suggested, that nitric oxide formation, which is required for IBA-action, was produced by NR rather than NOS (Kolbert et al. 2007). But this study failed to provide convincing results to link NR activity with IBA activity beside an IBA-insensitivity of the nitrate reductase mutant. More importantly, the inhibition of nitrate reductase prevents not only IBA but also IAA induced nitric oxide (Hu et al. 2005). This shows that NR is a general important source for auxin induced nitric oxide formation and is a reasonable explanation why nitrate reductase mutants show IBA insensitivity (Kolbert et al. 2007). It may rather be assumed that stimulation of NO production by IBA involves some cooperation between nitric oxide synthase-like activity and nitrate reductase activity, as both NOS and NR inhibitors block NO accumulation (Hu et al. 2005; Kolbert et al. 2007; Pagnussant et al. 2003, 2004). Moreover, auxin-induced acidification may also contribute to non-enzymatic NO production by spontaneous reduction of nitrite at acidic pH (Stöhr et al. 2002).

Taken together, the IBA-to-IAA conversion is needed for the bulk of IBA induced nitric oxide production. Despite the as yet unresolved questions concerning the NO-producing enzyme

systems it is clearly observable that the difference of nitric oxide level between IBA and IAA treatment is *NOA1* dependent.

An additional line of evidence shows the involvement of NO in IBA-induced lateral root formation. The lateral rootless (*lrt1*) maize mutant is insensitive to the auxins IAA, NAA and 2,4D in terms of lateral root initiation (see also Hochholdinger et *al*. 1998). But IBA as well as NO can induce lateral roots in this mutant, resulting in a qualitative rescue of the phenotype. The primary root shows local agglomerations of stunted lateral roots. Both treatments are amplified if applied together, resulting in a wild type like phenotype. An inhibition of NO production by cPTIO abolishes IBA´s ability to induce lateral roots completely, indicating - similar as in Arabidopsis (compare chapter 3.3.5 and 3.3.8) - a strong NO dependency of IBA activity in maize.

4.3.3. Auxin produced ROS and RNS implicates auxin as a redox-related stress factor

The fact that auxins promote ROS formation (e.g. Liszkay et *al.* 2004) could explain, why auxin signaling shares some key aspects with stress related signaling. The phytohormone abscisic acid (ABA) plays a crucial role in plant responses to abiotic stresses, such as anoxia. Interestingly, auxin induces the transcription of certain genes (e.g. Dc3), which are also induced by ABA (Rock and Sun 2005). It is known, that high concentrations of auxin induce ethylene and ABA synthesis (Raghavan et *al.* 2006), but even at lower concentrations the transcription of some *Daucus carota* genes under the control of the Dc3 promoter is induced, even though there is no appreciable amount of ABA synthesis (Raghavan et *al.* 2006). Similar to auxin, the production of NO and ROS is involved in a subset of the ABA induced activities (Mata and Lamattina 2001; Yan et *al.* 2007). ROS/RNS play crucial roles in root development and stomatal movement control (Desikan et *al*. 2004). Finally, the activation of ABA signalling pathways by ROS is well documented for stress-induced adaptations (Rock and Sun 2005).

Remarkably, pro3DC::GUS expression in root apices is activated by treatment with IAA, 2,4-D and NAA (Rock and Sun 2005). The staining pattern of the GUS-product is identical for all three auxins but differs from the pattern induced by ABA or by an osmoticum. IBA induces the same pattern as the other auxins (chapter 3.3.7). It is a peculiar finding that IBA is transported polar from cell to cell, but this transport is AUX1 and PIN1 independent and not sensitive to NPA (Rashotte et *al.* 2003, 2001) indicating a PGP independent transport. Given the weak capability of IBA to activate IAA-inducible genes (see above) and the different mode of intercellular transport, some other auxin feature has to be responsible for the pro3DC::GUS expression pattern. One such feature would be the ROS-formation. Moreover, the auxin induced peroxynitrite pattern in root

apices fits nicely the auxin induced pro3DC::GUS pattern, indicating a possible role of ROS/RNS and not auxin as actual transcriptional activator.

Considering the ROS/RNS dependency of auxin induced gravitropic bending (Joo et *al.* 2001, 2005; Hu et *al.* 2005) and auxin induced lateral root formation, a feedback regulation between auxin and stress related signaling molecules emerges, which together appear to orchestered plant root growth.

Auxin is used by fungi to communicate with host plants and to induce mycorrhizal symbiosis (e.g. Fitze et al. 2005). Members of the Glomus family of fungi (Fitze et *al.* 2005; Paszkowski and Boller 2002) manipulate "host" plants via IBA and not IAA. The IBA action modifies effectively root systems primarily by induced ROS and nitric oxide.

Differences in ROS formation between the two auxins IAA and IBA are probably linked with the IBA-to-IAA conversion that causes peroxisomal changes. The resulting compartimentation of auxin could also be linked with the changes of the ROS composition (see chapter 3.3.7).

An interesting side note is, that the ability of auxin to shape root architecture by inhibiting primary root elongation and formation of new lateral roots is not only linked to nitric oxide but also to ROS formation or more precisely to peroxidase activity. The lateral rootless (*lrt1*) rice mutant is insensitive to auxin (IAA, IBA and 2, 4-D) in terms of root elongation and lateral root initiation (Chhun et al., 2003). In the analogous maize mutant *lrt1* (Hochholdinger et *al.* 1998) auxin inhibits root elongation only moderate (compared to wild type root elongation inhibition). Proteomic analyses of maize *lrt1* showed that in addition to proteins, which are involved in lignin metabolism, one cytosolic ascorbate peroxidase is strongly up regulated (Hochholdinger et *al.* 2004). Not surprisingly, a treatment with the ascorbate peroxidase inhibitor, salicylhydroxamic acid (SHAM), induces lateral roots in *lrt1*. Another peroxidase over-expressing mutant (from tobacco) shows a phenotype lacking lateral roots almost completely and failing to react to IAA treatment by root elongation. Importantly, the level of free IAA is comparable to the wild type level (Lagrimini et *al.* 1997), indicating that peroxidase activity is counteracting auxin activity.

The role of transcription independent auxin pathways highlights several details, which corroborate stress related redox-signalling with auxin activity. This means that auxin may have evolved from a simple stress elicitor to one of the most important signaling molecule in plants and such it is not surprising that it still participates in general stress signaling pathways.

The comparison of IBA with IAA shows that the various forms of auxin affect not only gene transcription but also physiological pathways to unfold their broad spectrum of activity (see Fig.4.3).

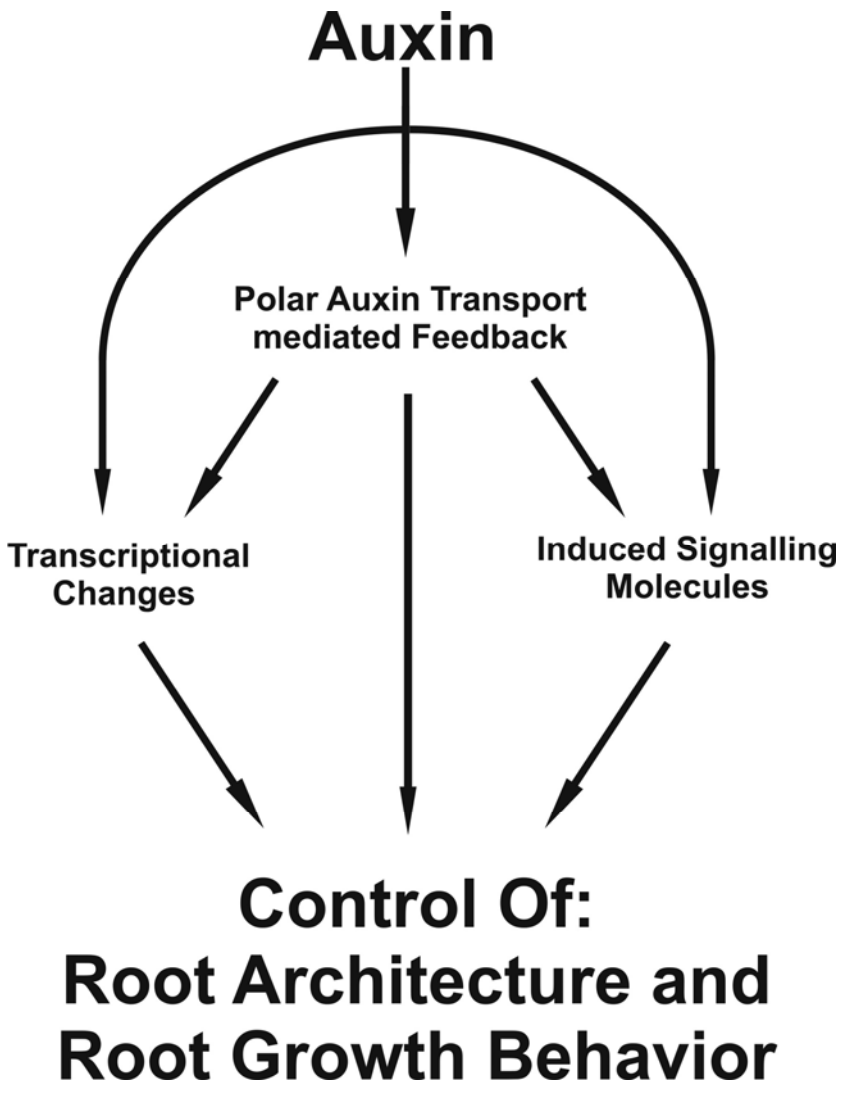

Fig.: 4.3.
Auxin shapes the root
Auxin modulates root architecture by at least two interwoven mechanisms, which are not directly PAT dependent. A direct effect of auxin on the transcriptional level which is sufficient to explain all longtime modifications and a second mechanism regarding primarily fast induced changes using several induced second messengers.

4.4. Summary

Nearly every developmental phase and every growth process of a plant is affected by auxin. Auxin is transported over long distance via the phloem but also polarly from cell-to-cell, along the entire plant body; from the shoot tip downwards and from the root tip upwards. This rather unique feature is not shared by any other known signaling molecule in plants. Auxin transport is always directional, energy dependent, and substrate specific. The mechanism of polar auxin transport (PAT) is described by the chemiosmotic model, proposed some 33years ago by Raven and independently by Rubery and Sheldrake. Since then it has obtained paradigm status receiving only marginal modifications by the discovery of some molecular components such as auxin influx and efflux transporters. However, the current study is describing and discussing observations, which contradict several predictions of the classical chemiosmotic theory of PAT, which makes it desirable to update our view of cellular auxin efflux.

For example, the chemiosmotic theory cannot explain the rapid inhibition of PAT by Brefeldin A, an inhibitor of secretion. Under these conditions, i.e., while PAT is inhibited, PIN auxin transporters are still present at the plasma membrane. This observation is the motivation and starting point in the current study to investigate the relationship between PAT and endosomal membrane recycling with some consideration of auxin action on root hair formation, and upstream effectors of auxin such as D´orenone and indole butyric acid (IBA).

A new IAA specific antibody has been used here to re-investigate several key aspects of polar auxin transport. The conclusions from this work are: (1) Endosomes and vesicle recycling are essential parts of the auxin transport machinery. Auxin is enriched at cross wall domains (end poles) of IAA transporting cells, but not of cells impaired in PAT either due to inhibitors or to genetic lesions. (2) The mere presence of PIN proteins at the plasma membrane is not sufficient to sustain auxin transport. (3) Continuous F-actin-dependent vesicle recycling between the plasma membrane and endosomes is necessary for polar positioning of PIN.

It is further shown, that auxin transport provides vectorial information for the localization of root hair initiation sites close to apical ends of hair-forming cells (ends that are oriented towards the root tip). Once initiated, root hair tip growth is based on a threshold level of auxin in the trichoblasts. Auxin export out of trichoblasts is driven by the PIN2 auxin efflux transporter to the next basal epidermis cell.

This study provides evidence, that one cleavage product of ß-carotene, called D'orenone, inhibits root hair formation and modifies the root architecture. Analysis of cellular changes after D´orenone treatment reveal an effect of this substance on PAT. In the D´orenone treated roots more PIN2 protein is found in root apices and the PIN2 expression zone is increased in size and shifted basally (away from the root apex). Root hair growth inhibition by D´orenone is rescued by externally applied IAA. Moreover, PIN2 knock-out mutants are insensitive towards D´orenone. Taken together, D´orenone targets root hair growth by upregulating PIN2 and thereby increasing the rate of PAT.

It is important to note, that auxin based modulation of root architecture involves second messengers such as reactive oxygen species and reactive nitrogen species (ROS/RNS). It is shown here, that mutants which are insensitive to the naturally occuring auxin, indole butyric acid (IBA), proove to be useful experimental tools to examine the relevance of the ROS/RNS dependent activity mechanism. Apparently there are two pathways involved in the action of IBA. One is that IBA is converted to IAA, which then feeds IAA into intracellular signalling pathways, and the other is that the IBA-conversion induces ROS/RNS production, though in a similar pattern as IAA within root tissues. Both generated IAA and alongside the IBA-to-IAA conversion produced nitric oxide are necessary for any IBA related root architecture altering effects. The comparison of IBA and IAA activity in this study implicates that all mentioned auxin-dependent changes of root growth and development are formed by complex feedback interactions between auxin and stress-related signalling molecules, which together underly environment-dependent phenotypic plasticity of the plant root system architecture.

5. References

- **Abas L, Benjamins R, Malenica N, Paciorek T, Wiśniewska J, Moulinier-Anzola JC, Sieberer T, Friml J, Luschnig C** (2006) Intracellular trafficking and proteolysis of the Arabidopsis auxin-efflux facilitator PIN2 are involved in root gravitropism. *Nat Cell Biol.* **8:** 249-256.
- **Abel S** (2007) Auxin is surfacing. *ACS Chem Biol.* **2:** 380-384.
- **Alder A, Holdermann I, Beyer P, Al-Babili S.** (2008) Carotenoid oxygenases involved in plant branching catalyze a highly specific, conserved apocarotenoid cleavage reaction.
- *Biochem J.* **18** [Epub ahead of print]
- **Aloni R, Schwalm K, Langhans M, Ullrich C** (2003) Gradual shifts in sites of free-auxin production during leaf-primordium development and their role in vascular differentiation and leaf morphogenesis. *Planta.* **216:** 841-853.
- **Aloni R, Aloni E, Langhans M, Ullrich CI** (2006a) Role of cytokinin and auxin in shaping root architecture: regulating vascular differentiation, lateral root initiation, root apical dominance and root gravitropism. *Ann Bot (Lond).* **97:** 883-893.
- **Aloni R, Aloni E, Langhans M, Ullrich CI** (2006b) Role of auxin in regulating Arabidopsis flower development. *Planta.* **223:** 315-328.
- **Appel K, Hirt H** (2004) Reactive oxygen species: metabolism, oxidative stress, and signal transduction. *Annu Rev Plant Biol.* **55:** 373-399.
- **Armstrong JI, Yuan S, Dale JM, Tanner VN, Theologis A** (2004) Identification of inhibitors of auxin transcriptional activation by means of chemical genetics in *Arabidopsis*. *Proc Natl Acad Sci USA.* **101:** 14978-14983.
- **Bailly A, Sovero V, Vincenzetti V, Santelia D, Bartnik D, König BW, Mancuso S, Martinoia E, Geisler M** (2008) Modulation of P-glycoproteins by auxin transport inhibitors is mediated by interaction with immunophilins *J Biol Chem* In press
- **Baluška F, Kubica S, Hauskrecht M** (1990) Postmitotic 'isodiametric' cell growth in the maize root apex. *Planta.* **181:** 269-274
- **Baluška F, Barlow PW, Kubica S** (1994) Importance of the post-mitotic 'isodiametric' growth (PIG) region for growth and development of roots. *Plant and Soil.* **167:** 31-42
- **Baluška F, Vitha S, Barlow PW, Volkmann D** (1997) Rearrangements of F-actin arrays in growing cells of intact maize root apex tissues: a major developmental switch occurs in the postmitotic transition region. *Eur J Cell Biol.* **72**: 113-121
- **Baluška F, Salaj J, Mathur J, Braun M, Jasper F, Šamaj J, Chua N–H, Barlow PW, Volkmann D** (2000) Root hair formation: F-actin-dependent tip growth is initiated by

local assembly of profilin-supported F-actin meshworks accumulated within expansin-enriched bulges. *Dev Biol.* **227:** 618-632.

- **Baluška F, Jasik J, Edelmann HG, Salajova T, Volkmann D** (2001) Latrunculin B induced plant dwarfism: plant cell elongation is F-actin dependent. *Dev Biol.* **231:** 113-124.
- **Baluška F, Hlavacka A, Šamaj J, Palme K, Robinson DG, Matoh T, McCurdy DW, Menzel D, Volkmann D** (2002) F-actin-dependent endocytosis of cell wall pectins in meristematic root cells: insights from brefeldin A-induced compartments. *Plant Physiol.* **130:** 422-431.
- **Baluška F, Samaj J, Menzel D** (2003) Polar transport of auxin: carrier-mediated flux across the plasma membrane or neurotransmitter-like secretion? *Trends Cell Biol*. **13**: 282-285
- **Baluška F, Mancuso S, Volkmann D, Barlow PW** (2004) Root apices as plant command centres: the unique 'brain-like' status of the root apex transition zone. *Biologia.* **59**: 9-17
- **Baluška F, Volkmann D, Menzel D** (2005a) Plant synapses: actin-based domains for cell-to-cell communiction. *Trends Plant Sci.* **10**: 106-111
- **Baluška F, Barlow PW, Baskin TI, Chen R, Feldman L, Forde BG, Geisler M, Jernstedt J, Menzel D, Muday GK, Murphy A, Samaj J, Volkmann D** (2005b) What is apical and what is basal in plant root development. *Trends Plant Sci.* **10:** 409-411
- **Baluška F, Hlavacka A, Mancuso S, Barlow PW** (2006) Neurobiological view of plants and their body plan. In: BALUŠKA, F., MANCUSO, S., and VOLKMANN, D. (Eds.): Communication in Plants. Neuronal Aspects of Plant Life. P. 19-35. Berlin, Heidelberg: Springer Verlag
- **Baluška F, Barlow PW, Volkmann D, Mancuso S** (2007) Gravity related paradoxes in plants: plant neurobiology provides the means for their resolution. In: WITZANY, G. (Ed.): Biosemiotics in Transdisciplinary Context, Proceedings of the Gathering in Biosemiotics 6, Salzburg. S. 122-133. Umweb: Helsinky
- **Baluška F, Schlicht M, Volkmann D, Mancuso S** (2008) Vesicular secretion of auxin: evidences and implications. *Plant Signal Behav.* **3:** 254-256.
- **Bandyopadhyay A, Blakeslee JJ, Lee OR, Mravec J, Sauer M, Titapiwatanakun B, Makam SN, Bouchard R, Geisler M, Martinoia E, Friml J, Peer WA, Murphy AS** (2007) Interactions of PIN and PGP auxin transport mechanisms. *Biochem Soc Trans.* **35:** 137-141.
- **Bartel B** (1997) Auxin biosynthesis. *Annu Rev Plant Physiol Plant Mol Biol.* **48**: 51-66.

- **Beauchamp C, Fridovich I** (1971) Superoxide dismutase: improved assays and assay applicable to acrylamide gels. *Anal. Biochem.* **44:** 276-287.
- **Bennett MJ, Marchant A, Green HG, May ST, Ward SP, Millner PA, Walker AR, Schulz B, Feldmann KA** (1996) Arabidopsis AUX1 gene: a permease-like regulator of root gravitropism. *Science.* **73:** 948-950.
- **Bennett T, Sieberer T, Willett B, Booker J, Luschnig C, Leyser O** (2006) The Arabidopsis MAX pathway controls shoot branching by regulating auxin transport. *Curr. Biol.* **16:** 553-563.
- **Bhalero RP, Bennett MJ** (2003) The case for morphogens in plants. *Nat Cell Biol*. **5:** 939-943.
- **Bhat RA, Panstruga R** (2005) Lipid rafts in plants. *Planta.* **223:** 5-19
- **Bianco C, Imperlini E, Calogero R, Senatore B, Pucci P, Defez R** (2006a) Indole-3-acetic acid regulates the central metabolic pathways in Escherichia coli. *Microbiology.* **152:** 2421-2431.
- **Bianco C, Imperlini E, Calogero R, Senatore B, Amoresano A, Carpentieri A, Pucci P, Defez R** (2006b) Indole-3-acetic acid improves Escherichia coli's defences to stress. *Arch Microbiol.* **185:** 373-382.
- **Blakeslee JJ, Peer WA, Murphy AS** (2005) Auxin transport. *Curr Opin Plant Biol.* **8:** 494-500.
- **Blakeslee JJ, Bandyopadhyay A, Lee OR, Mravec J, Titapiwatanakun B, Sauer M, Makam SN, Cheng Y, Bouchard R, Adamec J, Geisler M, Nagashima A, Sakai T, Martinoia E, Friml J, Peer WA, Murphy AS** (2007) Interactions among PIN-FORMED and P-glycoprotein auxin transporters in Arabidopsis. *Plant Cell.* **19:** 131-147.
- **Blaydes DF, Saus FL** (1978) Inhibition of coleoptile elongation by trisporic acids. *Plant & Cell Physiol.* **19:** 519-521.
- **Blilou I, Xu J, Wildwater M, Willemsen V, Paponov I, Friml J, Heidstra R, Aida M, Palme K, Scheres B** (2005) The PIN auxin efflux facilitator network controls growth and patterning in Arabidopsis roots. *Nature.* **433:** 39-44.
- **Bolwell GP, Blee KA, Butt VS, Davies DR, Gardner SL, Gerrish C, Minibayeva F, Rowntree EG, Wojtaszek P** (1999) Recent advances in understanding the origin of the apoplastic oxidative burst in plant cells. *Free Radic Res.* Suppl: S137-145.
- **Borner GH, Sherrier DJ, Weimar T, Michaelson LV, Hawkins ND, Macaskill A, Napier JA, Beale MH, Lilley KS, Dupree P** (2005) Analysis of detergent-resistant

membranes in Arabidopsis. Evidence for plasma membrane lipid rafts. *Plant Physiol.* **137:** 104-116.

- **Bouchard R, Bailly A, Blakeslee JJ, Oehring SC, Vincenzetti V, Lee OR, Paponov I, Palme K, Mancuso S, Murphy AS, Schulz B, Geisler M** (2006) Immunophilin-like TWISTED DWARF1 modulates auxin efflux activities of Arabidopsis P-glycoproteins. *J Biol Chem.* **281:** 30603-30612.
- **Boutté Y, Crosnier MT, Carraro N, Traas J, Satiat-Jeunemaitre B** (2006) The plasma membrane recycling pathway and cell polarity in plants: studies on PIN proteins. *J Cell Sci.* **119:** 1255-1265.
- **Bradford MM** (1976) A rapid and sensitive method for the quantification of microgram quantities of protein utilizing the principle of protein-dye binding. *Anal Biochem.* **72:** 248-254.
- **Campanoni P, Blatt MR** (2007) Membrane trafficking and polar growth in root hairs and pollen tubes. *J Exp Bot.* **58:** 65-74.
- **Campanoni P, Balsius B, Nick P** (2003) Auxin transport synchronizes the pattern of cell division in a tobacco cell line. *Plant Physiol.* **133:** 1251-1260.
- **Capaldi DJ, Taylor KE** (1983) A new peroxidase color reaction: oxidative coupling of 3-methyl-2-benzothiazolinone hydrazone (MBTH) with its formaldehyde azine application to glucose and choline oxidases. *Anal. Biochem.* **129:** 329-336.
- **Carol R J, Takeda S, Linstead P, Durrant MC, Kakesova H, Derbyshire P, Drea S, Zarsky V, Dolan L** (2005) A RhoGDP dissociation inhibitor spatially regulates growth in root hair cells. *Nature.* **438**: 1013-1016.
- **Casimiro I, Beeckman T, Graham N, Bhalerao R, Zhang H, Casero P, Sandberg G, Bennett MJ** (2003) Dissecting *Arabidopsis* lateral root development. *Trends Plant Sci.* **8:** 165-171.
- **Chak RK, Thomas TL, Quatrano RS, Rock CD** (2000) The genes ABI1 and ABI2 are involved in abscisic acid- and drought-inducible expression of the *Daucus carota* L. Dc3 promoter in guard cells of transgenic Arabidopsis thaliana. *Planta.* **210:** 875-883.
- **Chambon P** (1996) A decade of molecular biology of retinoic acid receptors. *FASEB J.* **10:** 940-954.
- **Chen R, Hilson P, Sedbrook J, Rosen E, Caspar T, Masson PH** (1998) The *Arabidopsis thaliana* AGRAVITROPIC 1 gene encodes a component of the polar-auxin-transport efflux carrier. *Proc. Natl. Acad. Sci. USA.* **95:** 15112-15117.

- **Cheng Y, Qin G, Dai X, Zhao Y** (2007) NPY1, a BTB-NPH3-like protein, plays a critical role in auxin-regulated organogenesis in Arabidopsis. *Proc Natl Acad Sci USA*. **104:** 18825-18829.
- **Chhun T, Taketa S, Tsurumi S, Ichii M** (2003) Interaction between two auxin-resistant mutants and their effects on lateral root formation in rice (Oryza sativa L.). *J Exp Bot.* **54:** 2701-2708.
- **Cho M, Lee SH, Cho HT** (2008) P-glycoprotein4 displays auxin efflux transporter-like action in Arabidopsis root hair cells and tobacco cells. *Plant Cell.* **19:** 3930-3943.
- **Christian M, Steffens B, Schenck D, Burmester S, Böttger M, Lüthen H** (2006) How does auxin enhance cell elongation? Roles of auxin-binding proteins and potassium channels in growth control. *Plant Biol (Stuttg).* **8:** 346-352.
- **Ciesielski T** (1872) Untersuchungen über die Abwärtskrümmung der Wurzel. *Beitr Biol Pflanze.* **1:** 1-30.
- **Cluis CP, Mouchel CF, Hardtke CS** (2004) The Arabidopsis transcription factor HY5 integrates light and hormone signaling pathways. *Plant Journal.* **38:** 332–347.
- **Corpas FJ, Barroso JB, del Río LA** (2001) Peroxisomes as a source of reactive oxygen species and nitric oxide signal molecules in plant cells. *Trends Plant Sci*. **6:** 145-150.
- **Corpas F J, Barroso JB, Carreras A, Quirós M, León AM, Romero-Puertas MC, Esteban FJ, Valderrama R, Palma JM, Sandalio LM, Gómez M, del Río LA** (2004) Cellular and subcellular localization of endogenous nitric oxide in young and senescent pea plants. *Plant Physiol.* **136:** 2722-2733.
- **Correa-Aragunde N, Graziano M, Lamattina L** (2004) Nitric oxide plays a central role in determining lateral root development in tomato. *Planta.* **218:** 900-905.
- **Correa-Aragunde N, Graziano M, Chevalier C, Lamattina L** (2006) Nitric oxide modulates the expression of cell cycle regulatory genes during lateral root formation in tomato. *J Exp Bot.* **57:** 581-588.
- **Curtis RHC** (2007) Do phytohormones influence nematode invasion and feeding site establishment? *Nematology.* **9:** 155-160.
- **Darwin C** (1880) The Power of Movements in Plants. London: John Murray
- **Dauphin A, Gérard J, Lapeyrie F, Legué V** (2007) Fungal hypaphorine reduces growth and induces cytosolic calcium increase in root hairs of Eucalyptus globules. *Protoplasma*. **231:** 83-88.

- **De Meutter J, Tytgat T, Prinsen E, Gheysen G, Van Onckelen H, Gheysen G** (2005) Production of auxin and related compounds by the plant parasitic nematodes *Heterodera schachtii* and *Meloidogyne incognita*. *Commun Agric Appl Biol Sci.* **70:** 51-60.
- **De Ruijter NCA, Miller DD, Bisseling T, Emons AMC** (1999) Lipochito-oligosaccharides re-initiate root hair tip growth in Vicia sativa with high calcium and spectrin-like antigen at the tip. *Plant J.* **17:** 141-154.
- **De Smet I, Jürgens G** (2007) Patterning the axis in plants--auxin in control. *Curr Opin Plant Biol.* **17:** 337-343.
- **Delbarre A, Muller P, Imhoff V, Guern J** (1996) Comparison of mechanisms controlling uptake and accumulation of 2,4-dichlorophenoxy acetic acid, naphthalene-1-acetic acid, and indole-3-acetic acid in suspension-cultured tobacco cells. *Planta.* **198:** 532-541.
- **Delbarre A, Muller P, Guern J** (1998) Short-lived and phosphorylated proteins contribute to carrier-mediated efflux, but not to influx, of auxin in suspension-cultured tobacco cells. *Plant Physiol.* **116:** 833-844.
- **Delledonne M, Xia Y, Dixon RA, Lamb C** (1998) Nitric oxide functions as a signal in plant disease resistance. *Nature.* **394:** 585-588
- **Desikan R, Cheung MK, Bright J, Henson D, Hancock JT, Neill SJ** (2004) ABA, hydrogen peroxide and nitric oxide signalling in stomatal guard cells. *J Exp Bot.* **55:** 205-212
- **Dettmer J, Hong-Hermesdorf A, Stierhof YD, Schumacher K** (2006) Vacuolar H^+-ATPase activity is required for endocytic and secretory trafficking in Arabidopsis. *Plant Cell.* ***18:*** 715-730.
- **Dewitte W, Chiappetta A, Azmi A, Witters E, Strnad M, Rembur J, Noin M, Chriqui D, Van Onckelen H** (1999) Dynamics of cytokinins in apical shoot meristems of a day-neutral tobacco during floral transition and flower formation. *Plant Physiol.* **199:** 111-122.
- **Dharmasiri N, Dharmasiri S, Estelle M** (2005) The F-box protein TIR1 is an auxin receptor. *Nature.* **435:** 441–445.
- **Dhindsa RS, Plumb-Dhindsa P, Thorpe TA** (1981) Leaf senescence:correlated with increased levels of membrane permeability and lipid peroxidation, and decrease levels of superoxide dismutase and catalase. *J Exp Bot.* **32:** 93-101.
- **Dhonukshe P, Baluska F, Schlicht M, Hlavacka A, Samaj J, Friml J, Gadella TW Jr.** (2006) Endocytosis of cell surface material mediates cell plate formation during plant cytokinesis. *Dev Cell.* **10:** 137-150.

- **Dhonukshe P, Aniento F, Hwang I, Robinson DG, Mravec J, Stierhof YD, Friml J** (2007) Clathrin-mediated constitutive endocytosis of PIN auxin efflux carriers in Arabidopsis. *Curr Biol.* **17:** 520-527.
- **Dhonukshe P, Grigoriev I, Fischer R, Tominaga M, Robinson DG, Hasek J, Paciorek T, Petrásek J, Seifertová D, Tejos R, Meisel LA, Zazímalová E, Gadella TW Jr, Stierhof YD, Ueda T, Oiwa K, Akhmanova A, Brock R, Spang A, Friml J** (2008) Auxin transport inhibitors impair vesicle motility and actin cytoskeleton dynamics in diverse eukaryotes. *Proc Natl Acad Sci USA.* **105:** 4489-4494.
- **Ditengou FA, Raudaskoski M, Lapeyrie F** (2003). Hypaphorine, an indole-3-acetic acid antagonist delivered by the ectomycorrhizal fungus *Pisolithus tinctorius*, induces reorganisation of actin and the microtubule cytoskeleton in *Eucalyptus globulus* ssp bicostata root hairs. *Planta.* **218:** 217-225.
- **Doke N** (1983) Involvement of superoxide generation in the hypersensitive response of potato tuber tissues to infection with an incompatible race of *Phytophthora infestans* and to hyphal wall components. *Physiol Plant Pathol.* **23:** 345-357.
- **Dolan L** (1998) Pointing roots in the right direction: the role of auxin transport in response to gravity. *Genes Dev*. **12:** 2091-2095.
- **Dolan L, Janmaat K, Willemsen V, Linstead P, Poethig S, Roberts K, Scheres B** (1993) Cellular organisation of the Arabidopsis thaliana root. *Development* **119:** 71-84.
- **Durner J, Wendehenne D, Klessig DF** (1998) Defense gene induction in tobacco by nitric oxide, cyclic GMP, and cyclic ADP-ribose. *Proc Natl Acad Sci USA*. **95:** 10328-10333.
- **Eklöf S, Astot C, Sitbon F, Moritz T, Olsson O, Sandberg G** (2000) Transgenic tobacco plants co-expressing Agrobacterium iaa and ipt genes have wild-type hormone levels but display both auxin- and cytokinin-overproducing phenotypes. *Plant J.* **23:** 279-284.
- **Epstein E, Ludwig-Müller J** (1993) Indole-3-butyric acid in plants: occurrence, synthesis, metabolism, and transport. *Physiologia Plantarum* **88:** 382–389.
- **Fischer U, Ikeda Y, Ljung K, Serralbo O, Singh M, Heidstra R, Palme K, Scheres B, Grebe M** (2006) Vectorial information for Arabidopsis planar polarity is mediated by combined AUX1, EIN2, and GNOM activity. *Curr Biol.* **16:** 2143-2149.
- **Fitze D, Wiepning A, Kaldorf M, Ludwig-Müller J** (2005) Auxins in the development of an arbuscular mycorrhizal symbiosis in maize. *J Plant Physiol*. **162:** 1210-1219.
- **Foissner I, Wendehenne D, Langebartels C, Durner J** (2000) In vivo imaging of an elicitor-induced nitric oxide burst in tobacco. *Plant J*. **23:** 817-824.

- **Foreman J, Demidchik V, Bothwell JHF, Mylona P, Miedema H, Torres MA, Linstead P, Costa S, Brownlee C, Jones JDG, Davies JM and Dolan L** (2003) Reactive oxygen species produced by NADPH oxidase regulate plant cell growth. *Nature* **422:** 442-446.
- **Friml J.** (2003) Auxin transport – shaping the plant. *Curr Opin Plant Biol* **6**:7-12.
- **Friml J, Wisniewska J, Benkova E, Mendgen K, Palme K** (2002a) Lateral redistribution of auxin efflux regulator PIN3 mediates tropism in Arabidopsis. *Nature* **415:** 806-809.
- **Friml J, Vieten A, Sauer M, Weijers D, Schwarz H, Hamann T, Offringa R, Jürgens G** (2003) Efflux-dependent auxin gradients establish the apical-basal axis of Arabidopsis. *Nature* **26**: 147-153.
- **Friml J, Benková E, Blilou I, Wisniewska J, Hamann T, Ljung K, Woody S, Sandberg G, Scheres B, Jürgens G, Palme K** (2002b) AtPIN4 mediates sink-driven auxin gradients and root patterning in Arabidopsis. *Cell* **108:** 661-673.
- **Friml J, Yang X, Michniewicz M, Weijers D, Quint A, Tietz O, Benjamins R, Ouwerkerk PB, Ljung K, Sandberg G, Hooykaas PJ, Palme K, Offringa RA** (2004) PINOID-dependent binary switch in apical-basal PIN polar targeting directs auxin efflux. *Science* **306:** 862-865.
- **Friml J, Wiśniewska J** (2005) Auxin as an intercellular signal. In: *Intercellular Communication in Plants*, Flemming A. (ed), Annual Plant Reviews 16, Blackwell Publishing.
- **Gälweiler L, Guan C, Wisman E, Mendgen K, Yephremov A, Palme K** (1998) Regulation of polar auxin transport by AtPIN1 in Arabidopsis vascular tissue. *Science* **282:** 2226-2230
- **Geisler M, Kolukisaoglu HU, Bouchard R, Billion K, Berger J, Saal B, Frangne N, Koncz-Kalman Z, Koncz C, Dudler R, Blakeslee JJ, Murphy AS, Martinoia E, Schulz B** (2003) TWISTED DWARF1, a unique plasma membrane-anchored immunophilin-like protein, interacts with Arabidopsis multidrug resistance-like transporters AtPGP1 and AtPGP19. *Mol Biol Cell.* **14:** 4238-4249.
- **Geisler M, Blakeslee JJ, Bouchard R, Lee OR, Vincenzetti V, Bandyopadhyay A, Titapiwatanakun B, Peer WA, Bailly A, Richards EL, Ejendal KF, Smith AP, Baroux C, Grossniklaus U, Müller A, Hrycyna CA, Dudler R, Murphy AS, Martinoia E** (2005) Cellular efflux of auxin catalyzed by the Arabidopsis MDR/PGP transporter AtPGP1. *Plant J.* **44:** 179-194.

- **Geldner N, Friml J, Stierhof YD, Jürgens G, Palme K** (2001) Auxin transport inhibitors block PIN1 cycling and vesicle trafficking. *Nature* **413:** 425-428.
- **Geldner N, Anders N, Wolters H, Keicher J, Kornberger W, Muller P, Delbarre A, Ueda T, Nakano A, Jürgens G** (2003) The Arabidopsis GNOM ARF-GEF mediates endosomal recycling, auxin transport, and auxin-dependent plant growth. *Cell.* **112:** 219-230.
- **Gerhardt B** (1992) Fatty acid degradation in plants. *Progress in Lipid Research.* **31:** 417–446.
- **Gessler NN, Sokolov AV, Belozerskaya TA** (2002) Reactive oxygen species in regulation of fungal development. *Appl Biochem Microbiol.* **38:** 536-543.
- **Gooday GW** (1978) Functions of trisporic acid. *Phil Trans R Soc Lond B*. **284:** 509-520.
- **Gooday GW** (1983) Hormones and sexuality in fungi. In *Secondary Metabolism and Differentiation in Fungi*, eds Bennett JW, Ciegler A (Marcel Dekker, New York), pp 239-266.
- **Grebe M, Xu J, Möbius W, Ueda T, Nakano A, Geuze HJ, Rook MB, Scheres B** (2003) Arabidopsis sterol endocytosis involves actin-mediated trafficking via ARA6-positive early endosomes. *Curr Biol.* **13:** 1378-1387.
- **Grebe M** (2004) Ups and downs of tissue and planar polarity in plants. *Bioessays.* **26:** 719-729.
- **Grebe M** (2005) Growth by auxin: when a weed needs acid. *Science.* **310**: 60-61.
- **Guo FQ, Okamoto M, Crawford NM** (2003) Identification of a plant nitric oxide synthase gene involved in hormonal signaling. *Science.* **302:** 100-103.
- **Guo FQ, Crawford NM** (2005) Arabidopsis nitric oxide synthase1 is targeted to mitochondria and protects against oxidative damage and dark-induced senescence. *Plant Cell*. **17:** 3436-3450.
- **Gutknecht J, Walter A** (1980) Transport of auxin (indoleacetic acid) through lipid bilayer membranes. *J Membr Biol.* **56:** 65-72.
- **Harlow E, Lane D** (1988) Antibodies - A Laboratory Manual, Cold Spring Harbor Laboratory, USA.
- **Heisler MG, Ohno C, Das P, Sieber P, Reddy GV, Long JA, Meyerowitz EM** (2005) Patterns of auxin transport and gene expression during primordium development revealed by live imaging of the *Arabidopsis* inflorescence meristem. *Curr. Biol.* **15:** 1899-1911.
- **Hesse T, Feldwisch J, Balshüsemann D, Bauw G, Puype M, Vandekerckhove J, Löbler M, Klämbt D, Schell J, Palme K** (1989) Molecular cloning and structural

analysis of a gene from Zea mays (L.) coding for a putative receptor for the plant hormone auxin. *EMBO J.* **8:** 2453-2461.

- **Himanen K, Vuylsteke M, Vanneste S, Vercruysse S, Boucheron E, Alard P, Chriqui D, Van Montagu M, Inzé D, Beeckman T** (2004) Transcript profiling of early lateral root initiation. *Proc Natl Acad Sci USA.* **101:** 5146-5151.
- **Hochholdinger F, Feix, G** (1998) Early post-embryonic root formation is specifically affected in the maize mutant *lrt1*. *Plant J.* **16:** 247-255.
- **Hochholdinger F, Guo L, Schnable PS** (2004) Lateral roots affect the proteome of the primary root of maize (Zea mays L.). *Plant Mol Biol*. **56:** 397-412.
- **Hu S, Brady SR, Kovar D, Staiger CJ, Clarke GB, Roux SJ, Muday G** (2000) Identification of plant F-actin-binding proteins by F-actin chromatography. *Plant J.* **24:** 127-137.
- **Hu X, Neill SJ, Tang Z, Cai W** (2005) Nitric oxide mediates gravitropic bending in soybean roots. *Plant Physiol* **137**: 663-670
- **Huang S, Gao L, Blanchoin L, Staiger CJ** (2006) Heterodimeric capping protein from Arabidopsis is regulated by phosphatidic acid. *Mol. Biol. Cell* **17:** 1946-1958.
- **Jacobs M, Rubery PH** (1988) Naturally Occurring Auxin Transport Regulators. *Science.* **41:** 346-349.
- **Jaillais Y, Fobis-Loisy I, Miège C, Rollin C, Gaude T** (2006) AtSNX1 defines an endosome for auxin-carrier trafficking in Arabidopsis. *Nature* **443:** 106-109.
- **Jaillais Y, Gaude T** (2007) Sorting out the sorting functions of endosomes in Arabidopsis. *Plant Signal. Behav.* **2:** 556-558.
- **Jaillais Y, Fobis-Loisy I, Miège C, Gaude T** (2008) Evidence for a sorting endosome in Arabidopsis root cells. *Plant J.* **53:** 237-247.
- **Jain A, Poling MD, Karthikeyan AS., Blakeslee JJ, Peer WA, Titapiwatanakun B, Murphy AS, Raghothama KG** (2007) Differential effects of sucrose and auxin on localized phosphate deficiency-induced modulation of different traits of root system architecture in Arabidopsis. *Plant Physiol.* **144:** 232-247.
- **Jenik PD, Barton MK** (2005) Surge and destroy: the role of auxin in plant embryogenesis. *Development* **132:** 3577-3585.
- **Joo JH, Bae YS, Lee JS** (2001) Role of auxin-induced reactive oxygen species in root gravitropism. *Plant Physiol* **126:** 1055-1060.

- **Joo JH, Yoo HJ, Hwang I, Lee JS, Nam KH, Bae YS** (2005) Auxin-induced reactive oxygen species production requires the activation of phosphatidylinositol 3-kinase. *FEBS Lett* **579:** 1243-1248
- **Katekaar JF, Geissler AE** (1980) Auxin transport inhibitors. IV. Evidence of a common mode of action for a proposed class of auxin transport inhibitors. *Plant Physiol.* **66,** 1190-1195.
- **Kawano T, Kawano N, Hosoya H, Lapeyrie F** (2001) Fungal auxin antagonist hypaphorine competitively inhibits indole-3-acetic acid-dependent superoxide generation by horseradish peroxidase. *Biochem Biophys Res Commun*. **288:** 546-551.
- **Kepinski S, Leyser O** (2005) The Arabidopsis F-box protein TIR1 is an auxin receptor. *Nature.* **435:** 446–451.
- **Kim I, Cho E, Crawford K, Hempel FD, Zambryski PC** (2005) Cell-to-cell movement of GFP during embryogenesis and early seedling development in *Arabidopsis*. *Proc. Natl. Acad. Sci. USA* **102:** 2227-2231.
- **Kindl H** (1993) Fatty acid degradation in plant peroxisomes: function and biosynthesis of the enzymes involved. *Biochiemie* **75:** 225–230.
- Kirkham M, Parton RG (2005) Clathrin-independent endocytosis: New insights into caveolae and non-caveolar lipid raft carriers *BBA* **1745**: 273-286
- **Kleine-Vehn J, Dhonukshe P, Sauer M, Brewer PB, Wisniewska J, Paciorek T, Benková E, Friml J** (2008) ARF GEF-Dependent Transcytosis and Polar Delivery of PIN Auxin Carriers in Arabidopsis. *Curr Biol.* **18:** 526-531.
- **Kolbert Z, Bartha B, Erdei L** (2007) Exogenous auxin-induced NO synthesis is nitrate reductase-associated in Arabidopsis thaliana root primordia. *J Plant Physiol.* In press
- **Lagrimini LM, Joly RJ, Dunlap JR, Liu TT** (1997) The consequence of peroxidase overexpression in transgenic plants on root growth and development. Plant *Mol Biol.* **33:** 887-895.
- **Lam SK, Tse YC, Robinson DG, Jiang L** (2007) Tracking down the elusive early endosomes. *Trends Plant Sci* **12:** 497-505.
- **Lamattina L, Garcia-Mata C, Graziano M, Pagnussat G** (2003) Nitric oxide: the versatility of an extensive signal molecule. *Ann Rev Plant Biol* **54:** 109-136.
- **Lanteri ML, Pagnussat GC, Lamattina L** (2006) Calcium and calcium-dependent protein kinases are involved in nitric oxide- and auxin-induced adventitious root formation in cucumber. *J Exp Bot* **57:** 1341-1351.

- **Lanteri ML, Laxalt AM, Lamattina L** (2008) Nitric oxide triggers phosphatidic acid accumulation via phospholipase D during auxin induced adventitious root formation in cucumber. *Plant Physiol*. In press
- **Larsson C, Widell S, Kjellbom P** (1987) Preparation of high-purity plasma membranes. Methods Enzymol. **148:** 558-568.
- **Lee SH, Cho H–T** (2006) PINOID positively regulates auxin efflux in Arabidopsis root hair cells and tobacco cells. *Plant Cell* **18:** 1604-1616.
- **Lee Y, Bak G, Choi Y, Chuang WI, Cho HT, Lee Y** (2008) Roles of Phosphatidylinositol 3-kinase in root hair growth. *Plant Physiol.* In press.
- **Lefebvre B, Furt F, Hartmann MA, Michaelson LV, Carde JP, Sargueil-Boiron F, Rossignol M, Napier JA, Cullimore J, Bessoule JJ, Mongrand S** (2007) Characterization of lipid rafts from Medicago truncatula root plasma membranes: a proteomic study reveals the presence of a raft-associated redox system. *Plant Physiol* **144:** 402-418.
- **Leyser O** (2005) Auxin distribution and plant pattern formation: how many angels can dance on the point of PIN? *Cell* **121:** 819-822.
- **Li J, Yang H, Peer WA, Richter G, Blakeslee JJ, Bandyopadhyay A, Titapiwatanakun B, Undurraga S, Khodakovskaya M, Richards EL, Krizek B, Murphy AS, Gilroy S, Gaxiola R** (2005) *Arabidopsis* H^+-PPase AVP1 regulates auxin-mediated organ development. *Science* **310:** 121-125.
- **Li L, Xu J, Xu ZH, Xue HW** (2002) Brassinosteroids stimulate plant tropisms through modulation of polar auxin transport in Brassica and Arabidopsis. *Plant Cell* **17:** 2738-2753.
- **Li G, Xue HW** (2007) Arabidopsis PLDzeta2 regulates vesicle trafficking and is required for auxin response. *Plant Cell* **19:** 281-295.
- **Li X, Zhang WS** (2008) Salt-avoidance tropism in Arabidopsis thaliana. *Plant Signal. Behav.* **3:** 351-353.
- **Liou J–C, Ho S–Y, Shen M–R, Liao Y–P, Chiu W–T, Kang K–H** (2005) A rapid, nongenomic pathway facilitates the synaptic transmission induced by retinoic acid at the developing synapse. *J. Cell Sci.* **118:** 721-730.
- **Liszkay A, van der Zalm E, Schopfer P** (2004) Production of reactive oxygen intermediates $O_2^{\cdot-}$, H_2O_2, and $^{\cdot}OH$ by maize roots and their role in wall loosening and elongation growth. *Plant Physiol*. **136:** 3114-3123.
- **Ljung K, Bhalerao RP, Sandberg G** (2001) Sites and homeostatic control of auxin biosynthesis in Arabidopsis during vegetative growth. *Plant Journal* **28:** 465–474.

- **Logan DC, Leaver CJ** (2000) Mitochondria-targeted GFP highlights the heterogeneity of mitochondrial shape, size and movement within living plant cells. *J Exp Bot*. **346:** 865-871
- **López-Bucio J, Hernández-Abreu E, Sánchez-Calderón L, Pérez-Torres A, Rampey RA, Bartel B, Herrera-Estrella L** (2005) An auxin transport independent pathway is involved in phosphate stress-induced root architectural alterations in *Arabidopsis*. Identification of *BIG* as a mediator of auxin in pericycle cell activation. *Plant Physiol.* **137:** 681-691.
- **Lucas M, Godin C, Jay-Allemand C, Laplaze L** (2008) Auxin fluxes in the root apex co-regulate gravitropism and lateral root initiation. *J Exp Bot*. **59**: 55-66.
- **Ludwig-Müller J, Epstein E** (1991) Occurrence and in Vivo Biosynthesis of Indole-3-Butyric Acid in Corn (Zea mays L.). *Plant Physiol.* **97:** 765-770.
- **Lupu R, Menendez JA** (2006) Pharmacological inhibitors of Fatty Acid Synthase (FASN)--catalyzed endogenous fatty acid biogenesis: a new family of anti-cancer agents? *Curr Pharm Biotechnol.* **7:** 483-493.
- **Malenica N, Abas L, Benjamins R, Kitakura S, Sigmund HF, Jun KS, Hauser MT, Friml J, Luschnig C** (2007) MODULATOR OF PIN genes control steady-state levels of Arabidopsis PIN proteins. *Plant J.* **51:** 537-550.
- **Malínská K, Malínský J, Opekarová M, Tanner W** (2003) Visualization of protein compartmentation within the plasma membrane of living yeast cells. *Mol Biol Cell.* **14:** 4427-4436.
- **Mata CG, Lamattina L** (2001) Nitric oxide induces stomatal closure and enhances the adaptive plant responses against drought stress. *Plant Physiol.* **126:** 1196-1204.
- **Mancuso S, Marras AM, Volker M, Baluška F** (2005) Noninvasive and continuous recordings of auxin fluxes in intact root apex with a carbon nanotube-modified and self-referencing microelectrode. *Anal. Biochem.* **341:** 344-351.
- **Mancuso S, Marras AM, Mugnai S, Schlicht M, Žársky V, Li G, Song L, Xue H-W, Baluška F** (2007) Phospholipase Dζ2 drives vesicular secretion of auxin for its polar cell-cell transport in the transition zone of the root apex. *Plant Signal. Behav.* **2:** 204-244.
- **Men S, Boutté Y, Ikeda Y, Li X, Palme K, Stierhof Y-D, Hartmann M-A, Moritz T, Grebe M** (2008) sterol-dependent endocytosis mediates post-cytokinetic acquisition of PIN2 auxin efflux carrier polarity *Nature.* In press.
- **Merks RM, Van de Peer Y, Inzé D, Beemster GT** (2007) Canalization without flux sensors: a traveling-wave hypothesis. *Trends Plant Sci*. **12:** 384-390.

- **Michniewicz M, Zago MK, Abas L, Weijers D, Schweighofer A, Meskiene I, Heisler MG, Ohno C, Zhang J, Huang F, Schwab R, Weigel D, Meyerowitz EM, Luschnig C, Offringa R, Friml J** (2007) Antagonistic regulation of PIN phosphorylation by PP2A and PINOID directs auxin flux. *Cell.* **130:** 1044-1056.
- **Mockaitis K, Howell SH** (2000) Auxin induces mitogenic activated protein kinase (MAPK) activation in roots of Arabidopsis seedlings. *Plant J.* **24:** 785-796.
- **Mongrand S, Morel J, Laroche J, Claverol S, Carde JP, Hartmann MA, Bonneu M, Simon-Plas F, Lessire R, Bessoule JJ** (2004) Lipid rafts in higher plant cells: purification and characterization of Triton X-100-insoluble microdomains from tobacco plasma membrane. *J Biol Chem.* **279:** 36277-36286.
- **Moore I** (2002) Gravitropism: lateral thinking in auxin transport. *Curr. Biol.* **12:** 452-455.
- **Morel J, Claverol S, Mongrand S, Furt F, Fromentin J, Bessoule JJ, Blein JP, Simon-Plas F** (2006) Proteomics of plant detergent-resistant membranes. *Mol Cell Proteomics.* **5:** 1396-1411.
- **Muday GK, DeLong A** (2001) Polar auxin transport: controlling where and how much. *Trends Plant Sci.* **6:** 535-542.
- **Müller A, Guan C, Gälweiler L, Tänzler P, Huijser P, Marchant A, Parry G, Bennett M, Wisman E, Palme** K (1998) AtPIN2 defines a locus of Arabidopsis for root gravitropism control. *EMBO J.* **17:** 6903-6911.
- **Murashige T, Skoog F** (1962) A revised medium for rapid growth and bio-assays with tobacco tissue cultures. *Physiol Plant.* **15:** 473-497.
- **Murphy A, Peer WA, Taiz L** (2000) Regulation of auxin transport by aminopeptidases and endogenous flavonoids. *Planta.* **211:** 315-324.
- **Murphy AS, Hoogner KR, Peer WA, Taiz L** (2002) Identification, purification, and molecular cloning of N-1-naphthylphthalmic acid-binding plasma membrane-associated aminopeptidases from Arabidopsis. *Plant Physiol.* **128:** 935-950.
- **Nadella V, Shipp MJ, Muday GK, Wyatt SE** (2006) Evidence for altered polar and lateral auxin transport in the *gravity persistent signal* (*gps*) mutants of *Arabidopsis*. *Plant Cell Environm.* **29**: 682-690
- **Nakamura A, Higuchi K, Goda H, Fujiwara MT, Sawa S** (2003) Brassinolide induces *IAA5*, *IAA19*, and DR5, a synthetic auxin response element in *Arabidopsis* implying a cross-talk point of brassinosteroid and auxin signaling. *Plant Physiol.* **133:** 1-11.
- **Nakano Y, Asada K** (1981) Hydrogen peroxide is scavenged by ascorbate-specific peroxidase in spinach chloroplasts. *Plant Cell Physiol.* **22:** 867-880.

- **Nemhauser JL, Mockler TC, Chory J** (2004) Interdependency of brassinosteroid and auxin signaling in Arabidopsis. *PLOS Biol*. **2:** 1460-1471.
- **Neuspiel M, Schauss AC, Braschi E, Zunino R, Rippstein P, Rachubinski RA, Andrade-Navarro MA, McBride HM** (2007) Cargo-selected transport from the mitochondria to peroxisomes is mediated by vesicular carriers. *Curr Biol* **18:** 102-108
- **Nichols BJ, Lippincott-Schwartz J** (2001) Endocytosis without clathrin coats: *Trends Cell Biol* **11**: 406-412
- **Njio G** (2004) Der Einfluss von reaktivem Sauerstoff und Stickstoffmonoxid auf das Wachstum und die Polarität von Pflanzenzellen *diploma thesis*
- **Nordström A-C, Jacobs FA, Eliasson L** (1991) Effect of exogenous indole-3-acetic acid and indole-3-butyric acid on internal levels of the respective auxins and their conjugation with aspartic acid during adventitious root formation in pea cuttings. *Plant Physiol* **96**: 856-861
- **Nordström A, Tarkowski P, Tarkowska D, Norbaek R, Åstot C, Dolezal K, Sandberg G** (2004) Auxin regulation of cytokinin biosynthesis in Arabidopsis thaliana: a factor of potential importance for auxin-cytokinin-regulated development. *Proc Natl Acad Sci USA.* **101:** 8039–8044.
- **Okada K, Ueda J, Komaki MK, Bell CJ, Shimura Y** (1991) Requirement of the auxin polar transport system in early stages of Arabidopsis floral bud formation. *Plant Cell.* **3:** 677–684.
- **Oono Y, Chen QG, Overvoorde PJ, Köhler C, Theologis A** (1998) Age mutants of *Arabidopsis* exhibit altered auxin-regulated gene expression. *Plant Cell* **10:** 1649-1662.
- **Ottenschläger I, Wolff P, Wolverton C, Bhalerao RP, Sandberg G, Ishikawa H, Evans M, Palme K** (2003) Gravity-regulated differential auxin transport from columella to lateral root cap cells. *Proc Natl Acad Sci USA.* **100:** 2987-2991.
- **Ovecka M, Lang I, Baluška F, Ismail A, Illeš P, Lichtscheidl IK** (2005) Endocytosis and vesicle trafficking during tip growth of root hairs. *Protoplasma.* **226**: 39-54.
- **Paciorek T, Friml J** (2005a) Auxin signaling. *J Cell Sci.* **119:** 1199-202.
- **Paciorek T, Zazímalová E, Ruthardt N, Petrásek J, Stierhof YD, Kleine-Vehn J, Morris DA, Emans N, Jürgens G, Geldner N, Friml J** (2005b) Auxin inhibits endocytosis and promotes its own efflux from cells. *Nature.* **435:** 1251-1256.
- **Pagnussat GC, Lanteri ML, Lamattina L** (2003) Nitric oxide and cyclic GMP are messengers in the indole acetic acid-induced adventitious rooting process. *Plant Physiol.* **132:** 1241-1248.

- **Pagnussat GC., Lanteri ML, Lombardo MC, Lamattina L** (2004) Nitric oxide mediates the indole acetic acid induction activation of a mitogen-activated protein kinase cascade involved in adventitious root development. *Plant Physiol.* **135:** 279-286.
- **Park S, Li J, Pittman JK, Berkowitz GA, Yang H, Undurraga S, Morris J, Hirschi KD, Gaxiola RA** (2005) Up-regulation of a H+-pyrophosphatase (H+-PPase) as a strategy to engineer drought-resistant crop plants. *Proc Natl Acad Sci USA.* **102:** 18830-18835.
- **Parry G, Estelle M** (2006) Auxin receptors: a new role for F-box proteins. *Curr Opin Cell Biol.* **18:**152-156
- **Paszkowski U, Boller T** (2002) The growth defect of lrt1, a maize mutant lacking lateral roots, can be complemented by symbiotic fungi or high phosphate nutrition. *Planta.* **214:** 584-590.
- **Peer WA, Murphy AS** (2007) Flavonoids and auxin transport: modulators or regulators? *Trends Plant Sci.* **12**: 556-563
- **Peer WA, Brown DE, Tague BW, Muday G K, Taiz L, Murphy AS** (2001) Flavonoid accumulation patterns of transparent testa mutants of arabidopsis. *Plant Physiol.* **126:** 536-548.
- **Peer WA, Bandyopadhyay A, Blakeslee JJ, Makam SN, Chen RJ, Masson PH, Murphy AS** (2004) Variation in expression and protein localization of the PIN family of auxin efflux facilitator proteins in flavonoid mutants with altered auxin transport in Arabidopsis thaliana. *Plant Cell.* **16:** 1898-1911.
- **Peer WA, Mahmoudian M, Freeman JL, Lahner B, Richards EL, Reeves RD, Murphy AS, Salt DE** (2006) Assessment of plants from the Brassicaceae family as genetic models for the study of nickel and zinc hyperaccumulation. *New Phytol*. **172:** 248-260.
- **Pence VC, Caruso JL** (1987) ELISA determination of IAA using antibodies against ring-linked IAA. *Phytochemistry* **26**: 1251-1255.
- **Pengelly W, Meins F** (1977) A specific radioimmunoassay for nanogram quantities of the auxin, indole-3-acetic acid. *Planta* **136:** 173-180.
- **Pérez-Pérez JM, Ponce MR, Micol JL** (2004) The ULTRACURVATA2 gene of Arabidopsis encodes an FK506-binding protein involved in auxin and brassinosteroid signaling. *Plant Physiol.* **134:** 101-117
- **Petrásek J, Cerná A, Schwarzerová K, Elckner M, Morris DA, Zazímalová E** (2003) Do phytotropins inhibit auxin efflux by impairing vesicle traffic? *Plant Physiol.* **131:** 254-263.

- **Petrásek J, Mravec J, Bouchard R, Blakeslee JJ, Abas M, Seifertová D, Wisniewska J, Tadele Z, Kubes M, Covanová M, Dhonukshe P, Skupa P, Benková E, Perry L, Krecek P, Lee OR, Fink GR, Geisler M, Murphy AS, Luschnig C, Zazímalová E, Friml J** (2006) PIN proteins perform a rate-limiting function in cellular auxin efflux. *Science*. **312:** 914-918.
- **Pitts RJ, Cernac A, Estelle M** (1998) Auxin and ethylene promote root hair elongation in Arabidopsis. *Plant J.* **16:** 553-560.
- **Poupart J, Waddell CS** (2000) The rib1 Mutant Is Resistant to Indole-3-Butyric Acid, an Endogenous Auxin in Arabidopsis. *Plant Physiol.* **124:** 1739-1751.
- **Poupart J, Rashotte AM, Muday GK, Waddell CS** (2005) The rib1 mutant of Arabidopsis has alterations in indole-3-butyric acid transport, hypocotyl elongation, and root architecture. *Plant Physiol.* **139:** 1460-1471.
- **Preuss ML, Schmitz AJ, Thole JM, Bonner HKS, Otegui MS, Nielsen E** (2006) A role for the RabA4b effector protein PI-4Kbeta1 in polarized expansion of root hair cells in Arabidopsis thaliana. *J Cell Biol.* **172:** 991-998.
- **Prusty R, Grisafi P, Fink GR** (2004) The plant hormone indoleacetic acid induces invasive growth in *Saccharomyces cerevisiae*. *Proc Natl Acad Sci USA.* **101:** 4153-4157.
- **Psahoulia FH, Drosopoulos KG, Doubravska L, Andera L, Pintzas A** (2007) Quercetin enhances TRAIL-mediated apoptosis in colon cancer cells by inducing the accumulation of death receptors in lipid rafts. *Mol Cancer Ther*. **6:** 2591-2599.
- **Pufky J, Qiu Y, Rao MV, Hurban P, Jones AM** (2003) The auxin-induced transcriptome for etiolated Arabidopsis seedlings using a structure/function approach. *Functional & Integrative Genomics.* **3:** 135–143.
- **Qi X, Zhou J, Jia Q, Shou H, Chen H, Wu P** (2005) A characterization of the response to auxin of the small GTPase, Rha1. *Plant Sci.* **169:** 1136-1145.
- **Raghavan C, Ong EK, Dalling MJ, Stevenson TW** (2006) Regulation of genes associated with auxin, ethylene and ABA pathways by 2,4-dichlorophenoxyacetic acid in Arabidopsis. *Funct Integr Genomics*. **6:** 60-70.
- **Rahman A, Hosokawa S, Oono Y, Amakawa T, Goto N, Tsurumi S** (2002) Auxin and ethylene response interactions during Arabidopsis root hair development dissected by auxin influx modulators. *Plant Physiol.* **130:** 1909-1917.
- **Rahman A, Bannigan A, Sulaman W, Pechter P, Blancaflor EB, Baskin TI** (2007) Auxin, actin and growth of the Arabidopsis thaliana primary root. *Plant J.* **50:** 514-528.

- **Rashotte AM, Brady SR, Reed RC, Ante SJ, Muday GK** (2000) Basipetal auxin transport is required for gravitropism in roots of Arabidopsis. *Plant Physiol.* **122:** 481-490.
- **Rashotte AM, DeLong A, Muday GK** (2001) Genetic and chemical reductions in protein phosphatase activity alter auxin transport, gravity response, and lateral root growth. *Plant Cell.* **13:** 1683-1697.
- **Rashotte AM, Poupart J, Waddell CS, Muday GK** (2003) Transport of the two natural auxins, indole-3-butyric acid and indole-3-acetic acid, in Arabidopsis. *Plant Physiol.* **133:** 761-772.
- **Ratajczak R, Hinz G, Robinson DG** (1999) Localization of pyrophosphatase in membranes of cauliflower inflorescence cells. *Planta.* **208:** 205-211.
- **Raven JA** (1975) Transport of indoleacetic acid in plant cells in relation to pH and electrical potential gradients and its significance for polar IAA transport. *New Phytol.* **74:** 163–172.
- **Rea PA, Poole RJ** (1999) Vacuolar H^+-translocating pyrophosphatase. *Annu Rev Plant Physiol Plant Mo. Biol.* **44:** 157-180.
- **Reboutier D, Bianchi M, Brault M, Roux C, Dauphin A, Rona JP, Legué V, Lapeyrie F, Bouteau F** (2002) The indolic compound hypaphorine produced by ectomycorrhizal fungus interferes with auxin action and evokes early responses in nonhost Arabidopsis thaliana. *Mol Plant Microbe Interact.* **15:** 932-938.
- **Rentel MC, Lecourieux D, Ouaked F, Usher SL, Petersen L, Okamoto H, Knight H, Peck SC, Grierson CS, Hirt H, Khight MR** (1994) OXI1 kinase is necessary for oxidative burst-mediated signalling in Arabidopsis. *Nature.* **427**: 858-891.
- **Rock CD, Sun X** (2005) Crosstalk between ABA and auxin signaling pathways in roots of Arabidopsis thaliana (L.) Heynh. *Planta.* **222:** 98-106.
- **Rubery P, Sheldrake A** (1974) Carrier-mediated auxin transport. *Planta.* **118:** 101-121.
- **Ruegger M, Dewey E, Hobbie L, Brown D, Bernasconi P, Turner J, Muday G, Estelle M** (1997) Reduced naphthylphthalamic acid binding in the tir3 mutant of Arabidopsis is associated with a reduction in polar auxin transport and diverse morphological defects. *Plant Cell.* **9:** 745-757
- **Ruzicka K, Ljung K, Vanneste S, Podhorská R, Beeckman T, Friml J, Benková E** (2007) Ethylene regulates root growth through effects on auxin biosynthesis and transport-dependent auxin distribution. *Plant Cell*. **19**: 2197-2212.

- **Sabatini S, Beis D, Wolkenfelt H, Murfett J, Guilfoyle T, Malamy J, Benfey P, Leyser O, Bechtold N, Weisbeek P, Scheres B** (1999) An auxin-dependent distal organizer of pattern and polarity in the *Arabidopsis* root. *Cell.* **99:** 463-472.
- **Sagi M, Fluhr R** (2001) Superoxide production by plant homologues of the gp91phox NADPH oxidase. Modulation of activity by calcium and by tobacco mosaic virus infection. *Plant Physiol.* **126:** 1281–1290.
- **Šamaj J, Ovecka M, Hlavacka A, Lecourieux F, Meskiene I, Lichtscheidl I, Lenart P, Salaj J, Volkmann D, Bögre L, Baluška F, Hirt H** (2002) Involvement of the mitogen-activated protein kinase SIMK in regulation of root hair tip-growth. *EMBO J.* **21:** 3296-3306
- **Šamaj J, Baluška F, Voigt B, Schlicht M, Volkmann D, Menzel D** (2004) Endocytosis, actin cytoskeleton and signalling. *Plant Physiol.* **135:** 1150-1161
- **Šamaj J, Read ND, Volkmann D, Menzel D, Baluška F** (2005a) The endocytic network in plants. *Trends Cell Biol*. **15:** 425-433
- **Šamaj J, Baluška F, Menzel D** (2005b) Endocytosis in Plants. Springer Verlag
- **Šamaj J, Chaffey NJ, Tirlapur U, Jasik J, Volkmann D, Menzel D, Baluška F** (2006) Actin and myosin VIII in plasmodesmata cell-cell channels. In *Cell-Cell Channels*, Baluška, F., Volkmann, D., Barlow, P.W. (eds), Landes Bioscience.
- **Sangiorgio V, Pitto M, Palestini P, Masserini M** (2004) GPI-anchored proteins and lipid rafts. *Ital J Biochem*. **53:** 98-111.
- **Santelia D, Vincenzetti V, Azzarello E, Bovet L, Fukao Y, Düchtig P, Mancuso S, Martinoia E, Geisler M** (2005) MDR-like ABC transporter AtPGP4 is involved in auxin-mediated lateral root and root hair development. *FEBS Lett.* **579:** 5399-5406**Sawa S, Ohgishi M, Goda H, Higuchi K, Shimada Y, Yoshida S, Koshiba T** (2002) The HAT2 gene, a member of the HD-Zip gene family, isolated as an auxin inducible gene by DNA microarray screening, affects auxin response in Arabidopsis. *Plant J.* **32:** 1011–1022.
- **Scanlon MJ, Henderson DC, Bernstein B** (2002) SEMAPHORE1 functions during the regulation of ancestrally duplicated knox genes and polar auxin transport in maize. *Development.* **129:** 2663-2673.
- **Schachtschabel D, Schimek C, Wöstemeyer J, Boland W** (2005) Biological activity of trisporoids and trisporoid analogues in *Mucor mucedo* (-). *Phytochemistry.* **66:** 1358-1365.
- **Schachtschabel D, Boland W** (2007) Efficient generation of a trisporoid library by combination of synthesis and biotransformation. *J Org Chem.* **72:** 1366-1372.

- **Schiefelbein JW** (2000) Constructing a plant cell. The genetic control of root hair development. *Plant Physiol.* **124:** 1525-1531.
- **Schlicht M** (2004) Die Polarität über die Querwände-Interaktionen zwischen Aktinzytoskelett, Vesikelrezyklierung und polarem Auxintransport. *diploma thesis*
- **Schlicht M, Strnad M, Scanlon MJ, Mancuso S, Hochholdinger F, Palme K, Volkmann D, Menzel D, Baluška F** (2006) Auxin immunolocalization implicates vesicular neurotransmitter-like mode of polar auxin transport in root apices. Plant Signal. Behav. 1: 122-133.
- **Schlicht M, Šamajová O, Schachtschabel D, Mancuso S, Menzel D, Boland W, Baluška F** (2008) D'orenone Blocks Polarized Tip-Growth of Root Hairs by Interfering with the PIN2-Mediated Auxin Transport Network in the Root Apex. *Plant J.* **55**: 709-717.
- **Schneider G** (1970). Morphactins: physiology and performance. *Annu Rev Plant Physiol.* **21:** 499-536.
- **Schopfer P, Liszkay A** (2006) Plasma membrane-generated reactive oxygen intermediates and their role in cell growth of plants. *Biofactors.* **28:** 73-81.
- **Schumacher K, Vafeados D, McCarthy M, Sze H, Wilkins T, Chory J** (1999) The Arabidopsis det3 mutant reveals a central role for the vacuolar H(+)-ATPase in plant growth and development. *Genes Dev.* **13:** 3259-3270.
- **Schwartz SH, Qin X, Loewen MC** (2004) The biochemical characterization of two carotenoid cleavage enzymes from *Arabidopsis* indicates that a carotenoid-derived compound inhibits lateral branching. *J Biol Chem.* **279**: 46940-46945.
- **Shin H, Shin HS, Guo Z, Blancaflor EB, Masson PH, Chen R** (2005) Complex regulation of Arabidopsis AGR1/PIN2-mediated root gravitropic response and basipetal auxin transport by cantharidin-sensitive protein phosphatases. *Plant J.* **42:** 188-200.
- **Shishova M, Yemelyanov V, Rudashevskaya E, Lindberg S** (2007) A shift in sensitivity to auxin within development of maize seedlings. *J Plant Physiol*. **164:** 1323-1330.
- **Sieberer T, Seifert GJ, Hauser MT, Grisafi P, Fink GR, Luschnig C** (2000) Post-transcriptional control of the Arabidopsis auxin efflux carrier EIR1 requires AXR1. *Curr. Biol.* **10:** 1595-1598.
- **Sieberer BJ, Ketelaar T, Esseling JJ, Emons AM** (2005) Microtubules guide root hair tip growth. *New Phytol*. **167:** 711-719.

- **Sieberer T, Willett B, Booker J, Luschnig C, Leyser O** (2006) The Arabidopsis MAX pathway controls shoot branching by regulating auxin transport. *Curr. Biol.* **16:** 553-563.
- **Spaepen S, Versées W, Gocke D, Pohl M, Steyaert J, Vanderleyden J** (2007) Characterization of phenylpyruvate decarboxylase, involved in auxin production of Azospirillum brasilense. *J Bacteriol.* **189:** 7626-7633.
- **Stadler R, Lauterbach C, Sauer N** (2005) Cell-to-cell movement of green fluorescent protein reveals post-phloem transport in the outer integument and identifies symplastic domains in *Arabidopsis* seeds and embryos. *Plant Physiol.* **139:** 701-712.
- **Staiger CJ** (2000) Signaling to the actin cytoskeleton in plants. *Annu Rev Plant Physiol Plant Mol Biol.* **51:** 257-288.
- **Stöhr C, Ullrich WR** (2002) Generation and possible roles of NO in plant roots and their apoplastic space. *J Exp Bot* **53**:2293-2303.
- **Strnad M, Vaněk T. Binarová P, Kamínek M, Hanuš J** (1990) Enzyme immunoassays for cytokinins and their use for immunodetection of cytokinins in alfalfa cell culture. *Molecular Aspects of Hormonal Regulation of Plant Development,* 41-54, Kutáček M, Elliott MC, Macháčková I, eds. SPB Academic Publ., The Hague
- **Strnad M, Vereš K, Hanuš J, Siglerová V** (1992a) Immunological methods for quantification and identification of cytokinins. *Physiology and Biochemistry of Cytokinins in Plants* 437-446, Kamínek M, Mok DWS, Zažímalová, E.,eds. SPB Academic Publ, The Hague
- **Strnad M, Peters W, Beck E, Kamínek M** (1992b) Immunodetection and identification of N^6-(o-hydroxybenzylamino)purine as a naturally occurring cytokinin in Populus x canadensis Moench cv Robusta leaves. *Plant Physiol.* **99:** 74-80.
- **Subczynski WK, Markowska E, Sielewiesiuk J** (1991) Effect of polar carotenoids on the oxygen diffusion-concentration product in lipid bilayers. An EPR spin label study. *Biochim Biophys Acta.* **1068:** 68-72.
- **Sun H, Basu S, Brady SR, Luciano RL., Muday GK** (2004) Interactions between auxin transport and the actin cytoskeleton in developmental polarity of *Fucus distichus* embryos in response to light and gravity. *Plant Physiol.* **135**: 266-278.
- **Sun F, Zhang W, Hu H, Li B, Wang Y, Zhao Y, Li K, Liu M, Li X** (2008) Salt modulates gravity signaling pathway to regulate growth direction of primary roots in Arabidopsis. *Plant Physiol.* **146:** 178-188.
- **Surpin M, Zheng H, Morita MT, Saito C, Avila E, Blakeslee JJ, Bandyopadhyay A, Kovaleva V, Carter D, Murphy A, Tasaka M, Raikhel N** (2003) The VTI family of

SNARE proteins is necessary for plant viability and mediates different protein transport pathways. *Plant Cell.* **15:** 2885-2899.

- **Sutter RP, Grandin AB, Dye BD, Moore WR** (1996) (-) mating type-specific mutants of Phycomyces defective in sex pheromone biosynthesis. *Fung Genet Biol.* **20:** 268-279.
- **Swarup R, Bennett M** (2003) Auxin transport: the fountain of life in plants? *Dev Cell.* **5**: 824-826.
- **Szabó C, Salzman AL, Ischiropoulos H** (1995) Peroxynitrite-mediated oxidation of dihydrorhodamine 123 occurs in early stages of endotoxic and hemorrhagic shock and ischemia-reperfusion injury *FEBS Lett.* **372:** 329-32.
- **Tachibana H, Fujimura Y, Yamada K** (2004) Tea polyphenol epigallocatechin-3-gallate associates with plasma membrane lipid rafts: lipid rafts mediate anti-allergic action of the catechin. *Biofactors.* **21:** 383-385.
- **Tarahovsky YS, Muzafarov EN, Kim YA** (2008) Rafts making and rafts braking: how plant flavonoids may control membrane heterogeneity. *Mol Cell Biochem.* In press
- **Taylor NL, Millar AH** (2007) Oxidative stress and plant mitochondria. *Methods Mol Biol.* **372:** 389-403.
- **Teale WD, Paponov IA, Ditengou F, Palme K** (2005) Auxin and the developing root of Arabidopsis thaliana. *Physiol Plant*. **123:** 130-138.
- **Teale WD, Paponov IA, Palme K** (2006) Auxin in action: signalling, transport and the control of plant growth and development. *Nat Rev Mol Cell Biol.* **7:** 847-859.
- **Terasaka K, Blakeslee JJ, Titapiwatanakun B, Peer WA, Bandyopadhyay A, Makam SN, Lee OR, Richards EL, Murphy AS, Sato F, Yazaki K** (2005) PGP4, an ATP binding cassette P-glycoprotein, catalyzes auxin transport in Arabidopsis thaliana roots. *Plant Cell.* **17:** 2922-2939.
- **Theologis A, Huynh TV, Davis RW** (1985) Rapid induction of specific mRNAs by auxin in pea epicotyl tissue. *J Mol Biol.* **183:** 53-68.
- **Tiedemann A** (1997) Evidence for a primary role of active oxygen species in induction of host cell death during infection of bean leaves with *Botrytis cinerea*. *Physiol Mol Plant Pathol.* **50**: 151-166
- **Titapiwatanakun B, Blakeslee JJ, Bandyopadhyay A,Yang H, Mravec J, Sauer M, Cheng Y, Adamec J, Nagashima A, Geisler M, Sakai T, Friml J, Peer WA, Murphy AS** (2008) ABCB19/PGP19 stabilises PIN1 in membrane microdomains in Arabidopsis. *Plant J* Accepted: **DOI**: 10.1111/j.1365-313X.2008.03668.x

- **Torres MA, Onouchi H, Hamada S, Machida C, Hammond-Kosack KE, Jones JD** (1998) Six Arabidopsis thaliana homologues of the human respiratory burst oxidase (gp91phox). *Plant J.* **14:** 365-370.
- **Utsuno K, Shikanai T, Yamada Y, Hashimoto** T (1998) *AGR*, an *Agravitropic* locus of *Arabidopsis thaliana*, encodes a novel membrane-protein family member. *Plant Cell Physiol.* **39:** 1111-1118.
- **van Noorden GE, Ross JJ, Reid JB, Rolfe BG, Mathesius U** (2006) Defective long-distance auxin transport regulation in the Medicago truncatula super numeric nodules mutant. *Plant Physiol.* **140:** 1494-506.
- **Verbelen J-P, De Cnodder T, Le J, Vissenberg K, Baluška F** (2006) The root apex of *Arabidopsis thaliana* consists of four distinct zones of cellular activities: meristematic zone, transition zone, fast elongation zone, and growth terminating zone. *Plant Signal Behav.* **1:** 296-304.
- **Vieten A, Vanneste S, Wisniewska J, Benková E, Benjamins R, Beeckman T, Luschnig C, Friml J** (2007) Functional redundancy of PIN proteins is accompanied by auxin-dependent cross-regulation of PIN expression. *Development.* **132:** 4521-4531.
- **Voigt B, Timmers ACJ, Šamaj J, Müller J, Baluška F, Menzel D** (2005a) GFP-FABD2 fusion construct allows in vivo visualization of the dynamic actin cytoskeleton in all cells of Arabidopsis seedlings. *Eur J Cell Biol.* **84**: 595-608.
- **Voigt B, Timmers A, Šamaj J, Hlavacka A, Ueda T, Preuss M, Nielsen E, Mathur J, Emans N, Stenmark H, Nakano A, Baluška F, Menzel D** (2005b) Actin-based motility of endosomes is linked to the polar tip growth of root hairs. *Eur J Cell Biol.* **84**: 609-621.
- **Volkmann D, Baluška F** (1999) The actin cytoskeleton in plants: from transport networks to signaling networks. *Microsc Res Tech.* **47:** 135-154.
- **Volkov AG, Adesina T, Markin VS, Jovanov E** (2008) Kinetics and mechanism of *Dionaea muscipula* Ellis trap closing. *Plant Physiol.* **146:** 694-702.
- **Weiler EW, Jourdan PS, Conrad W** (1981) Levels of indole-3-acetic acid in intact and decapitated coleoptiles as determined by a specific and sensitive solid-phase enzyme immunoassay. *Planta.* **153**: 561-571.
- **Went F** (1937) Wuchsstoff und Wachstum. *Rec Trav Bot Neerl.* **25:** 1-116.
- **Wilkinson S, Morris DA** (1994) Targeting of auxin carriers to the plasma membrane: effects of monensin on transmembrane auxin transport in *Cucurbita pepo* L. tissue. *Planta.* **193:** 194-202.

- **Wisniewska J, Xu J, Seifertová D, Brewer PB, Ruzicka K, Blilou I, Rouquié D, Benková E, Scheres B, Friml J** (2006) Polar PIN localization directs auxin flow in plants. *Science.* **312:** 883.
- **Woll K, Borsuk LA, Stransky H, Nettleton D, Schnable PS, Hochholdinger F** (2005) Isolation, characterization, and pericycle-specific transcriptome analyses of the novel maize lateral and seminal root initiation mutant *rum1*. *Plant Physiol*. **139:** 1255-1267.
- **Woodward AW, Bartel B** (2005) Auxin: regulation, action, and interaction. *Ann Bot (Lond.)* **95**: 707-735.
- **Woodward AW, Bartel B** (2005b) The Arabidopsis peroxisomal targeting signal type 2 receptor PEX7 is necessary for peroxisome function and dependent on PEX5. *Mol Biol Cell.* **16**: 573-583.
- **Woodward AW, Ratzel SE, Woodward EE, Shamoo Y, Bartel B** (2007) Mutation of E1-CONJUGATING ENZYME-RELATED1 decreases RELATED TO UBIQUITIN conjugation and alters auxin response and development. *Plant Physiol.* **144**: 976-987.
- **Wyatt SE, Rashotte AM, Shipp MJ, Robertson D, Muday GK** (2002) Mutations in the gravity persistence signal loci in *Arabidopsis* disrupt the perception and/or signal transduction of gravitropic stimuli. *Plant Physiol*. **130:** 1426-1435
- **Wymer CL, Bibikova TN, Gilroy S** (1997) Cytoplasmic free calcium distributions during the development of root hairs of Arabidopsis thaliana. *Plant J.* **12:** 427-439.
- **Xue HW, Chen X, Li G** (2007). Involvement of phospholipid signaling in plant growth and hormone effects. *Curr Opin Plant Biol.* **10:** 1-7.
- **Yamazoe A, Hayashi K, Kepinski S, Leyser O, Nozaki H** (2005) Characterization of terfestatin A, a new specific inhibitor for auxin signaling. *Plant Physiol.* **139:** 779-789.
- **Yan J, Tsuichihara N, Etoh T, Iwai S** (2007) Reactive oxygen species and nitric oxide are involved in ABA inhibition of stomatal opening. *Plant Cell Environ.* **30:** 1320-1325
- **Zažímalová E, Křeček P, Skůpa P, Hoyerová K, Petrášek J** (2007) Polar transport of the plant hormone auxin – the role of PIN-FORMED (PIN) proteins. *Cell Mol Life Sci.* **64:** 1621-1637.
- **Zegzouti H, Anthony RG, Jahchan N, Bögre L, Christensen SK** (2006) Phosphorylation and activation of PINOID by the phospholipid signaling kinase 3-phosphoinositide-dependent protein kinase 1 (PDK1) in Arabidopsis. *Proc Natl Acad Sci USA.* **103:** 6404-6409.

- **Zelko IN, Mariani TJ, Folz RJ** (2002) Superoxide dismutase multigene family: a comparison of the CuZn-SOD (SOD1), Mn-SOD (SOD2), and EC-SOD (SOD3) gene structures, evolution, and expression. *Free Radic Biol Med.* **33:** 337-349.
- **Zhang WH, Rengel Z, Kuo J** (1998) Determination of intracellular Ca^{2+} in cells of intact wheat roots: loading of acetoxymethyl ester of Fluo3 under low temperature. *Plant J.* **15**: 147-151.
- **Zolman BK, Yoder A, Bartel B** (2000) Genetic analysis of indole-3-butyric acid responses in Arabidopsis thaliana reveals four mutant classes. *Genetics.* **156**: 1323-1337.
- **Zolman BK, Silva ID, Bartel B** (2001a) The Arabidopsis pxa1 mutant is defective in an ATP-binding cassette transporter-like protein required for peroxisomal fatty acid beta-oxidation. *Plant Physiol.* **127**: 1266-1278.
- **Zolman BK, Monroe-Augustus M, Thompson B, Hawes JW, Krukenberg KA, Matsuda SP, Bartel B** (2001b) chy1, an Arabidopsis mutant with impaired beta-oxidation, is defective in a peroxisomal beta-hydroxyisobutyryl-CoA *hydrolase. J Biol Chem.* **276**: 31037-31046.
- **Zolman BK, Bartel B** (2004) An Arabidopsis indole-3-butyric acid-response mutant defective in PEROXIN6, an apparent ATPase implicated in peroxisomal function. *Proc Natl Acad Sci USA.* **101**: 1786-1791.

6. Index of Abbreviations:

2,4D	2,4-Dichlorophenoxyacetic acid
A23187	Calcium Ionophore or Calcimycin
ABA	abscisic acid
ABC transporter	ATP-Binding Cassette Transporter
ABD1	auxin binding protein 1
AGC kinase family	cAMP-dependent protein kinases (A), cGMP-dependent protein kinases (G), and phospholipid-dependent protein kinases (C)
agr1	agravitropic 1
APX	ascorbate peroxidase
ATP	Adenosine-5'-triphosphate
BA3	promoter consisting of 3 tandem auxin-responsive domains called A and B
BCIP	5-Bromo-4-chloro-3-indolyl phosphate
BFA	brefeldin A
BSA	Bovine serum albumin
Ca^{2+}	calcium cation
CAT	catalase
cGMP	cyclic guanosine monophosphate
CHX	cycloheximide
cm	centimeter
Col-0	Arabidopsis ecotype Columbia 0
cpi1	cyclopropylsterol isomerase 1
cPTIO	2-(4-Carboxyphenyl)-4,4,5,5-tetra-methylimidazoline-1-oxyl-3-oxide
Cu	copper
CW	cell wall
DAF-2 DA	4,5-diaminofluorescein diacetate
DMSO	dimethyl sulfoxide
DNA	desoxyribonucleic acid
DOR	2-deoxyribose
DPI	diphenyleneiodonium sulfate
DR5	promoter consisting of 7 tandem repeats of an auxin-responsive TGTCTC element and a minimal 35S CaMV promoter
DRM	detergent resistent membrane
DTT	dithiothreitol
EDTA	ethylenediamine tetraacetic acid
EGTA	ethylene glycol tetraacetic acid
eir1	ethylene insensitive root 1
ER	endoplasmatic reticulum
FABD	fimbrin actin-binding domain
F-actin	filamentous actin

Fig	figure
FITC	fluorescein isothiocyanate
Fluo 3-AM	4-(6-Acetoxymethoxy-2,7-dichloro-3-oxo-9-xanthenyl)-4'-methyl-2,2'-(ethylenedioxy) dianiline-N,N,N',N'-tetraacetic acid tetrakis(acetoxymethyl) ester
FM4-64	N-3-triethylammoniumpropyl-4-(6-(4-diethylaminophenyl)-hexa-trienyl)pyridinium dibromide
FYVE	zink finger domain named after four proteins: Fab1, YOTB, Vac1 & EEA1
G-actin	globular actin
GEF	guanine-nucleotide exchange factor
GFP	green fluorescent protein
GUS	ß-Glucoronidase
h/hrs	hour/hours
H^+	hydrogen ion
H_2O_2	hydrogen peroxide
HCl	hydrogen chloride
IAA	indole-3-acetic acid
IBA	indole-3-butyric acid
IGg	immunoglobulin
Jim5	acidic and unesterified pectins
KCl	potassium chloride
kDA	kilodalton
KNOX	knotted like homeobox
KOH	potassium hydroxide
lat B	latrunculin B
LRF	lateral root formation
ltr1	lateral rootless 1
MAP-kinase	Mitogen-activated protein kinases
MBTH	3-methylbenzothiazoline
MgCl	magnesium chloride
$MgSO_4$	magnesium sulphate
mm	millimeter
m-RNA	messenger ribonucleic acid
MDR	multidrug resistance
min	minute
mit	mitochondrial-targeting signal
MS	Murashige and Skoog
MVB	multivesicular body
MW	molecular weight
NAA	1-naphthalene acetic acid
NaCl	sodium chloride
NADPH	reduced form of nicotinamide adenine dinucleotide phosphate
NaN_3	sodium azide

NaOH	sodium hydroxide
NBD	NPA binding protein
NBT	nitro blue tetrazolium chloride
NO	nitric oxide
NOS	nitric oxide synthase
noa1	nitric oxide synthase associated 1
NPA	1-naphthylphthalamic acid
$O_2^{\cdot -}$	superoxide anion
O_3	ozone
$OH^{\cdot}$	hydroxyl radical
$ONOO^-$	peroxynitrite
PA	phosphatidic acid
PAT	polar auxin transport
PBS	phosphate buffered saline
PDK1	3-phosphoinositide dependent ***kinase*** 1
ped1	peroxisome defective 1
pex	peroxin
PGP	P-glycoprotein
PI(3)K	phosphatidylinositol 3-kinase
PID	pinoid
PIN	pin-formed
PIPES	Piperazine-N,N'-bis(2-ethanesulfonic acid)
PLD	phospholipase D
PM	plasma membrane
PP2A	protein phosphatase 2a
pro3DC	Daucus carota (L.) promoter
pxa1	***peroxisomal*** ABC transporter 1
pts1	peroxysomal targeting signal 1
PVP	polyvinylpyrrolidone
QC	quiescent centre
RG II	rhamnogalacturonan II
RNA	ribonucleic acid
RNS	reactive nitrogen species
ROS	reactive oxygen species
RT-PCR	reverse transcriptase- PCR
rpm	rounds per minute
rum1	rootless without meristems 1
SDS	sodium dodecyl sulfate
SHAM	salicylhydroxamic acid
SNAP	S-nitroso-N-acetyl-l,l-penicillamine
smt1	sterol methyltransferase 1

SOD	superoxide dismutase
TBA	thiobarbituric acid
TBS	TRIS buffered saline
TCA	trichloroacetic acid
TGN	trans golgi network
TIBA	2,3,5-triiodobenzoic acid
TIR1	transport inhibitor response 1
TRITC	tetramethyl rhodamine isothiocyanate
Trf A	Terfestatin A
TRIS	tris(hydroxymethyl) aminomethane
twd1	twisted dwarf 1
U	unit
ucu2	ultracurvata 2
µl	microliter
µm	micrometer
µM	micromol
µg	microgram
Wort	wortmannin
wt	wild type
XTT	2,3-bis(2-methoxy-4-nitro-5-sulfo-phenyl)-2H-tetrazolium-5-carbox-anilide
Zn	zinc

7. Index of Figures and Tables:

Erklärung

Ich versichere hiermit, dass ich die vorliegende Arbeit in allen Teilen selbst und ohne jede unerlaubte Hilfe angefertigt habe. Diese oder eine ähnliche Arbeit ist noch keiner anderen Stelle als Dissertation eingereicht worden. Die Arbeit ist an nachstehend aufgeführten Stellen auszugsweise veröffentlicht worden:

Mancuso S, Marras AM, Mugnai S, Schlicht M, Žársky V, Li G, Song L, Xue H-W, Baluška F (2007) Phospholipase Dζ2 drives vesicular secretion of auxin for its polar cell-cell transport in the transition zone of the root apex. *Plant Signal. Behav.* **2:** 204-244.

Schlicht M, Strnad M, Scanlon MJ, Mancuso S, Hochholdinger F, Palme K, Volkmann D, Menzel D, Baluška F (2006) Auxin immunolocalization implicates vesicular neurotransmitter-like mode of polar auxin transport in root apices. Plant Signal. Behav. 1: 122-133.

Schlicht M, Šamajová O, Schachtschabel D, Mancuso S, Menzel D, Boland W, Baluška F (2008) D'orenone blocks polarized tip-growth of root hairs by interfering with the PIN2-mediated auxin transport network in the root apex. *Plant J.* **55**: 709-717.

Ich habe früher noch keinen Promotionsversuch unternommen.

Bonn, den

Danksagung:

An dieser Stelle möchte ich mich bei all meinen Verwandten, Freunden und Bekannten bedanken, die mich in den Jahren der Erstellung der Dissertation vor allem moralisch unterstützten und somit zum Gelingen beigetragen haben.

Mein besonderer Dank gilt den Herren Prof. Dr. Frantisek Baluska und Prof. Dr. Diedrik Menzel für deren fachliche Betreuung und Beratung sowie für die Hilfe bei der Fertigstellung der Arbeit.
Meinen Kollegen Christian Burbach, Dr. Olga Samajova und Yin-Lang Wan danke ich für das angenehme Arbeitsklima. Ein großer Dank geht auch an meine ehemaligen Laborkollegen Gerald Njio, Kai Waßer und Andrej Hlavacka, sie gaben mir viele Anregungen für meine wissenschaftliche Arbeit. Ohne ihr Wissen, ohne ihre Ideen und ihre Kritik wäre mein Thema niemals soweit gekommen.
Allen Institutsangehörigen des IZMBs, die direkt oder indirekt zum Gelingen dieser Arbeit beigetragen haben und nicht namentlich erwähnt wurden, sei mein herzlicher Dank ausgesprochen.

Meiner Frau Alexandra bin ich dankbar für die Unterstützung, ihre Kraft und ihre Liebe, die mich all die Jahre durch mein Studium begleitet haben.
Und natürlich meine Tochter Akiko, ihr danke ich, dass sie nie versäumte mir ihre neuesten Abenteuer aus den Kindergarten zu erzählen, obwohl sie oft genug gegen den Computer oder das neueste Paper konkurrieren musste.